Oxidative stress and the role of downstream pathways in cardiovascular diseases

PhD Dissertation

Dr. Levente Kiss, MD

Semmelweis University
PhD School for Basic Medical Sciences

Supervisor: Dr. Csaba Szabó, MD, PhD, Dsc

Reviewers: Dr. Zsolt Radák, MD, PhD, DSc
Dr. Péter Ferdinándy, MD, PhD, DSc

Committee members: Dr. László Rosivall, MD, PhD, DSc
Dr. Balázs Sümegi, MD, PhD, DSc
Dr. Violetta Kékessi, MD, PhD

Budapest, Hungary

2009

CONTENTS

LIST OF ABBREVIATIONS

3-NT	3-nitrotyrosine
7K	7-ketocholesterol
AAR	Area-at-risk
ADP	Adenosine diphosphate
AIF	Apoptosis inducing factor
ANOVA	Analysis of variance
ApoE	Apolipoprotein E
ATP	Adenosine triphosphate
Bak	Bcl-2 homologous antagonist/killer
Bax	Bcl-2-associated protein
Bcl-2	B-cell chronic lymphocytic leukemia/lymphoma 2
Bcl-X_L	Bcl-2-like 1
Bid	BH3-interacting domain death agonist
BSA	Bovine serum albumin
BSO	Buthionine sulphoximine
CBS	Cystathionine β-synthase
CGL	Cystathionine γ-lyase
CHF	Chronic heart failure
cGMP	Cyclic guanosine monophosphate
CO	Carbon monoxide
cTnI	Cardiac-specific isoform of troponin-I
Cyt-c	Cytochrome-c
DAB	3,3'-diaminobenzidine-tetrahydrochloride
DNA	Deoxyribonucleic acid
DTPA	Dethylenetriaminepentaacetic acid
ECL	Enhanced chemiluminescence
EGTA	Ethylene glycol tetraacetic acid
ERK	Extracellular regulated kinase
ETC	Electron transport chain

$FADH_2$	Reduced flavin adenin dinucleotid
GAPDH	Glyceraldehyde 3-phosphate dehydrogenase
GSH	Reduced glutathione
GSSG	Oxidized glutathione
H&E	Hematoxylin and eosin
HClO	Hypochlorous acid
HEPES	4-(2-hydroxyethyl)-1-piperazineethanesulfonic acid
HIF-1	Hypoxia inducible factor
HO-1	Heme-oxygenase-1
HR	Heart rate
HRP	Horse-radish peroxidase
HW	Heart weight
H_2O_2	Hydrogen peroxide
H_2S	Hydrogen sulfide
HUVEC	Human umbilical vein endothelial cell
IAP	Inhibitors of apoptosis proteins
ICAM-1	Intercellular adhesion molecule
INF	Infarcted area
INO-1001	PARP-inhibitor
IL-1β	Interleukin-1 beta
IL-4	Interleukin-4
IL-6	Interleukin-6
IL-8	Interleukin-8
IL-10	Interleukin-10
KHB	Krebs-Henseleit bicarbonate
L-NAME	N-nitro-L-arginine methyl ester
LCA	Left coronary artery
LDL	Low density lipoprotein
LV	Left ventricular
LVESD	Left vetricular end-systolic dimension
LVEDD	Left vetricular end-diastolic dimension
MABP	Mean arterial blood pressure

MAPK	Mitogen activated protein kinase
MEK	Mitogen-activated protein kinase kinase
MEM	Minimal essential medium
MHC	Major histocompatibility complex
MI-R	Myocardial ischemia reperfusion
MPO	Myeloperoxidase
MPTP	Mitochondrial permeability transition pore
NO	Nitric oxide
NOS	Nitric oxide synthase
NAD^+	Nicotinamid adenine dinucleotide
NADPH	Nicotinamid adenine dinucleotide
NFκB	Nuclear factor of kappa light polypeptide gene enhancer in B-cells
$O_{2^{\cdot}}^-$	Superoxide anion
$OH^{\cdot}$	Hydroxyl radical
ONOO	Peroxynitrite
oxLDL	Oxidized low density lipoprotein
p53	Tumor protein 53
PARP	Poly-(ADP-ribose) polymerase
PARG	Poly-(ADP-ribose) glycohydrolase
PBS	Phosphate buffered saline
PJ34	PARP inhibitor
PHSS	Polarographic H_2S sensor
PKC	Protein kinase C
PLP	Pyridoxal 5'-phosphate
PVDF	Polyvinylidene fluoride
RNA	Ribonucleic acid
ROS	Reactive oxygen species
SD	Standard deviation
SEM	Standard error of mean
sGC	Soluble guanylate cyclase
SIR2α	Sirtuin, class III histone deacetylase

SOD	Superoxide dismutase
TAC	Transverse aortic constriction
TBST	TRIS-buffered saline tween-20
TCA	Trichloroacetic acid
TCV	Total cardiovascular
TL	Tibial length
TNF-α	Tumor necrosis factor alpha
TRIS	Trishydroxymethylaminomethane
TUNEL	Terminal deoxynucleotidyl transferase dUTP nick-end labeling
TTC	2,3,5-triphenyltetrazolium chloride
WT	Wild type
UK	United Kingdom
US	United States

1. INTRODUCTION

Cardiovascular diseases represent an enormous medical and social burden [1, 2]. Although substantial decreases occured in the number of total cardiovascular (TCV) mortality rates since 1970 in Western Europe and since the early 90's in Eastern Europe (Fig. 1.), the major cause of deaths in adults in the developed world is still of cardiovascular origin [3]. The main contributors to TCV mortality are atherosclerosis, ischemic heart disease and heart failure.

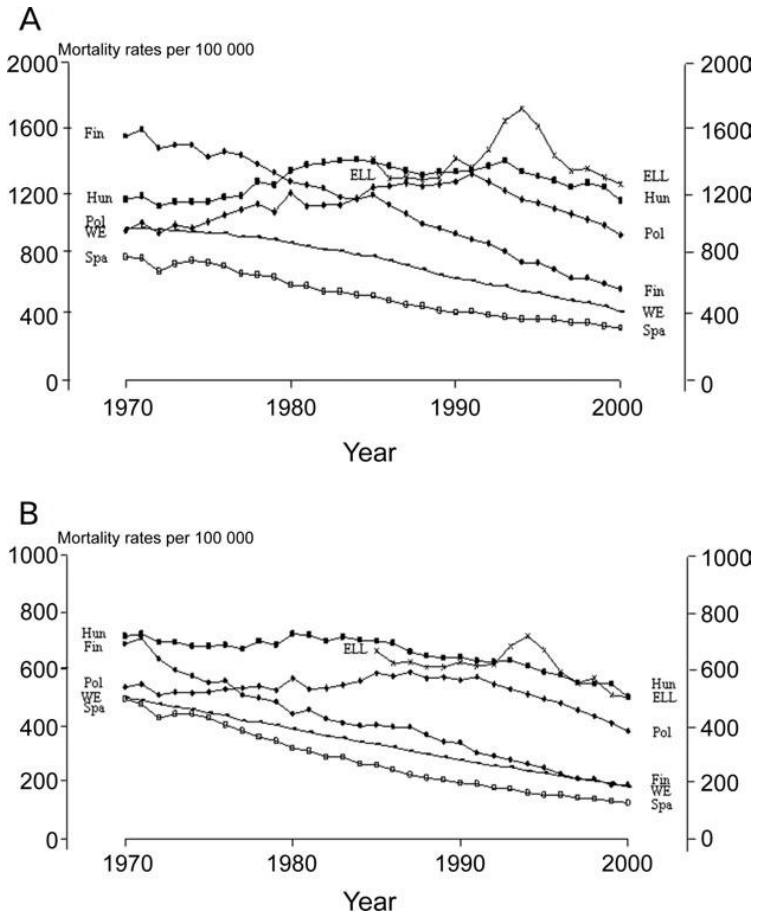

Figure 1. Time trends in TCV mortality in 1970-2000 *(A)* for men aged 45-74 years and *(B)* for women aged 45-74 years. (Hun: Hungary; ELL: Estonia, Latvia, Lithuania; Pol: Poland; Fin: Finland; WE: Austria, Denmark, England, Finland, France, Greece, Ireland, Italy, The Netherlands, Norway, Portugal, Scotland, Sweden, Switzerland and Wales; Spa: Spain) (*Kesteloot et al., Eur Heart J, 2006. 27(1): p. 107-13.)*

Atherosclerosis is a disease of large and medium-sized muscular arteries and is characterized by endothelial dysfunction, vascular inflammation, and the buildup of lipids, cholesterol, calcium, and cellular debris within the intima of the vessel wall. This buildup results in plaque formation, vascular remodeling, acute and chronic luminal obstruction, abnormalities of blood flow, and diminished oxygen supply to target organs [4-6]. In case of the heart this diminished oxygen supply leads to ischemic heart disease also known as coronary artery disease [7-9]. Atherosclerosis is the leading cause of deaths in the developed world. It is responsible for more than half of the yearly mortality in the United States (US): atherosclerosis-related cerebrovascular disease is responsible for over 200,000 deaths per year; more than 11 million US citizens have chronic coronary artery disease; approximately 1.5 million myocardial infarctions occur a year and more than 500,000 people die annually of myocardial infarction alone. This rate of mortality costs more than $100 billion a year [10]. More than 50 million people in the US are candidates for some form of dietary and/or drug treatment to modify their lipid profile. Although an encouraging decrease in mortality due to coronary heart disease has occurred in the developed world, this decrease has not happened in the developing world [11], and an exponential increase in tobacco habituation and the adoption of a Western diet high in saturated fats likely predicts that atherosclerosis will be the leading cause of deaths in the developing world within the first quarter of the 21st century [12].

Congestive heart failure (CHF) is a progressive syndrome deriving from multiple etiologies and is defined by impaired cardiac contractility, multiorgan failure and death [13, 14]. Although TCV mortality rates tend to decrease in the developed world, the incidence of this condition continues to steadily increase. It affects more than 2% of the US population, or almost 5 million people [15]. The total annual cost of treatment for heart failure in the United States is approximately $28 billion, and it consumes approximately 2% of the National Health Service budget in the United Kingdom. Moreover, the financial burden of heart failure will increase in coming decades because of the aging population and the improved treatments of its causes. The molecular mechanisms by which CHF develops are multifactorial and currently available therapies have only modest impacts on patient survival as 50% of CHF patients die within 5 years of diagnosis [16].

1.1. Free radicals and their derivatives in living organisms

Potentially harmful free radicals are generated continuously in living organisms, but under physiological conditions protective mechanisms lead to a well-balanced equilibrium, during which the levels and the deleterious effects of these free radicals are regulated and these free radicals even control several physiological functions via redox-sensitive pathways [17]. When this carefully regulated equilibrium is disturbed the so-called oxidative stress occurs. The knowledge regarding the role of oxidative stress in the pathogenesis of a wide variety of diseases has broadened enormously recently. Oxidative stress is now implicated in such pathophysiological conditions as cancer, autoimmun diseases, diabetes, hypertension, atherosclerosis, ischemic heart disease, cardiac heart failure [18-29].

1.1.1. Reactive oxygen species (ROS)

Sources of reactive oxygen species in living cells are generated enzymatically and from aerobic metabolism that utilizes life-sustaining oxygen to oxidize fuels [30]. Superoxide anion ($O_2^{\cdot -}$) is the precursor of most ROS and a mediator in oxidative chain reactions. The main producers of superoxide anion are NAD(P)H oxidases, xanthine oxidase and the mitochondrial electron transport chain (Fig. 2.). NAD(P)H (nicotinamide adenine dinucleotide phosphate) oxidases are located on the cell membrane of polymorphonuclear cells, macrophages, vascular smooth muscle cells, cardiac myocytes, fibroblasts and endothelial cells [31-38]. The enzyme generates superoxide by transferring electrons from NADPH inside the cell across the membrane and coupling these

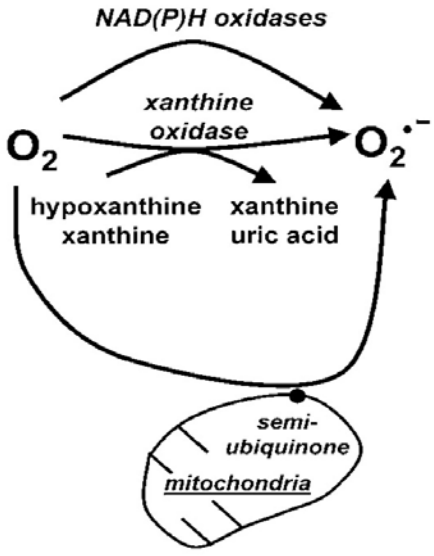

Figure 2. The sources of $O_2^{\cdot -}$

to molecular oxygen. Xanthine oxidase, which forms after the proteolytic conversion of xanthine dehydrogenase, provides another enzymatic source of $O_2^{\cdot -}$. This enzyme catalyzes the oxidation of hypoxanthine to xanthine and can further catalyze the oxidation of xanthine to uric acid. The non-enzymatic production of $O_2^{\cdot -}$ occurs when a single electron is directly transferred to oxygen by reduced coenzymes or prosthetic groups. The mitochondrial electron transport chain contains several redox centres that may leak electrons to oxygen. It is calculated that 1-4% of oxygen reacting with the respiratory chain is incompletely reduced to ROS [30]. Figure 3. shows the mitochondrial electron transport chain and the route of electrons through it with the possible site of superoxide generation.

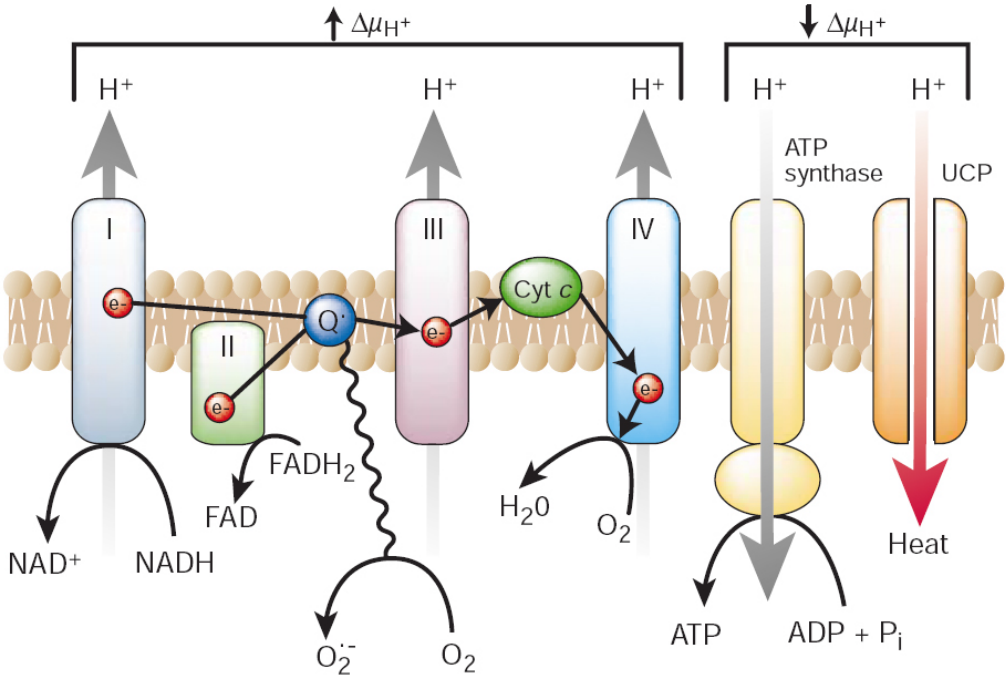

Figure 3. The mitochondrial electron transport chain and the production of superoxide. (*Brownlee, M., Nature, 2001. 414(6865): p. 813-20.)*

Dismutation of $O_2^{\cdot -}$ (either spontaneously or by the reaction catalyzed by superoxide dismutases) produces hydrogen peroxide (H_2O_2) [39]. In the presence of reduced transition metals (e.g. ferrous ions), hydrogen peroxide can be converted into the highly reactive hydroxyl radical ($OH^{\cdot}$). Besides superoxide anion, hydrogen peroxide and

hydroxyl radicals, there are also other sources of free radicals like singlet oxygen [40], peroxides [41], reactive aldehydes [42], reactive nitrogen species [43], and other reactive molecules [44]. Frequently, different reactive species coexist in the reactive environment and make it difficult to identify which agent is responsible for a given biological effect.

1.1.2. Reactive nitrogen species (RNS)

The NO radical ($NO^{\cdot}$) is produced by the oxidation of one of the terminal guanido-nitrogen atoms of L-arginine [45]. This process is catalyzed by the enzyme nitric oxide synthase (NOS) (Fig. 4).

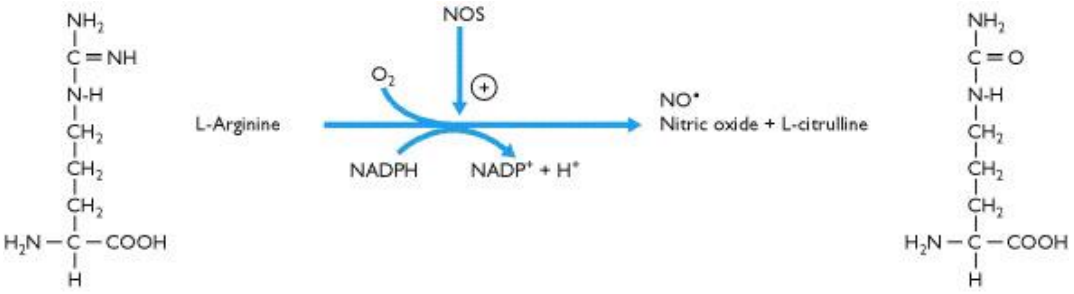

Figure 4. The enzymatic process to form NO catalyzed by NOS. This reaction utilizes dioxygen and nicotinamide-adenine dinucleotide phosphate (NADPH) as co-substrates and tetrahydropteridin, flavin adenine dinucleotide, flavin mononucleotide, thiol and heme as co-factors.

There are three isoforms of NOS enzyme: neuronal (nNOS; type I) [46], inducible (iNOS; type II) [47], and endothelial NOS (eNOS; type III) [48]. Many tissues express one or more of these isoforms. The isoforms nNOS and eNOS are constitutively expressed, but their activity is regulated by the intracellular calcium concentration. The isoform iNOS is inducibly expressed in macrophages after stimulation with cytokines, lipopolysaccharides and other immunologically relevant agents [49]. Expression of iNOS is regulated at the transcriptional and posttranscriptional level by signaling pathways that involve agents such as the redox-responsive transcription factor NF-κB (nuclear factor of kappa light polypeptide gene enhancer in B-cells) or mitogen-activated protein kinases (MAPKs) [50]. Depending on the microenvironment NO

produced by these enzymes can be converted to various other reactive nitrogen species such as nitrosonium cation (NO^+), nitroxyl anion (NO^-) or reacting with superoxide it forms the extremely reactive peroxynitrite ($ONOO^-$) [51].

1.1.3. Protective mechanisms against free radicals. Redox homeostasis.

To control the level of continuously forming oxidative and nitrosative species cells have developed various enzymatic and nonenzymatic systems to protect themselves. Superoxide anions can be scavenged by superoxide dismutase (SOD), an enzyme, present in all aerobic organisms, which catalyzes the conversion of two of these radicals into hydrogen peroxide and molecular oxygen. Three known types of SOD are present in mammalian tissues. MnSOD is encoded in the nuclear genome, but localizes to mitochondria via a mitochondrial targeting sequence, and makes up ~70% of the SOD activity in the heart [52]. The remaining intracellular SOD consist primarily of Cu/ZnSOD which is localized in the cytosol. Extracellular SOD, localized in intravascular spaces is also a Cu- and Zn-containing enzyme. As the only known SOD located in the mitochondria, MnSOD plays a critical role in the control of mitochondrial ROS-formation during normal oxidative phosphorylation. The importance of MnSOD in the myocardium was demonstrated using homozygous knockout mice which developed normally, but died soon after birth in cardiomyopathy [53]. Hydrogen peroxide formed by superoxide dismutase and by the uncatalysed reaction of hydroperoxy radicals are scavenged by catalase, an ubiquitous heme protein that catalyzes the conversion of hydrogen peroxide into water and molecular oxygen. Peroxidases are also heme enzymes and catalyze an analogous reaction in which hydrogen peroxide is reduced to water by a reductant. Glutathione has a key role in detoxification by reacting with hydrogen peroxide and organic peroxides. Glutathione, which is present in high concentrations (5mM) in animal cells, serves as a sulfhydril buffer [54, 55]. Glutathione cycles between a reduced thiol form (GSH) and an oxidized form (GSSG), in which two tripeptides are linked by a disulfide bond. GSSG is reduced to GSH by glutathione reductase, a flavoprotein utilizing NADPH derived from the pentose phosphate pathway as the electron source. Figure 5. summarizes the enzymatic processes regulating free radical levels.

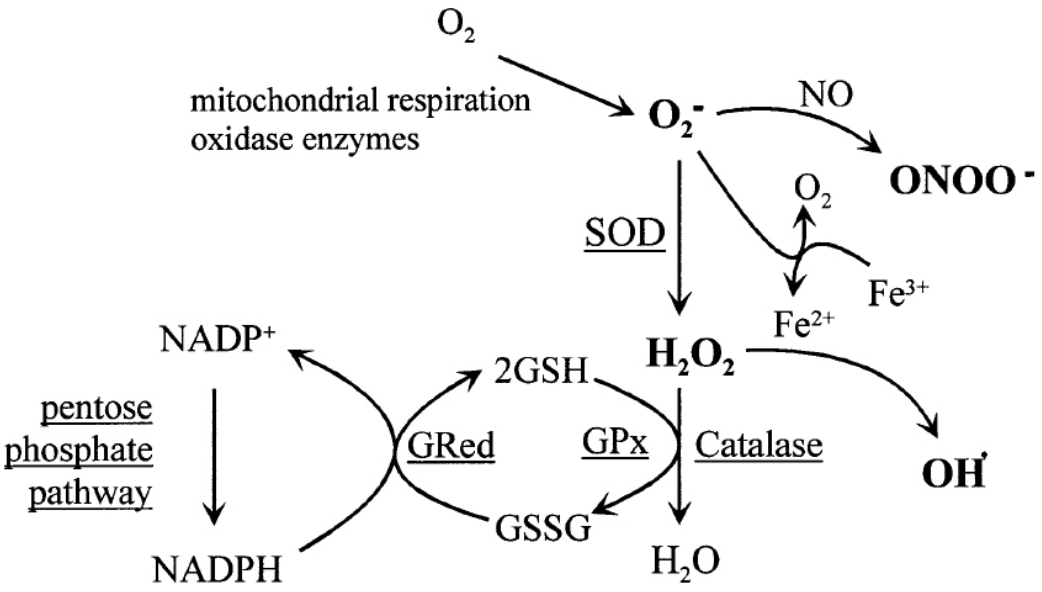

Figure 5. Free radicals and the enzymes that regulate their levels. *(Sawyer et al., J Mol Cell Cardiol, 2002. 34(4): p. 379-88.)*

Other important physiological antioxidants are vitamin E and reduced coenzyme Q. Vitamin E is regarded as the most important lipid-soluble antioxidant. In vitamin E-deficient microsomal fractions, the protection against lipid-peroxidation diminished [56]. Ascorbate and reduced glutathione are water-soluble antioxidants, which regenerate alpha-tocopherol. However, the protective effect of ascorbate and GSH against oxidative stress can attenuate or even reverse in the absence of vitamin E within the membranes [57]. In addition to its function as an electron and proton carrier in mitochondrial and bacterial electron transport coupled to ATP synthesis, coenzyme Q acts in the reduced form (ubiquinol) as an antioxidant, inhibiting lipid peroxidation in biological membranes and in serum low-density lipoprotein (LDL). It can also protect mitochondrial inner-membrane proteins and DNA against oxidative damage [58]. Physiological molecules such as urate, bilirubin and ceruloplasmin, can also protect against oxidative attack [59-61]. The novel gasotransmitter hydrogen sulfide (H_2S) may also be an important redox-controlling molecule similar to other small thiols, such as cysteine and glutathione. There are, indeed, indications for reactions of sulfide that are consistent with its “antioxidant effect” [62]. In addition, there are other compounds that

have a relatively low specific antioxidative capacity, i. e., on a molar basis, but, when present at high concentrations, can contribute significantly to the overall ROS scavenging activity. The most prominent examples of such high-level, low efficiency antioxidants are free amino acids, peptides and proteins. Practically all amino acids can serve as targets for oxidative attack by ROS, although some amino acids such as tryptophan, tyrosine, histidine and cysteine are particularly sensitive to ROS [63-65]. Because the cumulative intracellular concentration of free amino acids is on the order of 10^{-2}M [66], free amino acids are quantitatively important ROS scavengers (Fig. 6.).

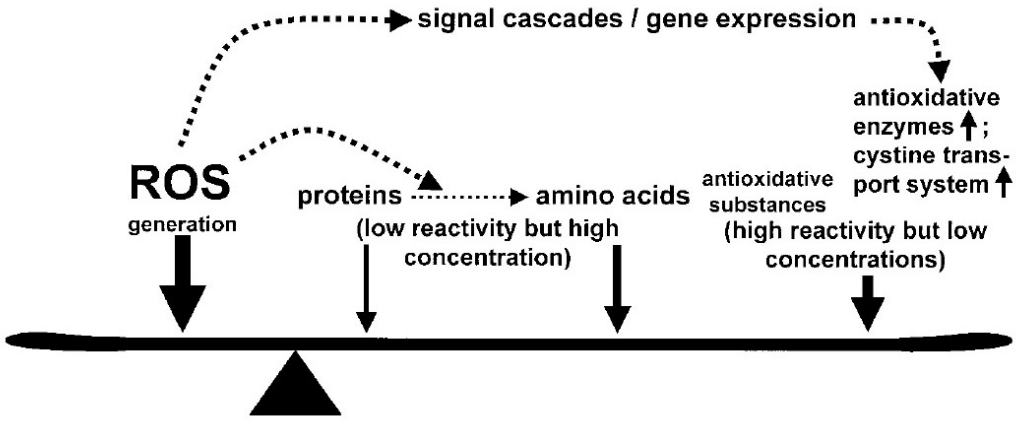

Figure 6. The redox homeostasis. Balance between free radical production and various types of scavengers. *(Droge, Physiol Rev, 2002. 82(1): p. 47-95.)*

1.1.4. The physiological role of free radicals

Although reactive oxygen and nitrogen species are often regarded as potentially dangerous molecules, numerous physiological functions are controlled by them. These cases of redox regulation typically involve the regulated production of NO or ROS by NOS or NAD(P)H oxidase, respectively, and the effects of these compounds on specific signaling cascades. The redox-sensitive target molecules of these signaling cascades and their chemical modification by oxidative agents are, in most cases, not yet well understood. However, the surprisingly large number of NAD(P)H oxidase isoforms and NO synthases is by itself a strong indication for the physiological relevance of redox

signaling in biological regulation. In the following, a few well-studied examples demonstrate how ROS and RNS affect and control various physiological conditions.

1.1.4.1. ROS in the defense against pathogens

Activated macrophages and neutrophil granulocytes can produce large amounts of superoxide and its derivatives via the phagocytic isoform of NAD(P)H oxidase. In an inflammatory environment hydrogen peroxide produced by activated macrophages can reach a concentration of 10-100 μM in the vicinity of these cells [67, 68]. The massive production of antimicrobial and tumoricidal ROS in an inflammatory environment is called „oxidative burst“ and plays an important role in the first line defense against environmental pathogens. The combined activities of NAD(P)H oxidase and myeloperoxidase (MPO) in phagocytes leads, in addition, to the production of hypochlorous acid (HClO), one of the strongest physiological oxidants and a powerful antimicrobial agent [69]. Importantly, phisiologically relevant ROS production can also modulate redox-sensitive signal cascades and enhance immunological function of lymphocytes [70].

1.1.4.2. Effects involving guanylate cyclase

Guanylate cyclase belongs to the family of heterodimeric heme proteins and catalyzes the formation of cGMP. NO binds to the heme moiety of guanylate cyclase and the resulting conformational change activates the enzyme [71] and the resulting cGMP is utilized as an intracellular amplifier and second messenger in a large range of physiological responses [72] and it modulates the function of protein kinases, phosphodiesterases, ion channels, and other phisiologically important targets [73]. The most important effects include the regulation of smooth muscle tone [74] and the inhibition of platelet adhesion [75]. Vascular smooth muscle relaxation is mediated by a cGMP-dependent protein kinase that phosphorylates and activates a calcium-sensitive potassium channel [76]. Superoxide and hydrogen peroxide may also play a role in the activation of guanylate cyclase [77-79]. Since micromolar concentrations of hydrogen peroxide stimulate NOS, there is a strong possibility that the activation of guanylate cyclase by superoxide and hydrogen peroxide may be also mediated by NOS. Figure 7. shows the possible mechanisms for NO-mediated vasodilation.

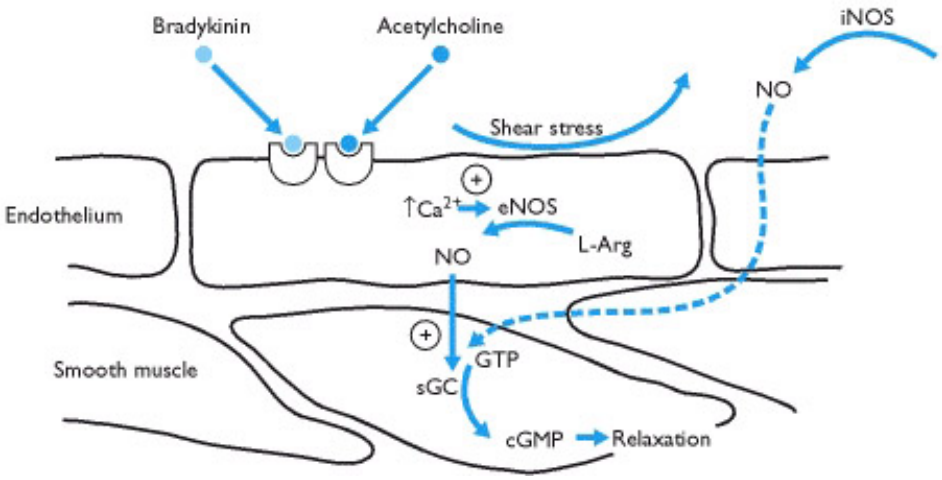

Figure 7. Vasodilatory effects of NO on vascular smooth muscle cells. A rise in intracellular Ca^{2+}, induced by chemicals or shear stress on the endothelial lining, activates endothelial nitric oxide synthase (eNOS) that converts L-arginine to citrulline and NO. NO diffuses into smooth muscle cells to activate soluble guanylate cyclase (sGC) and the rise in cGMP causes muscle relaxation. In infections, e.g. sepsis, circulating concentrations of NO can rise as a result of inducible iNOS activity and this can have the same vasodilator effect as locally produced NO. *(Nussey, S.S. and Whitehead, S.A. Endocrinology: An Integrated Approach , 2001)*

1.1.4.3. ROS in the regulation of oxygen homeostasis

Oxygen homeostasis is maintained in higher organisms by a tight regulation of the red blood cell mass. Not surprisingly, the regulatory processes involve ROS. The erythropoietin gene in renal interstitial cells is controlled by the transcription factor hypoxia-inducible factor 1 (HIF-1) [80]. HIF-1 is a heterodimeric protein expressed ubiquitously in tissues and composed of the subunits HIF-1α and HIF-1β. The cytoplasmic HIF-1α and HIF-1β subunits are constitutively expressed, and changes in oxygen tension do not affect the concentration of the HIF-1β subunit, but, under normoxic conditions, HIF-1α is rapidly degraded by proteasomes. Therefore hypoxia decreases the ROS-mediated degradation of HIF-1α enhancing the formation of the active heterodimeric complex and leading to nuclear translocation [81, 82] (Fig. 8.).

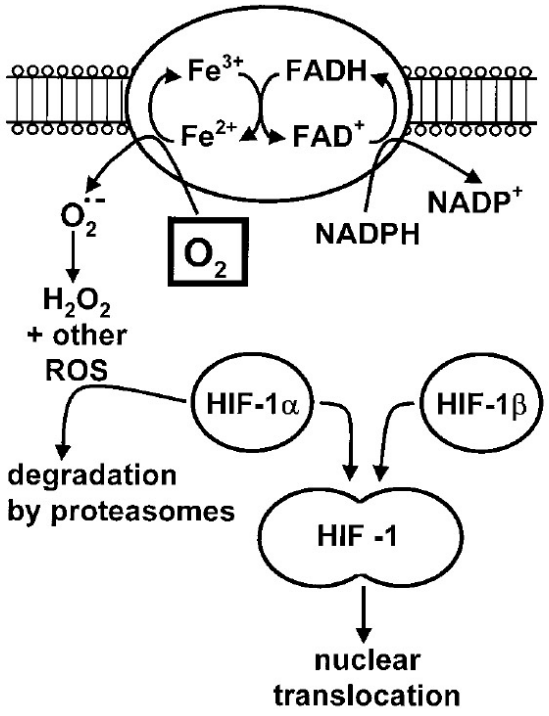

Figure 8. Regulation of the transcription factor hypoxia-inducible factor 1 (HIF-1). *(Droge, Physiol Rev, 2002. 82(1): p. 47-95.)*

The number of target genes activated by HIF-1 continues to increase, and targets include genes whose protein products are involved in angiogenesis, cell proliferation and viability, vascular remodeling and vasomotor responses [81]. ROS production is implicated in the control of ventilation as well as HIF-1 was demonstrated to control the production of tyrosine hydroxylase, an enzyme which is thought to be involved in the control of ventilation by the carotid body [81, 82]. Carotid bodies are sensory organs that detect changes in arterial blood oxygen. They are composed of glomus type I chemoreceptor cells that release neurotransmitters in response to hypoxia. Exactly how hypoxia leads to this release is not entirely clear but recent experiments suggest that either cytochrome-like ROS-producing proteins sense the altered oxygen concentration or the changes in the rate of mitochondrial ROS production may play a major role in the oxygen sensing [83-85].

1.2. Downstream pathways in oxidative stress

Despite the complexity of the antioxidant systems, free radicals generated excessively in certain circumstances can break this barrier and cause oxidative stress to the cell. Reactive oxygen species injure a wide variety of biomolecules and cell compartments. ROS initiate lipid peroxidation [86], protein oxidation [87] and the formation of DNA breaks [88]. The major product of lipid peroxidation is 4-hydroxy-2-nonenal, which is highly citotoxic and can readily react with and damage proteins. In various forms of oxidative stress there are different sources of ROS. During ischemia-reperfusion, mitochondrial respiratory complexes, especially complex III, are the main sources of toxic oxygen intermediers [89]. Hydrogen peroxide- or doxorubicine-induced oxidative injury in turn has at least two components. They can cause an enhanced mitochondrial ROS production, but their reaction with transition metals (e.g. Fe^{2+}) inducing a site-specific oxyradical formation is also very important in the mediation of oxidative cell injury [90, 91]. Mitochondrial respiratory chain complexes have a central role in the development of postischemic damage. They are the main sources of ROS during reoxygenation, but themselves are also injured by ROS and reactive aldehydes, such as 4-hydroxy-2-nonenal, and they exhibit a reduced activity during oxidative stress. Due to the injury of ion channels and the decrease of high-energy phosphate levels sodium and calcium accumulate intracellularly. The high level of intracellular Ca^{2+} activates caspases (Ca^{2+} dependent aspartate-specific proteases) and it causes the conversion of xanthine dehydrogenase to xanthine oxidase [92]. High intracellular Ca^{2+} level also induces the opening of mitochondrial permeability transition pores (MPTPs). As a consequence of opening of the MPTPs, the mitochondrial membrane potential will collapse and the mitochondrial energy production will be ceased [93]. The consequences are reduced energy generation, an increased ROS production, ROS and NO-induced single-strand DNA break formation that activates the nuclear poly(ADP-ribose) polymerase (PARP) pathway and eventually cell death [94-96]. Therefore the oxidative injury finally leads to some form of cell death via various pathways. The way the injured cell dies depends largely on the severity of the insult. The two main forms of cell death are apoptosis and necrosis. Apoptosis is a well-regulated sequence of morphological events [97]. The cell first undergoes nuclear and cytoplasmic

condensation with blebbing of the plasma membrane, then breaks up into membrane-enclosed fragments, so-called apoptotic bodies, which are rapidly recognized and engulfed by macrophages or by neighbouring cells. Figure 9. summarizes the main signaling pathways that lead to apoptosis [98].

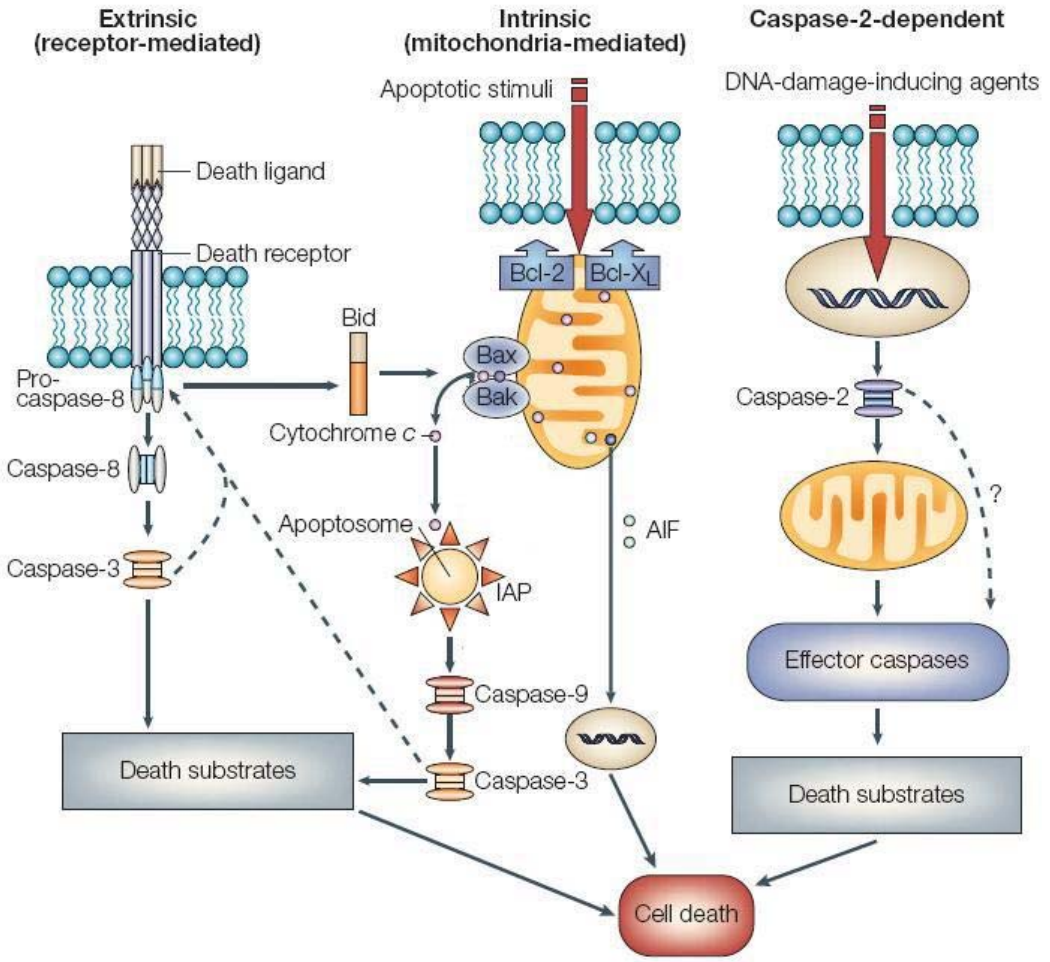

Figure 9. Ligation of death receptors results in the activation of caspase-8 and caspase-3 activation and Bid induced release of cytochrome c from the mitochondrial intermembrane space. The intrinsic, mitochondria-mediated pathway leads to the same end and cytochrome c forms the apoptosome complex with apoptosis activating factor-1 (Apaf-1) and pro-caspase-9. Bcl-2 family proteins and inhibitors of apoptosis proteins (IAPs) regulate this pathway and it also involves the translocation of the mitochondrial apoptosis inducing factor (AIF) to the nucleus, a process linked to chromatin condensation. The activation of procaspase-2 by DNA damage can lead to apoptosome formation as well. These effects lead to the cleavage of death substrates, such as PARP *(Modified after Orrenius et al., Nat Rev Mol Cell Biol, 2003. 4(7): p. 552-65.).*

The other form of cell death - necrosis - is characterized by irreversible swelling of the cytoplasm and its organelles. Loss of membrane integrity results in cell lysis and the release of noxious cellular constituents which leads to the inflammation of the surrounding tissue. Inflammatory processes contribute to the progression of oxidative injury, leading to worsening of the tissue damage. Ischemia-reperfusion increases the release of proinflammatory cytokines such as TNF-α and IL-1β [99]. TNF-α and IL-1β stimulate up-regulation of other proinflammatory (IL-6, IL-8) and anti-inflammatory cytokines (IL-4, IL-10). Proinflammatory cytokines promote expression of adhesion molecules (selectins), integrins, intercellular adhesion molecules (ICAM-1 and 2) on endothelial cells and leukocytes resulting in microvascular plugging and secondary ischemia [100].

The present thesis is focused on two aspects of the events occuring during or after oxidative stress. On one hand it investigates the role of PARP enzyme in cardiovascular diseases. On the other, it further elucidates the complex role of the new gasotransmitter H_2S in oxidative circumstances as - apart from its radical scavenging effect - H_2S was found to be involved in several other biological interactions and its role was implicated in a variety of animal disease models [101].

1.2.1. Poly(ADP-ribose) polymerase

Poly(ADP-ribose) polymerase is an abundant nuclear enzyme with complex regulatory function [102-109]. Poly(ADPribose) polymerase-1 (PARP-1, E.C. 2.4.2.30) [also known as poly(ADP-ribose) synthetase (PARS)], the major PARP isoform, is a member of the PARP enzyme family consisting of PARP-1 and many additional, recently identified poly(ADP-ribosylating) enzymes (minor PARP isoforms). Because the role of the minor PARP isoforms is poorly understood, in the present thesis PARP refers to 'PARP-1'. PARP is a DNA damage sensor and signaling molecule and binds to both single- and double stranded DNA breaks, becomes activated, forms homodimers and initiates an energy-consuming cycle by transferring ADP ribose units from NAD^+ onto nuclear acceptor proteins such as histones, transcriptional factors, DNA replication factors and signaling molecules (NFκB, p53) with PARP itself being the major acceptor (Fig. 10.).

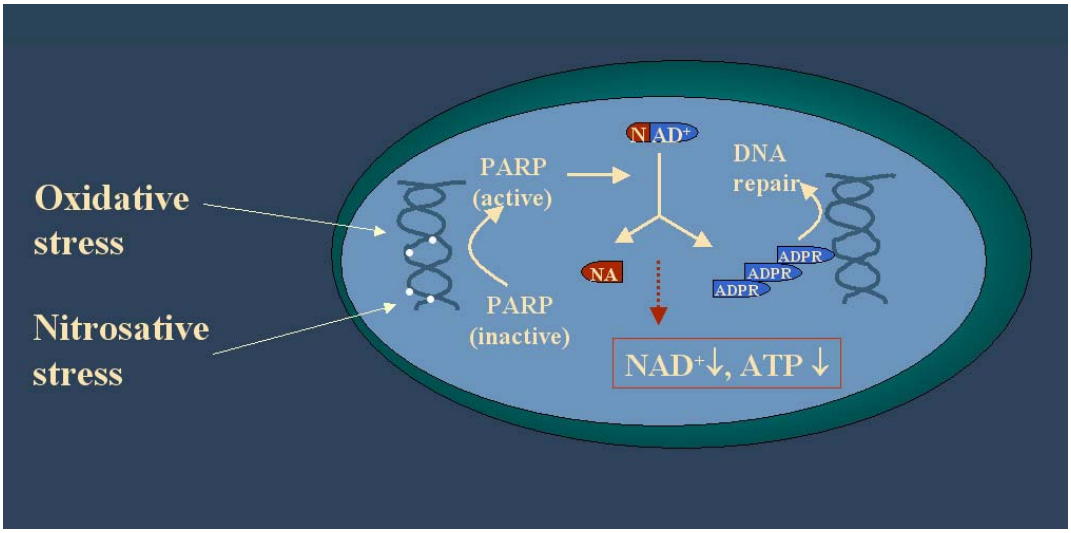

Figure 10. Activation and function of poly(ADP-ribose) polymerase (PARP).

Auto-poly(ADP-ribosyl)ation represents a major regulatory mechanism for PARP resulting in the downregulation of the enzyme activity. Poly(ADP-ribosyl)ation alters the activity of the other acceptor proteins also, due to the high negative charge of the attached ADP-ribose. In case of the histones, this process leads to electrostatic repulsion between DNA and loosening up the chromatin structure thereby making genes more accessible for gene transcription ([110-115]. The effect of PARP on the function of these proteins is carried out by non-covalent protein-protein interactions and by covalent poly(ADP-ribosylation) [109]. Poly(ADP-ribosylation) is a dynamic process as the polymer is rapidly degraded by two enzymes: poly(ADP-ribose) glycohydrolase (PARG) and ADP-ribosyl protein lyase. These enzymes are involved in the catabolism of poly(ADP-ribose) with PARG cleaving ribose-ribose bonds of both linear and branched portions of poly(ADP-ribose) and the lyase removing the protein proximal ADP-ribose monomer [108].

The biological role of PARP is complex. One of the most important functions is related to the fact that mild genotoxic noxa cause PARP activation that facilitates DNA repair and cell survival. Under pathophysiological conditions, reactive species trigger severe DNA damage, the overactivation of PARP and the activation of DNA-repair enzymes such as DNA glycosylases and DNA ligases [116, 117]. Peroxynitrite is considered a key trigger of DNA strand breakage because it can travel significant distances and

readily crosses cell membranes. When excessively activated by DNA breaks, PARP initiates an energy-consuming cycle resulting in the depletion of NAD^+ and ATP, slowing the rate of glycolysis and mitochondrial respiration, eventually leading to cellular dysfunction and necrotic cell death. Necrosis, as mentioned earlier, is the least desirable form of cell death as the cellular content is released into the tissue exposing neighbouring cells to proteases and various pro-inflammatory factors, thereby triggering positive feedback pathways of inflammatory tissue injury [109]. PARP-overactivation induced necrosis is also related to intracellular acidification [115, 118] (Fig. 11.).

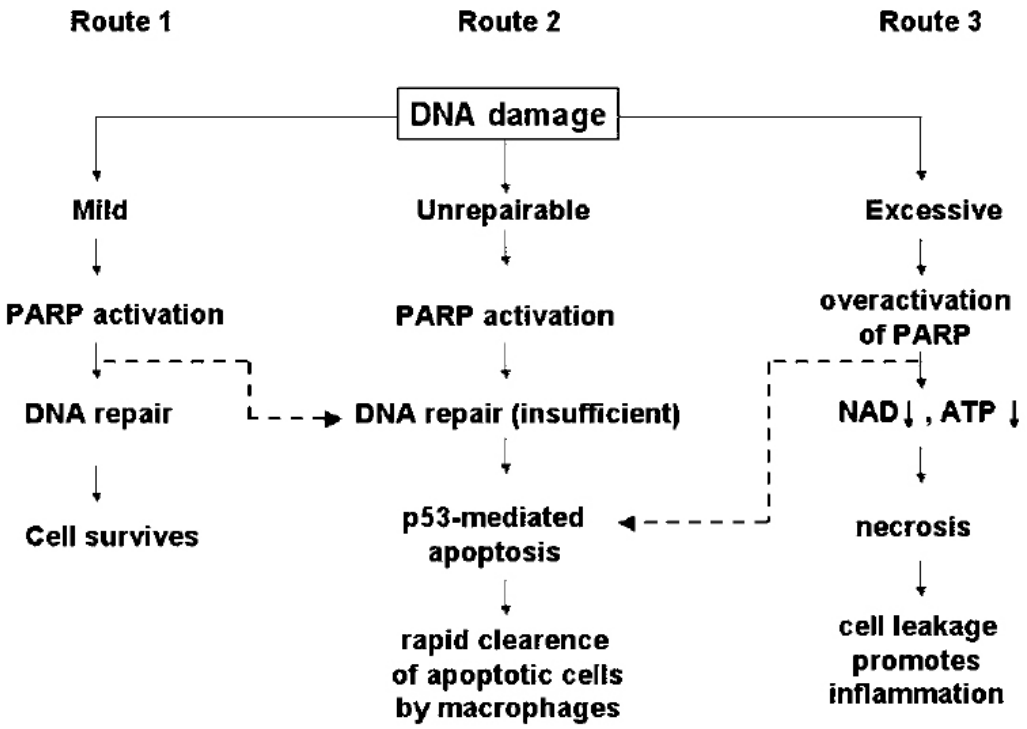

Figure 11. Depending on the intensity of the DNA-damaging stimulus, genotoxic agents can trigger three different pathways. In the case of mild DNA damage, poly(ADP-ribosylation) facilitates DNA repair and thus survival (route 1). More severe genotoxic stimuli activate the p53-dependent (or possibly independent) apoptotic pathway (route 2). The most severe DNA damage may cause excessive PARP activation, depleting cellular NAD^+/ATP stores. NAD^+/ATP depletion blocks apoptosis and results in necrosis (route 3). The inhibition of PARP in cells entering route 1 inhibits repair and thus diverts cells to route 2 (broken arrow). The inhibition of PARP in cells entering route 3 preserves cellular energy stores and thus enables apoptotic machinery to operate (broken arrow). *(Virág L. and Szabó C., Pharmacol Rev, 2002. 54(3): p. 375-429.)*

Another mechanism for PARP-mediated cell death is considered to be dependent on the linkage between the PARP pathway and class III histone deacetylases (sirtuins; e.g., SIR2α), which are NAD^+ dependent [119, 120]. Several studies have shown that SIR2α has profound roles in chromatin remodeling, gene silencing, cell viability, and longevity [121]. Because the enzymatic activity of SIR2α is absolutely dependent on NAD^+, it is suggested that the activation of PARP downregulates SIR2α through depletion of cell NAD^+ content, which then promotes cell death via activation of p53-mediated apoptosis [120, 122, 123]. PARP has been also shown to induce translocation of AIF from the mitochondria to the nucleus [124] and the cleavage of PARP is considered a hallmark of caspase-mediated apoptosis [125].

Another important function of this enzyme is the regulation of the production of inflammatory mediators such as inducible nitric oxide synthase (iNOS), intercellular adhesion molecule-1 (ICAM-1) and major histocompatibility complex class II (MHC Class II) [102, 126-128]. NFκB is a key transcription factor in this regulatory process and PARP has been shown to act as a coactivator in the NFκB-mediated transcription.

Other roles of PARP include its involvement in the regulation of replication and differentiation. It has been shown that poly(ADP-ribose) polymer can also serve as an emergency source of energy used by the base excision machinery to synthesize ATP [129]. Furthermore, poly(ADP-ribose) may also serve as a signal for protein degradation in oxidatively injured cells [130].

It must be stressed that moderate activation of PARP can be of physiological importance via enhancement of the DNA repair, but overactivation of it represents an important mechanism of tissue damage in various pathological conditions associated with oxidative and nitrosative stress, including myocardial reperfusion injury [127], heart failure [131, 132], stroke [133, 134], circulatory shock [135-140], and autoimmune β-cell destruction associated with diabetes mellitus [141, 142]. Activation of PARP and beneficial effects of various PARP inhibitors have been demonstrated in various forms of endothelial dysfunction such as the one associated with circulatory shock, hypertension, atherosclerosis, preeclampsia and aging [143-146].

1.2.2. Hydrogen sulfide

Hydrogen sulfide (H_2S) has been best known for decades as a pungent toxic gas in the contaminated environmental atmosphere, dubbed 'gas of rotten eggs' or 'swamp gas' [147]. However, H_2S has been recognized recently to have various biological effects and it is regarded as a novel gasotransmitter in the central nervous and in the circulatory systems, similar to the other gasotransmitters nitric oxide (NO) and carbon monoxide (CO). The endogenous production of H_2S was initially described in the brain [148]. It is formed endogenously by pyridoxal-5'-phosphate-dependent enzymes such as cystathionine-β-synthetase (CBS; E.C. 4.2.1.22) and cystathionine-γ-lyase (CGL; E.C. 4.4.1.1) and has a negative feedback effect on these enzymes [149] (Fig. 12.). CBS is highly expressed in the brain, but not detectable in the blood vessels, while CGL is expressed in various vessels of the vascular system [150-152]. *In situ* hybridization has shown the presence of CGL mRNA in the vascular smooth muscle, but not in the endothelial layer [150].

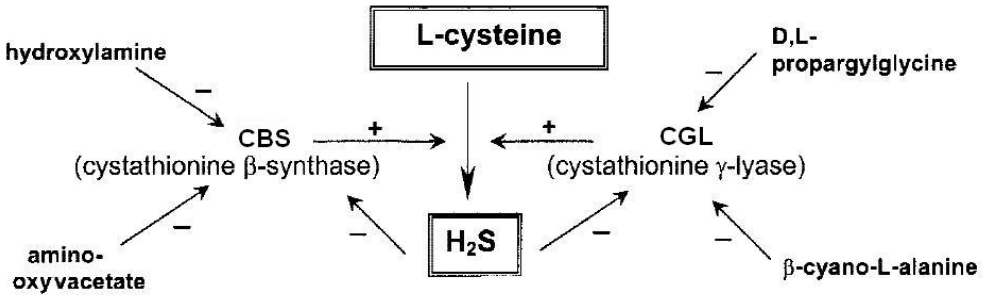

Figure 12. The formation of H_2S and the inhibitors of the involved enzymes.

As H_2S is chemically present in different forms under physiological pH *in vivo* (H_2S, HS^- or S^{2-}) and the active one is yet to be clearly determined, in the present thesis the term 'sulfide' collectively defines all these species. The physiological concentration of sulfide in blood and in tissues is in a broad range (1-160 μM) and appears to be dependent on the method used to detect it [150, 153, 154]. H_2S *in vivo* is metabolized by oxidation in mitochondria or by methylation in cytosol and can be scavenged by methemoglobin or by metallo- or disulfide-containing molecules such as oxidized

glutathione [155, 156]. Excretion of H_2S takes place mainly in the kidney as free or conjugated sulfate and as thiosulfate [155].

The effects of H_2S are multiple and there is no single sulfide receptor that is responsible for these biological actions. The effects can be classified to 3 reaction groups: chelation of metalloproteins, covalent addition to proteins and redox reactions [101] (Fig. 13.).

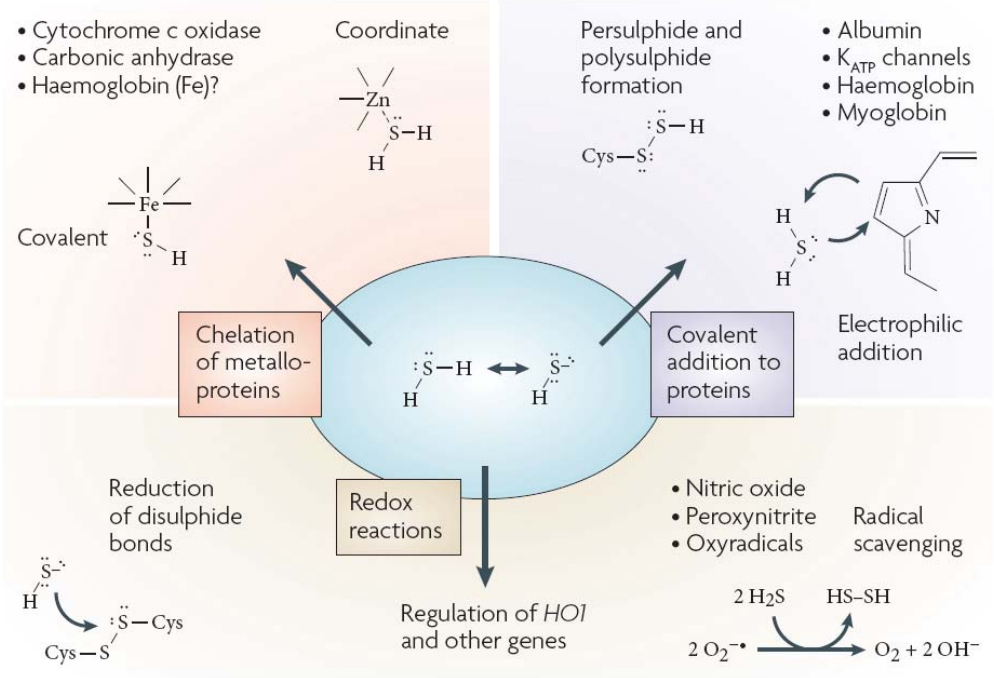

Figure 13. Effects of H_2S *(Szabó, Nat Rev Drug , 2007. 6(11): p. 917-35.)*

Carbonic anhydrase (E.C. 4.2.1.1) and cytochrome c oxidase (E.C. 1.9.3.1) are two known cellular targets in the first group [157, 158]. The physiological or pathophysiological effect of the chelation of carbonic anhydrase is unknown, but it is linked to the intrapulmonary receptors of CO_2 [159]. H_2S is also known [160] to be a potent and reversible inhibitor of cytochrome c oxidase (part of complex IV of the mitochondrial electron transport chain) and the profound nature of H_2S ability to influence whole organism metabolism was recently demonstrated by its ability to induce a suspended animation-like state in mice [161]. Sulfide can bind covalently to albumin and it can activate ATP-activated potassium (K_{ATP}) channels in the myocardium, vascular smooth muscle and cardiac myocytes [149, 150]. Finally, the redox reactions in

which H_2S participates can lead to the reduction of disulfide bonds, as well as reactions with various ROS and RNS, resulting in free-radical scavenging and anti-oxidant effects. Sulfide has also been demonstrated to regulate cellular signal transduction pathways, resulting in alterations of various genes and gene products such as interleukin-1β and and heme oxigenase 1 (HO-1) [162] [163]. By upregulating HO-1, H_2S can trigger the production of CO, another gasotransmitter with well-documented cytoprotective and anti-inflammatory effects [164], including inhibition of the NFκB pathway and the dowregulation of iNOS expression and NO production by inflammatory stimuli [165]. The exact physiological roles of these effects are still mostly obscure, but emerging evidence suggests a role as a regulator of the *N*-methyl-D-aspartate receptor and it may be central in long-term-potentiation of neuronal circuitry [151, 166]. In addition, H_2S is known to be produced in the vasculature by CGL where it is proposed to mediate smooth muscle relaxation and subsequent vasodilation independent of the GC/cGMP pathway [167-169].

Regarding pathophysiology, H_2S has been implicated in many inflammatory, neural and cardiovascular diseases [101, 170]. The beneficial effect of lowering H_2S levels was demonstrated in carrageenan-induced hindpaw edema [171], acute pancreatitis [154] and in septic shock [153]. Inhibition of H_2S synthesis accelerated the recovery of mean arterial pressure in a haemorrhagic shock model as well [172]. The possible underlying mechanism could be the effect of H_2S on K_{ATP} channels as these channels have been implicated in the pathogenesis of haemorrhagic shock associated hypotension [173]. In contrast, in many other investigations it was shown beneficial to use H_2S donors [163, 174, 175]. For instance, in a rat model of ballon-induced intimal hyperplasia NaHS (a sulfide donor) reduced restenosis and vascular inflammation and improved coronary artery reactivity [176]. The effect of H_2S to modulate cellular respiration via inhibition of mitochondrial electron transport chain has prompted many investigations using models of oxidative stress, because mitochondrial production of ROS has been implicated in various ischemia-reperfusion related diseases. Indeed, H_2S has been shown to protect against oxidative injury in in vivo and in vitro models of myocardial ischemia-reperfusion models [177, 178], but the exact mechanisms of its protective effects are still to be established.

1.3. Oxidative stress in various cardiovascular diseases

Oxidative stress has been demonstrated to play an important role in the pathogenesis of several cardiovascular diseases [120, 124-133]. The present thesis focuses on its role in atherosclerosis, ischemic heart disease and chronic heart failure.

1.3.1. Oxidative stress and atherosclerosis

The pathogenesis of atherosclerosis involves a complex and incompletely understood interaction between the critical cellular elements (endothelial cells, smooth muscle cells, platelets and leucocytes) of the atherosclerotic lesion. Vasomotor function, thrombogenicity, the state of activation of the coagulation cascade, the fibrinolytic system, smooth muscle cell migration and proliferation, and cellular inflammation are complex and interrelated biological processes that contribute to atherogenesis (Fig. 14.). Oxidative and nitrosative stress play an important role in these interactions [179, 180]. Elevated levels of oxidative DNA-damage have been shown in atherosclerotic plaques [144] and oxidative DNA damage activates the PARP enzyme which was shown to play a role in the neointima formation [181]. The inhibition of PARP was also demonstrated to improve the endothelial function of apoE deficient mice [182]. ApoE is essential for the normal catabolism of triglyceride-rich lipoprotein constituents. Low density lipoproteins (LDL) are the major vehicles transporting cholesterols in the plasma from the liver to the tissues and in patients with atherosclerosis the LDL levels are usually high and the oxidation of these particles are considered to be a major factor in their atherogenicity [183]. Elevated serum levels of oxidized LDL cholesterol overwhelm the antioxidant properties of the healthy endothelium and result in abnormal endothelial metabolism of this lipid moiety. Oxidized LDL is capable of a wide range of toxic effects and cell/vessel wall dysfunctions that are characteristically and consistently associated with the development of atherosclerosis [184]. These dysfunctions include impaired endothelium-dependent dilation and paradoxical vasoconstriction and are the results of direct inactivation of nitric oxide by the excess production of free radicals and reduced transcription of nitric oxide synthase messenger RNA (mRNA) [185]. The decrease in the availability of nitric oxide is also associated with increased platelet adhesion, increased plasminogen activator inhibitor, decreased plasminogen activator,

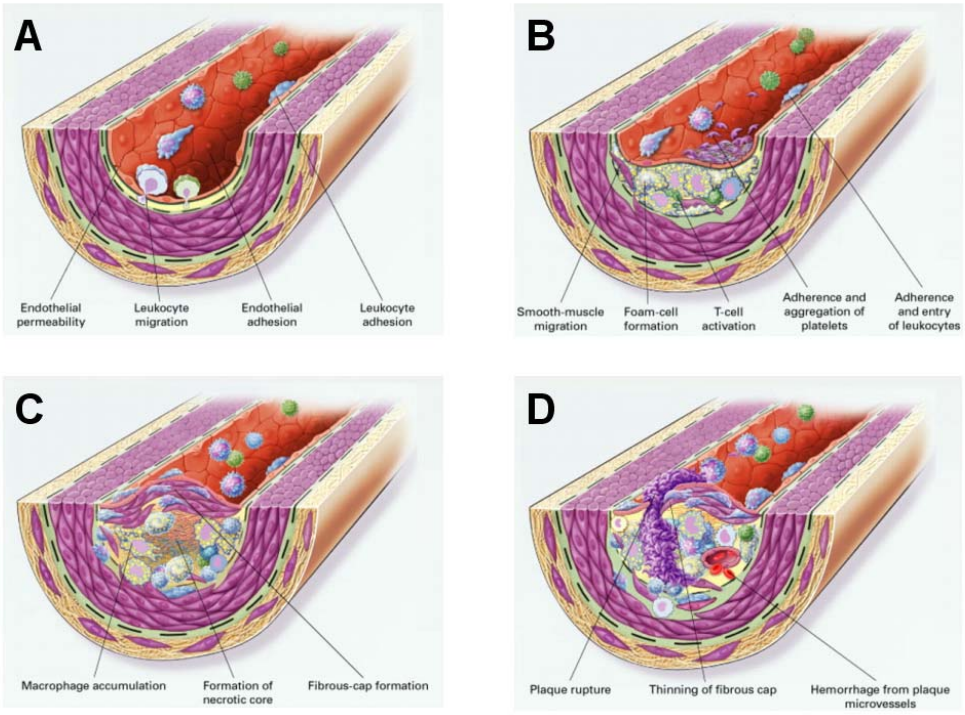

Figure 14. The pathogenesis of atherosclerosis. *(A)* The earliest pathologic stage is related to the decreased availability of NO leading to increased leukocyte adhesion and migration, impaired endothelium-dependent dilation and a procoagulant milieu. *(B)* The next step is the formation of fatty streaks which are the results of focal accumulation of serum lipoproteins, foam-cells, T lymphocytes, and smooth muscle cells in varying proportions within the intima of the vessel wall. *(C)* The fatty streak may progress to form a fibrous plaque, the result of progressive lipid accumulation and the migration and proliferation of smooth muscle cells. These smooth muscle cells are responsible for the deposition of extracellular connective tissue matrix and form a fibrous cap that overlies a core of lipid-laden foam cells, extracellular lipid, and necrotic cellular debris. *(D)* Denudation of the overlying endothelium or rupture of the fibrous cap may result in exposure of the thrombogenic contents of the core of the plaque to the circulating blood resulting in thrombus formation, partial or complete occlusion of the blood vessel, and progression of the atherosclerotic lesion. (*Ross, N Engl J Med, 1999. 340(2): p. 115-26.*)

increased tissue factor, decreased thrombomodulin levels [186]. The consequences include a procoagulant milieu and enhanced platelet thrombus formation. Furthermore, oxidized LDL activates inflammatory processes at the level of gene transcription by upregulation of NFκB, expression of adhesion molecules, and recruitment of monocytes/macrophages [187]. One of the main oxysterols in oxidized LDL (oxLDL) is 7-ketocholesterol [188]. 7-ketocholesterol (7K) was shown to inhibit arterial endothelium-dependent relaxation in rabbits aortas [189] and was reported to activate PARP in microglial cells [190]. The potential role of 7K to activate PARP in endothelial cells leading to endothelial dysfunction, therefore contributing to the early development of atherosclerosis, has not yet been established.

1.3.2. Oxidative stress and ischemic heart disease

It has been clearly established that myocardial cells cannot survive under severe prolonged ischemia. Coronary reperfusion, therefore, appears to be the only appropriate therapeutic strategy [191]. Reperfusion may prevent the development of necrosis, but experimental studies have demonstrated that it is accompanied by various characteristic disturbances, generally referred to as reperfusion injury [192]. On one hand, this injury is the consequence of the inflammatory response of the damaged tissue. On the other, it relates to the excessive production of reactive oxygen and nitrogen species. Early research led to the belief that during cardiac ischemia, oxygen content would rapidly decrease to complete anoxia, with all oxygen consumed by cytochrome oxidase. Because of the limitation of oxygen that is present during ischemia, the initial focus on oxidative damage to myocardium historically involved reperfusion. A detectable burst of ROS is generated early in reperfusion [89, 193-197]. However, during the initial progression of myocardial ischemia, oxygen remains available [198]. During simulated ischemia in cardiomyocytes, under conditions of oxygen depletion, the ROS generation actually increases [199, 200]. In the setting of low-flow ischemia, ROS production occurs continuously [196]. Even during stop flow ischemia in the isolated perfused heart, tissue oxygen remains detectable by sensitive electron paramagnetic resonance measurement at least during the initial 10 min of ischemia [198]. The production of ROS increases during global ischemia, which is consistent with the presence of oxygen during the evolution of ischemic injury [194, 201-203]. Mitochondria sustain progressive damage during ischemia and are the primary source for ROS production [204-211]. Ten to twenty minutes of ischemia decreases complex I activity [205, 210]. Damage to the phosphorylation apparatus, including complex V [210] and the adenine nucleotide transporter [204, 212], also occurs relatively early in ischemia. As ischemic periods are lengthened to 30 and 45 min, oxidative phosphorylation through complex III [213] and cytochrome oxidase decreases [208, 209, 211, 214]. Damage to the phosphorylation apparatus does not explain the decrease in state 3 respiration observed as ischemia progresses since dinitrophenol-uncoupled respiration is decreased, localizing the functionally significant site of damage to the electron transport chain (ETC) [208, 213-216]. Thus, while a complex I defect occurs early, as ischemia continues, damage progresses to involve complexes III and IV. Superoxide production

during simulated ischemia in cardiac myocytes is decreased by blockade of electron transfer [199, 200]. Complex III is emerging as the major site for the production of ROS that are detected within the cardiomyocyte during ischemia [217, 218]. Ischemia leads to release of cytochrome c from mitochondria. Cardiolipin, a component of the inner mitochondrial membrane, binds cytochrome c via nonionic [219-221] and electrostatic [222] mechanisms that localize cytochrome c at the inner membrane [222]. Cardiolipin depletion delocalizes cytochrome c from the inner membrane [222, 223], the first step in cytochrome c release from mitochondria [222]. A subsequent increase in permeability of the mitochondrial outer membrane then allows the loss of delocalized cytochrome c [222]. Outer membrane permeability increases due to disruption of the outer membrane lipid bilayer, as a result of the activation of cytosolic and perhaps mitochondrial phospholipases [224], or the insertion of proapoptotic peptides into the mitochondrial outer membrane [225]. Cytochrome c release into cytosol occurs during ischemia in isolated rat and rabbit hearts [208, 216, 226-228]. Release of cytochrome c during ischemia activates downstream caspase 3 leading to an increase in the number of cardiomyocytes displaying apoptotic markers [228] that becomes increasingly evident during reperfusion [228-231]. In the isolated perfused rabbit heart, the decrease in mitochondrial cytochrome c content occurs during ischemia, without additional decreases during reperfusion [232]. Thus injury to mitochondria during ischemia is sufficient to release cytochrome c for activation of apoptotic pathways. During reperfusion, ischemically damaged mitochondria further augment oxidative damage, calcium-driven myocyte injury, and the activation of apoptotic programs [233]. Transient blockade of mitochondria during early reperfusion, by ischemia, hypoxia, or pharmacological inhibition paradoxically decreases myocardial injury, presumably by blunting the deleterious consequences of respiration in mitochondria that suffered ischemic damage [199, 200, 234]. Thus the restriction of mitochondrial oxidative metabolism by therapeutic intervention via the modification of signaling cascades could constitute a key mechanism of cardiac protection during ischemia and reperfusion. As H_2S was shown to modulate cellular respiration via inhibition of mitochondrial electron transport chain the possible beneficial effects of sulfide has prompted many investigations using models of oxidative stress. The early results are encouraging [235, 236], but the exact mechanisms of its protective effects are still to be established.

1.3.3. Oxidative stress and cardiac heart failure

In the setting of hemodynamic overload, there are progressive changes in myocardial structure and function that are referred to as myocardial remodeling. This process is characterized by ventricular enlargement, alterations in chamber geometry and pump dysfunction [237]. At the cellular level, the changes in ventricular structure in heart failure include myocyte growth [238], loss of myocytes via apoptosis or necrosis [239] and/or myocyte slippage [240], the latter perhaps caused by degradation of fibrillar collagen struts due to the activation of matrix metalloproteases [241, 242]. Pump dysfunction may result from loss of functional myocytes and/or a shift in myocyte contractility in part due to reexpression of fetal isoforms involved in contraction (e.g. β-myosin heavy chain) [243] and/or calcium homeostasis (e.g. sarcoplasmic reticulum Ca^{2+} ATP-ase) [244]. Ultimately, progressive remodeling can result in clinical heart failure, a syndrome associated with disabling symptoms, exercise limitation and death. Increasing evidence from experimental models of heart failure supports the concept that there is increased oxidative stress in the failing heart, and that this contributes to the pathogenesis of myocardial remodeling and failure [21, 27, 28]. One of the most toxic radical is peroxynitrite ($ONOO^-$) formed in the nearly-instantenous reaction of nitric oxide with superoxide anion [245]. $ONOO^-$ can participate in multiple oxidative chemistries, and has a high affinity to nitrate tyrosine residues relative to other biological oxidants, resulting in posttranslational modification of protein-bound tyrosine to 3-nitrotyrosine (3-NT) [246]. Protein nitration is a important phenomenon in cardiovascular disease and the extent of protein nitration is statistically correlated to the extent of cardiac dysfunction in vivo [247, 248]. Although protein nitration is known to mediate some toxic effects of $ONOO^-$ in vitro, including enzyme inhibition, the putative cellular targets of $ONOO^-$ in vivo are just beginning the to be investigated [249]. One established site of action is DNA as $ONOO^-$ leads to single-stranded DNA breaks, which in turn (over)activates PARP enyzme and eventually leads to apoptotic or necrotic cell death.

Myocardial cell death and cardiac muscle gene dysregulation associated with heart failure have long been documented [250-254]. However, the mechanism of cell death remains highly disputed [251, 253, 255] and conflicting data exist concerning the influence of caspases. Whereas some investigators have failed to detect activation of

caspases or a beneficial effect of caspase inhibitors in endangered myocardium, others have found positive results [251, 256]. During early stages of cardiac hypertrophy (or physiological hypertrophy), no activation of caspases has been reported; however, apoptosis has been seen accompanying the adaptive phase of pressure overload hypertrophy [257, 258]. Some studies have shown that during sustained pressure overload, caspase activation peaks only during hypertrophy of the myocardium; thereafter it declines in failing hearts [259]. It is therefore likely that caspase activation is an epiphenomenon occurring at a particular stage of hypertrophy, possibly during transition to heart failure. The time window between activation of caspases and their downstream effects, including PARP cleavage and finally DNA fragmentation, also may be very narrow. As a result, conflicting results could have been seen, depending on the severity of the disease and the time point when tissue was taken for the analysis. It has been demonstrated that the number of necrotic cells is 7-fold greater than the number of apoptotic cells in patients with cardiac failure [252]. This is in agreement with other reports showing failing heart myocytes to be negative for active caspase 3 but positive for DNA damage markers, including PARP-activation [254, 260-262]. As it was discussed earlier, once activated, PARP induces protein poly-ADP-ribosylation by utilizing cellular NAD^+ content leading to apoptosis or cell necrosis depending on the severity of the stimulus [125, 263]. A role of inflammatory cytokines and NFκB in the induction of pathological hypertrophy is well established [264]. Recent reports indicate that PARP, together with other cofactors, regulates the transcriptional activity of cytokines and NFκB; thus PARP could initiate the process of pathological hypertrophy via changing the activity of these intermediary factors [265]. Although several studies are investigating PARP-mediated myocyte cell death the precise mechanism is yet to be established.

2. OBJECTIVES

The main objective of the present thesis was to further elucidate the role of PARP and H_2S in models of cardiovascular diseases involving oxidative stress. The specific aims were as follows:

1. To clarify the potential effects of the main oxysterol 7-ketocholesterol on the activity of endothelial poly(ADP-ribose) polymerase and on endothelium-dependent relaxant function.

2. To investigate the role of PARP in the process of cardiac remodeling and heart failure in a mouse model of heart failure induced by transverse aortic constriction.

3. To determine whether H_2S has a potential to ameliorate myocardial ischemia-reperfusion injury in vivo and to explore what could be the possible underlying mechanism of action.

3. MATERIALS AND METHODS

3.1. Animals

In the study to elucidate the role of oxysterols in PARP activation male BALB/c mice 8 wk of age were used (Charles River Laboratories, Inc). To investigate the role of PARP in the process of cardiac remodeling and heart failure male C57BL/6 mice were purchased from Charles River Laboratories, Inc. (Wilmington, MA). $PARP^{-/-}$ and wild-type $PARP^{+/+}$ mice were derived from Dr. Z. Q. Wang's laboratory [266]. In the third study regarding H_2S male C57BL6/J mice 8 wk of age were purchased from the Jackson Laboratory (Bar Harbor, ME). αMHC-CGL-Tg mice were developed and bred in-house at Albert Einstein College of Medicine (AECOM). The animals were exposed to a cycle of 12-h light/12-h dark and had free access to water and food. An acclimatization period of at least 1 week was provided before initiating the experimental protocols. All investigations conformed to the Guide for the Care and Use of Laboratory Animals published by the National Institutes of Health and was performed with the approval of the local Animal Care and Use Committee.

3.2. Experimental protocols

3.2.1. Experiments on the role of 7-ketocholesterol

To elucidate the effects of the main oxysterol 7-ketocholesterol on the activity of endothelial poly(ADP-ribose) polymerase and on endothelium-dependent relaxant function in vitro and in vivo experiments were both used. HUVEC cells were used to assess PARP activation after 7K exposure (2-20 μg/ml). BALB/c mice were treated for 1 week with 7-ketocholesterol or vehicle applied subcutaneously at a daily dose of 10 mg/kg. In a separate set of experiments vascular rings were incubated with 7K (90 μg/ml) or vehicle for 2 hours, followed by the determination of endothelium-dependent vascular function. In both set of experiments subgroups pretreated subcutaneously with 1g/kg buthionine sulphoximine (BSO, Sigma)/24h for the inhibition of γ-glutamylcysteine synthetase, thus lowering antioxidant capacity [267] were also used.

Aortic rings from these animals were used in isometric force functional studies and in PAR immunohistochemistry.

3.2.2. Experiments on the role of PARP in cardiac remodeling and heart failure

To investigate the role of PARP in the process of cardiac remodeling and heart failure transverse aortic constriction (TAC) was performed acording to Rockman's method [268]. Briefly, male mice were anesthetized with a mixture of ketamine (65 mg/kg) and xylazine (5 mg/kg). The chest and neck were shaved, and mice were placed in a supine position under body temperature control, and a midline cervical incision was made to expose the trachea. Mice were orally intubated with 20-gauge tubing and ventilated with a tidal volume of 0.2 ml at a rate of 110 strokes/min using a rodent respirator (model 683; Harvard Apparatus Inc., Holliston, MA). The chest was opened at the second intercostal space. The transverse aortic arch was ligated between the innominate artery and left common carotid artery with a 27-gauge needle using 7-0 silk suture with the aid of dissecting microscope, and then the needle was promptly removed to yield a constriction of 0.4 mm in diameter. The chest was closed in layers. The mice were kept on a heating pad until recovery from anesthesia. For the sham operation, the aorta was not ligated. Mice were studied at 9 weeks (pharmacological inhibitor studies) or 29 weeks (wild-type versus PARP-1 knockout mice) after TAC. The former group received either the isoindolinone-based PARP inhibitor INO-1001 [269, 270] (30 mg/kg/day) or vehicle orally (via drinking water) after surgical operation and continuosly afterwards for 9 weeks. The drug solution was changed every 2 days. At the conclusion of the studies, mice were sacrificed by an overdose of ketamine/xylazine mixture. Before the heart was isolated, the chest was opened to determine whether pleural effusion was present. The heart, lung, and liver were removed and their weights were measured. Organ weights were normalized to body weight. In addition, in a separate set of studies C57BL/6 mice treated with INO-1001 and undergoing aortic banding were sacrificed at 1 and 9 weeks, plasma samples and myocardial tissues were obtained and concentration of INO-1001 was measured by high-performance liquid chromatography (n = 5 animals/group). In mice that died spontaneously, organs were also removed at autopsy. In these mice, the deaths were ascribed to heart failure, if pleural effusion had occurred, and then increased lung weight to body weight was confirmed. The effect of

hemodynamic loading conditions were examined with cardiac function measurements at 9 weeks after banding. Further experiments on the excised hearts included collagen staining, PAR and AIF immunohistochemistry and western blot studies. The PARP inhibiting effects of INO-1001 were tested on isolated cardiomyocytes.

3.2.3. Experiments on the role of H_2S in myocardial ischemia-reperfusion injury

In order to investigate the possible effects of H_2S in myocardial ischemia-reperfusion (MI-R) multiple approaches were taken: (1) in vivo model of myocardial ischemia-reperfusion using wild type and transgenic mice and further experiments on in situ and excised hearts; (2) in vitro studies using cardiomyocyte derived mitochondria; (3) in vitro studies using cardiomyocytes. In the first model mice were anesthetized via an intraperitoneal (ip) injection of sodium pentobarbital (50 mg/kg) and ketamine (60 mg/kg). Additionally, mice were given sodium heparin (200 units/kg) prior to surgery to prevent clot formation and allow for consistent and complete reperfusion post-ligation. The mice were then placed in a supine position with paws taped to the operating table. Animals were intubated with an endotracheal tube (PE-60) and ventilated with 100% oxygen (0.5 liter/min) by a rodent ventilator, Minivent (HugoSachs, Model 845) at a rate of 110 strokes/minute, 230 µl tidal volume. Effective ventilation was visually confirmed by vapor condensation in the endotracheal tube and rhythmic rising of the chest. Mice were maintained at a constant temperature of 37°C monitored via a rectal probe connected to a Digisense K-Type digital thermometer. The mice were then depilated using Nair hair removal lotion and the exposed regions were wiped with alcohol and Betadine solution. A midline incision was made along the sternum exposing the ribcage. Next, a thoracotomy was performed just to the left of the midline utilizing a thermal cautery unit (Geiger). The second and third ribs were cauterized creating a small vertical opening approximately 1 cm in size. The left coronary artery (LCA) was then visually identified with the aid of an Olympus SZ61 stereomicroscope with a Schott ACE1 fiber optic light source. The LCA was ligated with a 7-0 silk suture passed with a tapered BV-1 needle in close approximation just under the coronary artery. A small piece of PE-10 tubing was then placed inline with the LCA and the 7-0 suture was tightly tied compressing the LCA and rendering the left ventricle ischemic. Ischemia was visually confirmed by cyanosis of the affected left ventricle. During the ischemic

period the incision was covered with parafilm creating an effective barrier against desiccation and dehydration. After 30 or 45 min of ischemia the LCA was allowed to reperfuse by the removal of the 7-0 suture and the sternum and skin was closed separately with 5-0 BIOSYN glycomer monofilament suture. Animal recovery was supplemented by 100% oxygen and butorphanol (0.3 mg/kg) analgesia as well as a single dose of the antibiotic cefazolin (80 mg/kg) to prevent infection. In the surgical recovery area, a heat lamp was utilized to maintain the appropriate body temperature of the mice. In addition, food and water were made available immediately and for the remainder of the first 24 hours of recovery. Further experiments on the excised hearts included H&E staining, Evan's Blue and TTC staining, MPO assay, IL1β, TNF-α, IL-10 ELISAs, transmission electron microscopy, TUNEL assay, immunohistochemistry and western blot studies. Isolated cardiac mitochondria were evaluated for mitochondrial respiration in an in vitro hypoxia assay, and isolated cardiomyocytes were used to measure caspase-3 activation.

3.3. Functional and structural studies

3.3.1. Measurement of isometric force in aortic rings of mice

The method to determine endothelium-dependent vascular relaxation in thoracic aortic rings from mice was done according to Pacher's method [271]. Briefly, the thoracic aorta was cleared from periadventitial fat and cut into rings 3mm wide using operation microscope, mounted in organ baths filled with warmed (37 ˚C) and oxygenated (95% O_2, 5% CO_2) Krebs' solution ($CaCl_2$ 1.5 mM; $MgSO_4$ 1.2 mM; NaCl 118 mM; $NaHCO_3$ 14.8 mM; KCl 4.6 mM; NaH_2PO_4 1.2 mM; Glucose 11.1 mM). Isometric tension was measured with isometric force transducers (HBM, Q11), which was connected to a transducer–amplifier (HBM, MGA II) and recorded on paper (Kipp Zonen, BD300). A tension of 1 gram was applied and the rings were equilibrated for 60 minutes. Fresh Krebs was provided at 20 min intervals. After equilibration the contractile response of arterial rings to a depolarizing solution of a modified Krebs solution enriched in K^+ (124 mM) was first tested to evaluate their functional integrity. For the measurement of endothelial functionality rings were precontracted with phenylephrine (10^{-6} M) and then

dose–response curves to acetylcholine (10^{-8} M - 10^{-5} M) were constructed. Experiments were conducted on 20 rings in each experimental group.

3.3.2. Measurement of cardiac function

To measure arterial pressure, 2 high-fidelity catheter tip transducers (1.4F; Millar Instruments Inc., Houston, TX) were used. One was inserted into the right carotid artery and advanced to the left ventricle for measurement of left ventricular (LV) pressure and LV dP/dt. After measurement of LV function, the transducer was pulled back to carotid artery and another transducer was inserted into the left carotid artery. The pressure in both carotid arteries was measured simultaneously and the pressure gradient between carotid arteries was calculated.

3.3.3. Collagen staining

For collagen staining, fixed blocks of ventricular tissue were embedded in paraffin, and 5-μm-thick sections were cut from each block. The section was deparaffinized, rehydrated, and stained with Masson's trichrome using a staining kit (HT15; Sigma-Aldrich, St. Louis, MO).

3.3.4. Echocardiograhic assessment of left-ventricular structure and function

Mice were lightly anesthetized to effect with isoflurane in 100% O_2 and secured to the Visualsonics Rail System III mouse handling table with paws taped to electrode leads for the continuous monitoring of ECG and respiration rate. A rectal thermometer was inserted to maintain core body temperature at 37ºC via digital adjustment of the heated platform. Wetting drops were applied to the eyes, hair was removed using depilatory cream and ultrasonic gel was applied to the chest wall for transducer interface. Transthoracic high-resolution echocardiography of the LV utilizing a 30-MHz RMV scanhead interfaced with a Vevo 770 (Visualsonics, Toronto, Canada) was performed 1 week prior to myocardial infarction. Parasternal-long-axis (PLA) B-mode images were acquired (1000 frames/sec) for a period of 7 min. These images then underwent EKV (ECG-based Kilohertz Visualization) reconstruction yielding a 1000 Hz EKV loop spanning one complete heart cycle. Additionally ECG, body temperature and respiratory rate data were acquired throughout the procedure. Off-line measurements

and calculations were made on a Dell Precision 380 computer running VS V2.2.3 software for the accurate assessment of LV structure and function. Seventy-two hours post myocardial infarction mice again underwent high-resolution echocardiography just prior to the assessment of infarct size.

3.3.5. Assessment of infarct size

Infarct size was determined after 24 or 72 hr of reperfusion. Evan's blue dye (1 ml of a 5% solution) was injected into the carotid artery catheter to delineate the ischemic zone from the nonischemic zone. The heart was rapidly excised and cross-sectioned into 1mm thick sections, which were then incubated in 1.0% 2,3,5-triphenyltetrazolium chloride (TTC) to demarcate the viable and nonviable myocardium within the risk zone. Images of each side of every 1mm heart section were acquired and weighed. The areas of infarction, risk, and nonischemic LV were assessed by a blinded technician using computer-assisted planimetry (NIH Image 1.57).

3.3.6. Blood pressure and heart rate measurements

To check if H_2S alters the hemodynamics of mice aortic blood pressures (systolic, diastolic and mean) and heart rate were measured in the conscious state using radiotelemetry techniques. Mice were surgically implanted with the PA-C10 radiotelemeter pressure transducers (DSI, St. Paul, MN) and the catheters were placed in the aorta. Mice were anesthetized with ketamine (50 mg/kg, ip) and xylazine (8 mg/kg, ip) and the skin on the ventral surface was treated with chemical hair remover. The skin was then washed, wiped clean with topical antiseptic and then wiped with alcohol. An incision was made from the chin to the superior sternum. The right carotid artery was surgically exposed from the bifurcation of internal and external carotid toward the heart. About 1 cm of the common carotid artery was isolated and ligated at the bifurcation using 4-0 silk suture and an additional tie was placed midway on the vessel for securing the catheter and hemostasis. Distal and proximal traction was used to stabilize the vessel. A small incision was made in the artery adjacent to the bifurcation and the catheter was placed in the artery and advanced 1.2 cm so that the tip of the catheter was in the aorta. A pulsing radio signal was used to confirm a functional implant by a distinctive high-frequency oscillating tone on a portable AM radio set at

500 kHz. The catheter was then firmly tied in place and the radiotelemeter was secured in place under the skin of the right flank with tissue adhesive. All skin wounds were closed with interrupted 6-0 silk sutures. The mice were treated with antibiotic (cefazolin, GlaxoSmithKline, 80 mg/kg, sc) and also received buprenorphine (Buprenex, 0.3 mg/kg) for analgesia. Mice were placed in a warm recovery area supplemented with 100% oxygen and allowed to recover. At 7 days following implantation hemodynamic measurements were conducted using DSI Open Art interfaced with IOX software (EMKA Technologies, Church Falls, VA). Mice were lightly anesthetized with isoflourane and the femoral vein exposed for injection of various concentrations (0-1 mg/kg) of the H_2S donor. Data were recorded every second over the entire time of the experiment.

3.3.7. Mitochondrial respiratory rate

Cardiac mitochondria were isolated from C57BL6/J mice 8 wk of age from the following groups: control, sham operated, vehicle-treated, or mice that received 50 μg/kg H_2S donor after 45 min ischemia and 24 h reperfusion. Briefly, the heart was quickly excised and washed in buffer containing 250 mM sucrose, 10 mM Tris, 1 mM EGTA, pH 7.4 at 4°C. After changes of buffer, the cardiac samples were cut into small pieces and homogenized. The samples were centrifuged at 3000 g for 3 min to remove debris, and mitochondria were obtained by a differential centrifugation technique [272]. All isolated mitochondria were kept on ice and used within 3 hr of isolation. Oxygen consumption of cardiac mitochondria was measured in a multichannel sealed chamber magnetically stirred at 37˚C using calibrated Clark-type electrodes connected to an Instech amplifier and data recorded on a Dell Precision PC running Windaq software, adapted from Shiva et al. [272]. Isolated mitochondria (1 mg/ml) were incubated in respiration buffer composed of 120 mM KCl, 3 mM HEPES, 1 mM EGTA, 25 mM sucrose, 5 mM $MgCl_2$, 5 mM KH_2PO_4, pH 7.4. Complex I respiration was initiated by the addition of 5 mM pyruvate plus 2.5 mM malate to the respiration buffer prior to the mitochondria followed by the addition of 1 mM ADP. To measure oxygen consumption mediated by complex II, 8 mM succinate plus 4 mM glycerol-3-phosphate plus 5 μM rotenone was added to the respiration buffer prior to the addition of mitochondria followed by the addition of 1 mM ADP. In the in vitro mitochondria hypoxia assay state

3 respiration was initiated and the mitochondria were allowed to consume all oxygen until the chamber became anoxic. The mitochondria were left anoxic for 30 min in the sealed chamber. To reoxygenate, mitochondria were centrifuged and resuspended in oxygenated buffer containing fresh substrate and ADP for reestablishment of state 3 respiration. Post anoxic respiratory rate was expressed as a percentage of preanoxic rate and is referred to as recovery of mitochondrial respiration.

3.4. Immunohistochemistry

Immunohistochemistry was used in 7K studies (PAR) and in experiments involving transverse aortic constriction (PAR& AIF). Tissues were fixed in 4% buffered formalin and paraffin sections were prepared. Sections were treated with 0.6% H_2O_2 in methanol to quench endogenous peroxidase activity and microwaved in 0.2 M citrate buffer (pH 3.0) to retrieve antigenic epitopes. After blocking in 1.5% normal goat serum, a polyclonal anti-PAR antibody (Calbiochem, San Diego, CA, USA) was applied at 1:100 dilution. A biotinylated secondary antibody and the ABC method were used to visualize PAR polymers with 3, 3'-diaminobenzidine-tetrahydrochloride (DAB) + nickel sulphate and H_2O_2 as substrate (Vector, Laboratories, Burlingame, CA, USA). Slides were counterstained with Gill's hematoxyline (Accustain, Sigma Diagnostics, St. Louis, MO, USA). A similar approach was used with AIF staining using rabbit polyclonal anti-AIF antibody (Chemicon International, Temecula, CA).

3.5. Measurements on cells

3.5.1. Measurements of PARP activation in HUVEC cells

Human umbilical vein endothelial (HUVEC) cells were plated at a density of 250 000 cells per well in a 12-well plate and grown in M199 media supplemented with 10% fetal calf serum and 0.03 mg/mL endothelial cell growth supplement. After 24 h, the media was replaced and the cells were treated with increasing concentrations of 7K (2, 4, 8, 16 μg/ml) for 24h with or without buthionine-sulphoximine (BSO, 1mM). In subsequent experiments HUVEC cells were treated with H_2O_2 (positive control) or with 20μg/mL 7K with or without pretreatment with the PARP inhibitor PJ-34 (3μM, 1h) or the nitric

oxide synthase (NOS) inhibitor, *N*-nitro-L-arginine methyl ester (L-NAME, 3mM, 1h, Sigma). For the measurement of cellular PARP activity (12,13), the media was removed and replaced with 0.5 mL N-2-hydroxyethylpiperazine- N'-2'-ethanesulfonic acid (pH 7.5) containing 0.01% digitonin and 3H-NAD^+ (0.5 μCi/mL), and the cells were incubated for 20 min at 37°C. The cells were then scraped from the wells and placed in Eppendorf tubes containing 200 μL ice-cold 50% trichloroacetic acid (TCA) (w/v). The tubes were then placed at 4°C. After 4 h, the tubes were centrifuged at 1800*g* for 10 min and the supernatant removed. The pellet was washed twice with 500 μL ice-cold 5% TCA. The pellet was solubilized in 250 μL NaOH (0.1 M) containing 2% sodium dodecyl sulfate overnight at 37°C. The PARP activity was then determined by measuring the radioactivity incorporated using a Wallac scintillation counter (Wallac, Turku, Finland) [273]. The solubilized protein (250 μL) was mixed with 5 mL scintillant (ScintiSafe Plus, Fisher, Pittsburgh, PA, USA) before being counted for 10 min. Results are expressed as a percentage of the PARP activity observed in untreated cells. Cell viability was measured by the 3-[4, 5-dimethylthiazol-2-yl]-2, 5-diphenyltetrazolium bromide assay and was unaffected by the pharmacological inhibitors used.

3.5.2. In vitro myocyte isolation and PARP inhibition studies

Isolation of ventricular myocytes from mice was conducted according to Chen's method [274]. Hearts were excised and mounted in a Langendorff perfusion apparatus and perfused for ~5 min with Ca^{2+}-free Krebs-Henseleit bicarbonate (KHB) buffer containing 120 mM NaCl, 5.4 mM KCl, 1.2 mM $MgSO_4$, 1.2 mM NaH_2PO_4, 5.6 mM glucose, 20 mM $NaHCO_3$, 10 mM 2,3-butanedione monoxime (Sigma-Aldrich), and 5 mM taurine (Sigma-Aldrich), gassed with 95% O_2, 5% CO_2, followed by a 15 to 20 min perfusion with same KHB buffer containing 25 μM $CaCl_2$ and 0.1% collagenase (Worthington Biochemicals, Freehold, NJ) and 0.1% BSA. Thereafter, ventricular tissue was chopped and incubated for 10 min in the same medium supplemented with 1% BSA. The ventricular tissue was then dispersed and filtered. The resultant myocytes were washed twice with fresh KHB buffer containing 1% BSA and 25 μM $CaCl_2$, and then the Ca^{2+} concentration was increased to 1.0 mM gradually. Finally, the myocyte pellets were washed and suspended in MEM medium containing 1.2 mM Ca^{2+} (M1080'

Sigma-Aldrich). Myocytes were plated in laminin-precoated plates or glass coverslips at a density of 10^5 cells/cm^2. After 1h plating in MEM medium with 5% fetal calf serum, the medium was changed to fetal bovine serum free MEM. After overnight culture, myocytes were subjected to H_2O_2 treatment at 200 μM in the presence or absence of various concentrations of INO-1001. Activation of PARP was measured by incorporation of radiolabeled NAD^+ as described previously.

3.5.3. Caspase-3 activity in cardiomyocytes

Adult cardiomyocytes were isolated as previously stated and were randomly divided into three groups. Hypoxia-reoxygenation (HR) was initiated by 6 hr of hypoxia (95% N_2, 5% CO_2) and followed by 12 hr reoxygenation (5% CO_2). Myocytes were dosed with either vehicle or the H_2S donor (100μM) at the time of reoxygenation. Caspase-3 activity was determined by AC-DEVD-AFC fluorescence (BIOMOL Int) and read on a microplate fluorescence plate reader (400nm and 508nm). Activity was calculated as pmol/min/mg protein.

3.6. Western blot analysis

To examine the presence of AIF in different cell fractions fresh ventricles were cut into small pieces in ice-cold MSE buffer (225 mM mannitol, 75 mM sucrose, 1.0 mM EGTA, and 20 mM HEPES (KOH), pH 7.4). The samples were then resuspended in 3 volumes of MSE buffer supplemented with 1 mM dithiothreitol and protease inhibitors (200x cocktail solution; Sigma). Subcellular fractions were prepared as described previously, followed by Western blotting for AIF [229, 275]. The heart was further homogenized for 5s at power 3 output by a Polytron homogenizer (PT1200 C; Kinematica, Basel, Switzerland). The homogenates were filtered through a 50-mesh screen to remove unbroken tissue and then centrifuged at 600g at 4°C for 10 min. The supernatant was centrifuged for 10 min at 8000g. The pellet obtained was used as mitochondrial fraction and was washed twice and resuspended in MSE buffer. The 8000g supernatant was recentrifuged at 15 000g at 4°C for 20 min, and the resulting supernatant was used as soluble cytosolic fraction. To obtain nuclear extracts, the 600g nuclear pellet was washed twice with TMS buffer (240 mmol/l sucrose, 10 mmol/l Tris,

pH 7.4, and 1.5 mmol/l $MgCl_2$) and incubated with 0.1% of Triton X-100 in TMS buffer for 15 min on ice. The nuclei were pelleted by centrifugation at 600g for 10 min and washed three times with 5 ml of TMS buffer without Triton X-100. The final pellet of nuclei was resuspended 1/1 (v/v) in extract buffer (400 mmol/l NaCl, 20 mmol/l Tris, pH 7.5, 1.5 mmol/l MgCl2, 1 mmol/l dithiothreitol, and 25% glycerol), and incubated at 4°C with gentle shaking for 1 h. The nuclei were pelleted again at 600g for 10 min, and the resulted supernatant was further centrifuged at 15 000g for 20 min to obtain nuclear extract. Samples containing 30μg of protein were subjected to electrophoresis on polyacrylamide gels (Invitrogen, Carlsbad, CA) and then transferred to nitrocellulose membrane. After blocking in 3% nonfat milk and 0.05% Tween 20 in phosphate-buffered saline, blots were incubated with antibody to AIF (murine polyclonal; Chemicon International).

A slightly different method was used for the analysis of myocardial CGL protein in the transgenic mice. Myocardial tissue lysates were centrifuged to remove any particulate, and protein concentration of the cleared lysate was measured using the BioRad Dc protein assay. Equal amounts of protein (20 μg) were loaded into each lane and separated on a 8% polyacrilamide gel. Protein was transferred to polyvinylidene fluoride membrane overnight at 30 V and then blocked in 5% milk in TRIS-buffered saline tween-20 (TBST) at room temperature for 3 hr. Membranes were washed three times with TBST and then incubated with anti-CGL (1:3000), in 5% BSA TBST overnight at 4°C. Membranes were then washed three times with TBST and then incubated with HRP-linked anti-mouse secondary (Amersham) at 1:2000 in 5% BSA TBST at room temperature for 3 hr. Membranes were then washed three times with TBST, incubated with enhanced chemiluminescence (ECL) reagents (Amersham), and then exposed to film. Membranes used to detect CGL were then stripped and incubated with mouse anti-α-tubulin (as a loading control) at 1:5000 in 5% BSA TBST at 4°C overnight. Membranes were then washed and incubated with HRP linked anti-mouse secondary at 1:2000 in 5% BSA TBST at room temperature for 3 hr, washed and incubated with ECL reagents, and then exposed to film. Densitometric analysis was performed using Quantity One software (Bio-Rad).

3.7. Additional methods on elucidating the role of H_2S in MI-R

3.7.1. Cardiac troponin-I assay

Mice were completely exsanguinated after 45 min of LCA ischemia and 4 hr reperfusion. This time point was chosen after preliminary studies that revealed 4 hr to be the time point for peak cardiac enzyme levels in the circulating plasma. Serum levels of the cardiac-specific isoform of troponin-I were assessed using an ELISA from Life Diagnostics (West Chester, PA).

3.7.2. Myocardial histology

After 45 min of ischemia and 24 hr reperfusion hearts were rapidly excised, cross-sectioned and fixed in 10% buffered formalin. Fixed tissue was then paraffin embedded and sectioned in a standard fashion and stained with H&E. Slides were then assessed in a blinded fashion by a pathologist and scored for the following: percentage of LV involvement, myodegeneration, cardiomyocyte hydropic changes, neutrophilic infiltrate, hemorrhage, lymphohistiocytic infiltrate and acute myocardial necrosis.

3.7.3. Quantitative assessment of neutrophil accumulation

Whole heart lysates from mice subjected to 45 min of ischemia and 4 hr reperfusion were assessed for myeloperoxidase (MPO) activity as a marker of neutrophil accumulation. Cardiac tissues were homogenized in a solution containing 0.5% hexadecyltrimethylammonium bromide dissolved in 10 mmol/liter potassium phosphate buffer (pH 7) and centrifuged for 30 min at 20 000 g at 4°C. An aliquot of the supernatant was allowed to react with a solution of tetramethylbenzidine (1.6 mmol/liter) and 0.1 mmol/liter H_2O_2. The rate of change in absorbance was measured by spectrophotometry at 650 nm. Myeloperoxidase activity was defined as the quantity of enzyme degrading 1 mmol of hydrogen peroxide per minute at 37°C and expressed in milliunits per milligram protein. For the measurements of IL-1β, TNF-α and IL-10 ELISA kits were used according to the manufacturer's instructions (R&D Systems, Inc., Minneapolis, MN, USA).

3.7.4. Intravital microscopy

Postcapillary venules (20μm to 40μm diameter) were observed under fluorescence microscopy according to Ouedraogo's method [276].

3.7.5. Transmission electron microscopy

After 45 min of ischemia and 24 h reperfusion, hearts were rapidly excised and fixed with 2% paraformaldehyde and 2.5% glutaraldehyde in 0.1M sodium cacodylate buffer, postfixed with 1% osmium tetroxide followed by 1% uranyl acetate, dehydrated through a graded series of ethanol and embedded in LX112 resin (LADD Research Industries). Ultrathin (80nm) sections were cut on a Reichert Ultracut UCT, stained with uranyl acetate followed by lead citrate, and viewed on a JEOL 1200EX transmission electron microscope at 80 kV.

3.7.6. TUNEL assay

TUNEL assay was conducted by using a kit according to the manufacturer's instructions (ApopTag HRP kit, DBA). The number of TUNEL-positive nuclei/high-power field was counted in a minimum of 20 fields for each section (n = 6/group).

3.7.7. Polarographic assessment of H_2S production

The polarographic technique for assessment of H_2S production in tissue homogenates was conducted according to Koenitzer's method [277]. Briefly, mouse hearts were rapidly flushed with PBS (pH 7.3 at 37°C) containing protease inhibitors and 50μM diethylenetriaminepentaacetic acid (DTPA) to chelate trace metals that catalyze H_2S oxidation and homogenized using a glass dounce. H_2S concentration in the vessel organ bath was recorded with a polarographic H_2S sensor (PHSS) connected to a multichannel analyzer (Apollo 4000, WPI, Sarasota, FL). In all experiments, the PHSS was calibrated prior to and after the experiment by adding Na_2S stock standard to check calibration. H_2S production rates were determined after the addition of substrate and cofactor at the initial steepest slopes of each trace.

3.8. Chemicals

The phenanthridinone-based PJ34 and isoindolinone-based INO-1001 PARP inhibitors were both from Inotek Pharmaceticals Corp. (Beverly, MA). PJ34 was dissolved in M199 media used for HUVEC and INO-1001 was dissolved in 5% dextrose (Abbott Labs, Pomezia, Italy) and diluted 100 times with water. The hydrogen sulfide formulation (pharmaceutical name: IK-1001) was a pharmaceutical-grade aqueous solution of H_2S produced and formulated to pH neutrality and isoosmolarity by Ikaria Inc. (Seattle, WA) using H_2S gas (Matheson, Newark, CA) as a starting material. The sealed bottles containing the H_2S formulation were freshly opened prior to each experiment and diluted in Krebs' solution to the desired concentration and used immediately. All other chemicals were purchased from the companies indicated in parentheses.

3.9. Statistics

All values are reported as mean ± SEM or SD as indicated in the results section. Statistics were performed by using JMP 5.1 statistical software with the Student t-test, ANOVA and Dunnett post hoc tests when appropriate. Probability values of less than 0.05 were considered significant.

4. RESULTS

4.1. Effects of 7-ketocholesterol on the activity of endothelial poly(ADP-ribose) polymerase and on endothelium-dependent relaxant function

PARP in HUVEC cells were activated by 7-ketocholesterol in a dose-dependent manner. This activation was even higher with the pretreatment of BSO (Fig. 15A) The further analysis of this activation showed that 20 μg/ml 7K has nearly the same potential in activating PARP as 0.5mM H_2O_2, and this activation can be blocked by the PARP inhibitor PJ34 and by the non-selective NOS-inhibitor L-NAME (Fig. 15B).

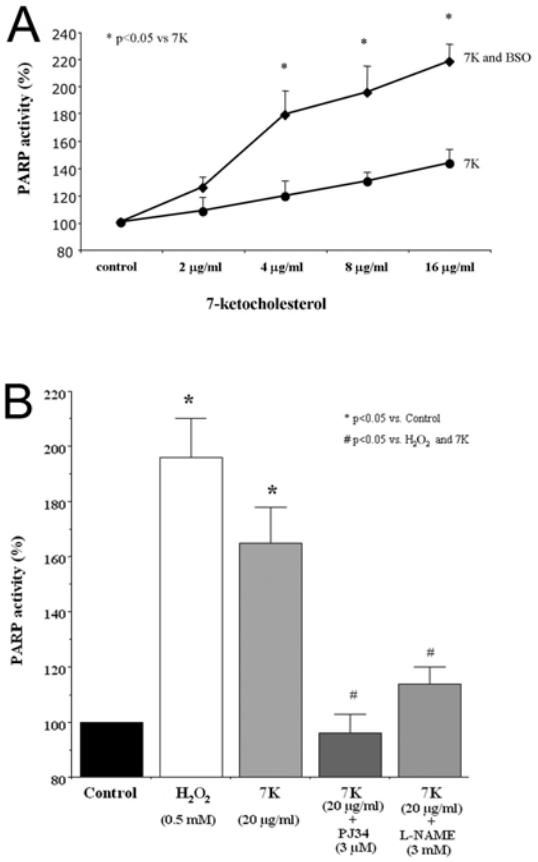

Figure 15. 7-ketocholesterol treatment activates PARP in HUVEC cells in a dose dependent manner. *(A)* Further analysis of this effect showed that BSO pretreatment augments this activation suggesting an oxidant effect of the 7K. *(B)* The degree of PARP activation by 7K was comparable with the degree elicited by H_2O_2. 7K-induced PARP activation was blocked by PARP inhibitor PJ34 and the non-isoform-selective NOS inhibitor L-NAME. Data represent mean ± SD.

The experiments conducted on vascular rings showed no difference in Ach induced relaxations, neither after incubation of rings with 7K, nor after subcutaneous treatment of mice with 7K, even in the presence of BSO pretreatment (Fig. 16.).

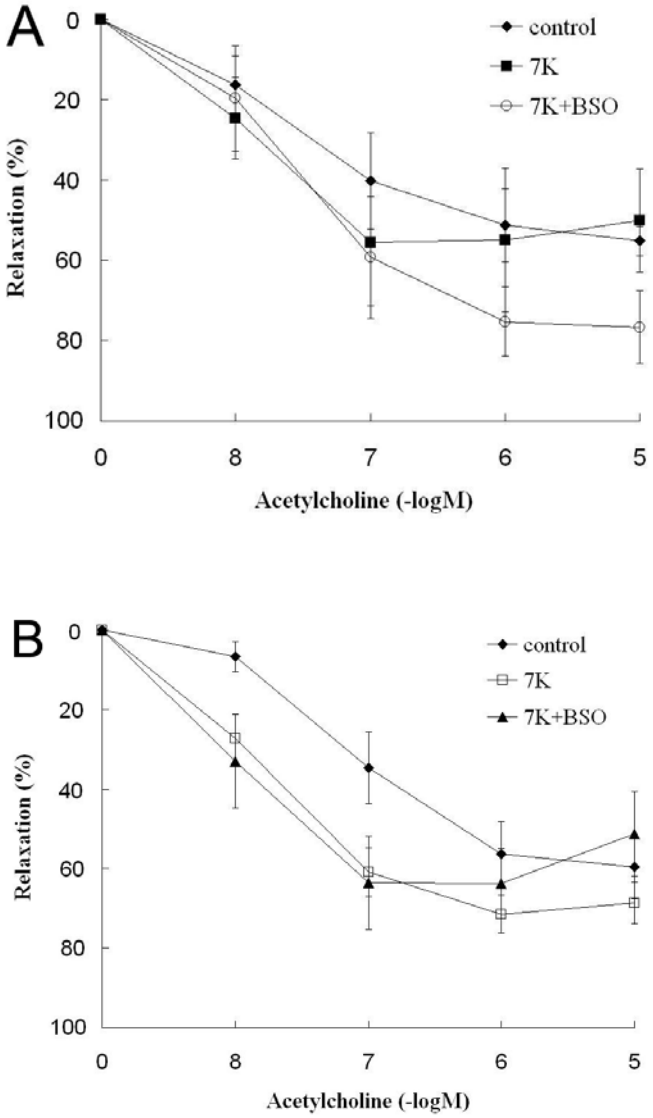

Figure 16. The effect of 7-ketocholesterol treatment on endothelium dependent vasodilatation. *(A)* Incubation with 90 µg/ml for 2 hours did not cause significant dysfunction compared to control. *(B)* Pretreatment of mice with 10 mg/kg /day 7K caused no difference compared to vehicle treated animals either. Data represent mean ± SD.

Based on nuclear PAR-staining, the PARP activity of endothelial cells in the vessel wall showed no significant difference between the groups studied (Fig. 17.).

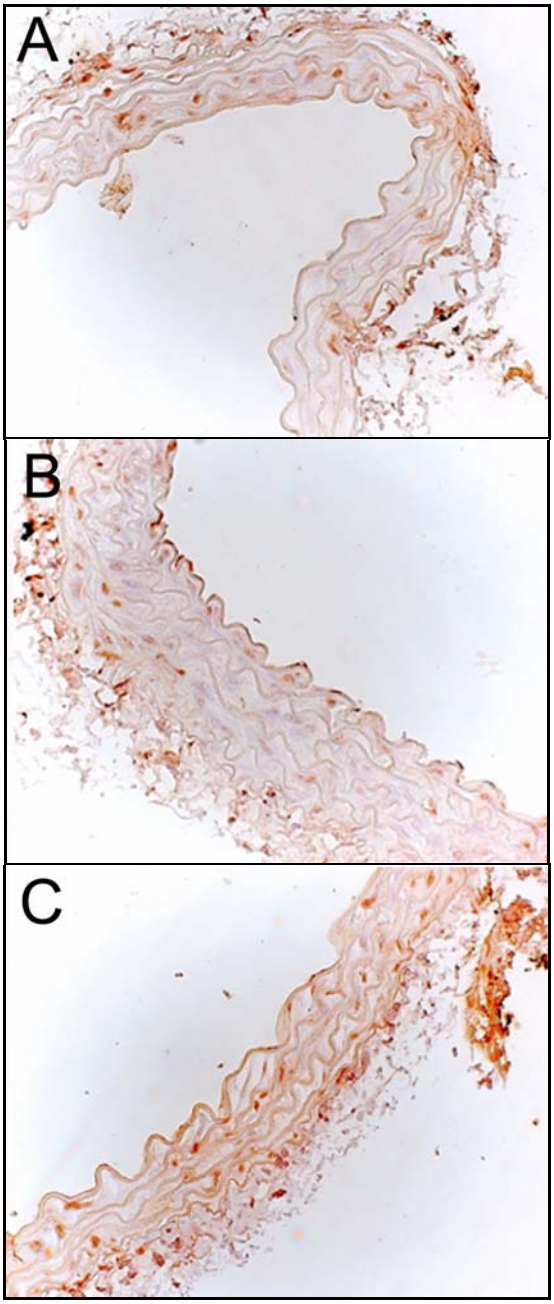

Figure 17. No difference could be observed in nuclear PAR staining, therefore the PARP activity of endothelial cells in the vessel wall did not differ among the groups studied: (*A)* 7K incubation, *(B)* 7K pretreatment, *(C)* control. Anti-PAR staining (1:100), hematoxylin background.

4.2. Poly(ADP-Ribose) polymerase promotes cardiac remodeling, contractile failure and translocation of apoptosis-inducing factor in a murine experimental model of aortic banding and heart failure

4.2.1. Effect of INO-1001 on hemodynamics

To examine the effect of INO-1001 on hemodynamic loading conditions of aortic banded mice, we measured the mechanical function. Table 1. summarizes the hemodynamic results. At 9 weeks after banding, left ventricular systolic pressure increased significantly in banded mice compared with sham-operated mice. Hearts from vehicle-treated banded mice showed a 22 and 14% reduction in maximal dP/dt (+dP/dt) and minimal dP/dt (-dP/dt) compared with those from sham-operated mice, indicating pressure overload-impaired cardiac function. Treatment with INO-1001 prevented the pressure overload-induced decrease in contractile function despite that the pressure gradient between both carotid arteries was comparable in the vehicle-treated banded group (51.2 ± 5.1 mm Hg) versus the INO-1001-treated banded group (50.2 ± 9.5mmHg).

4.2.2. Effect of INO-1001 on the load-induced increase in heart weight and mortality

To examine whether INO-1001 attenuates load-induced cardiac hypertrophy, we treated aortic banded mice with INO-1001 or vehicle for 9 weeks after surgery. Aortic banded mice had a significant increase in heart weight at the end of the experiment compared with sham-operated mice. Heart weight or left ventricular weight to tibial length (HW/TL, LVW/TL) ratio increased by 100.5 or 117.9% in the vehicle-treated banded mice. Importantly, however, in INO-1001-treated banded mice, HW/TL or LVW/TL ratio rose by 39.0 or 60.9%, which was significantly lower than in the vehicle-treated banded mice (Fig. 18.).

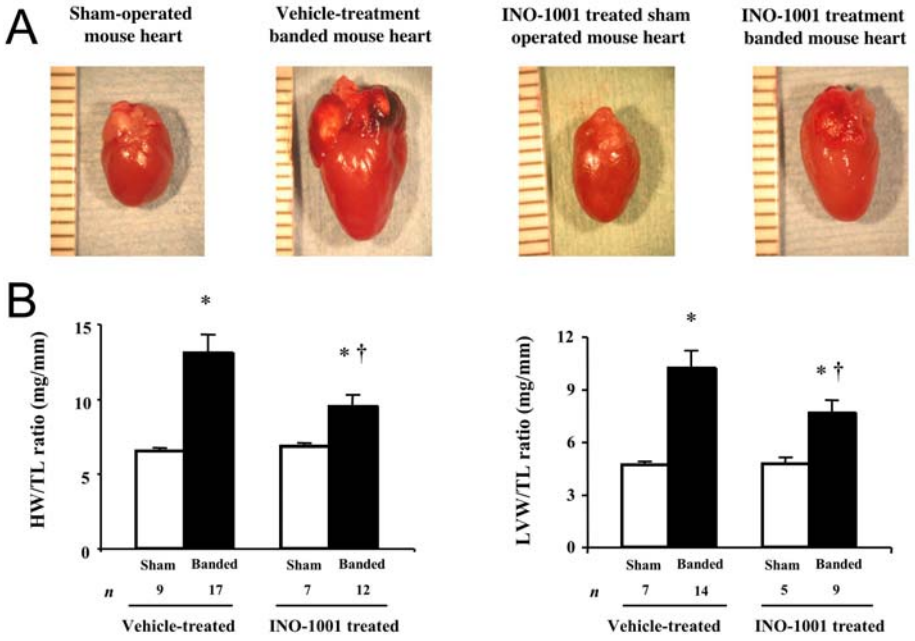

Figure 18. Reduced hypertrophic response to pressure overload in mice subjected to aortic banding in the presence of the PARP inhibitor INO-1001. *(A)* Representative photographs of heart from vehicle-treated banded, INO-1001-treated banded, and respective sham-operated mice 9 weeks after TAC. Scales represent millimeters. *(B)* Heart weight/tibial length and left ventricular weight/tibial length ratio were determined 9 weeks after TAC or sham operation. The error bars represent the SEM. *, $p<0.05$ versus respective sham-operative mice. †, $p<0.05$ INO-1001-treated versus vehicle-treated banded mice.

The body weights and tibial lengths were not different among the groups. Furthermore, 9 weeks after TAC, aortic banded mice exhibited increased lung weight (Table 1.), indicating the development of pulmonary congestion. In contrast, INO-1001-treated banded mice showed a significant decrease in lung weight.

	Vehicle		INO-1001	
	Sham	Banded	Sham	Banded
	(n = 7–12)	(n = 9–17)	(n = 5–8)	(n = 10–16)
Body weight, g	31.2 ± 0.9	29.8 ± 0.8	33.1 ± 0.6	31.8 ± 0.6
Lung weight, mg	184.1 ± 7.8	289.8 ± 41.3*	175.8 ± 4.6	206.4 ± 16†
Liver weight, g	1.29 ± 0.05	1.30 ± 0.04	1.33 ± 0.08	1.30 ± 0.03
Lung weight/body weight, mg/g	5.9 ± 0.3	10.3 ± 1.8*	5.3 ± 0.2	6.5 ± 0.5†
Aortic pressure gradient, mm Hg	3.1 ± 1.4	51.2 ± 5.0*	2.8 ± 0.7	50.2 ± 9.5*
Heart rate, bpm	352 ± 36	323 ± 21	322 ± 24	326 ± 31
LVSP, mm Hg	126.5 ± 3.0	152.4 ± 6.9*	123.8 ± 7.9	169.9 ± 7.5*
dP/dt, mm Hg/mS	5.78 ± 0.24	4.51 ± 0.21*	5.53 ± 0.30	5.48 ± 0.24†
−dP/dt, mm Hg/mS	5.47 ± 0.20	4.71 ± 0.32*	5.69 ± 0.23	6.13 ± 0.34†

Table 1. Improvement in cardiac function by PARP inhibition in chronic heart failure induced by aortic banding. Hemodynamic measurement and organ weight of 9-week aortic banded mice treated with vehicle or INO-1001. Results are presented as mean ± SEM. *, $p<0.05$ versus respective sham-operated group; †, $p<0.05$ versus vehicle-treated banded group

The all-cause mortality rate of TAC was not different for vehicle-treated banded mice and INO-1001-treated banded mice (Fig. 19.). All sham-operated mice survived to the time of experiment. Forty-five mice of 72 in the vehicle-treated banded group and 32 mice of 61 in the INO-1001-treated mice died prematurely. Twenty-one mice in vehicle-treated banded mice (29.2%), and 11 mice in the INO-1001-treated banded mice (18.1%) died of heart failure, judged by postmortem findings. These mice had massive pleural effusion, severe lung congestion (lung wet weight 400.1 ± 29.6 mg, range 189–782 mg) and developed severe cardiac hypertrophy (heart weight 216 ± 12.7 mg, range 135–451.8 mg).

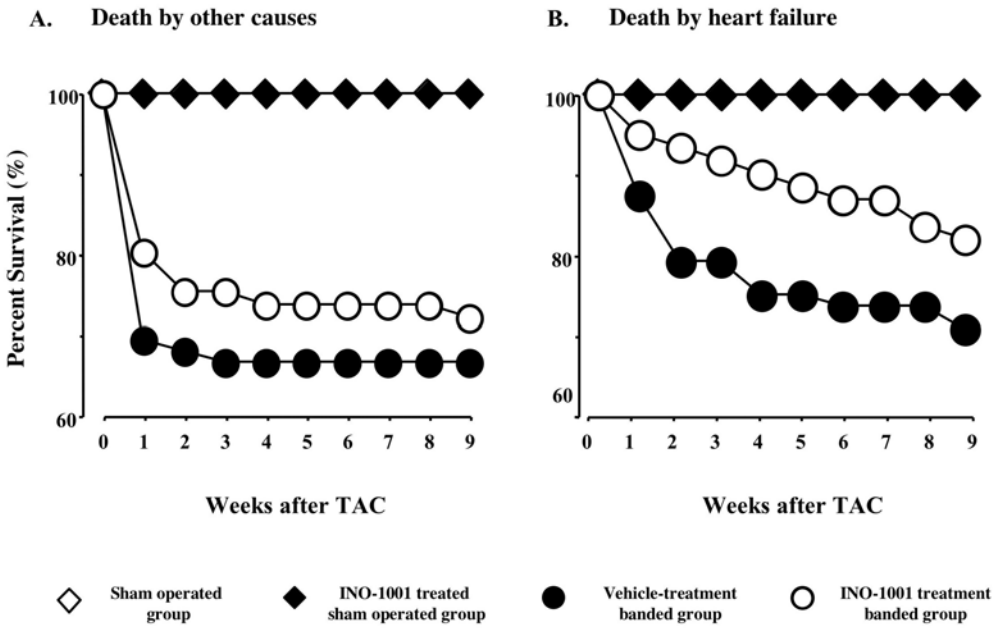

Figure 19. Survival of mice subjected to aortic banding in the presence and absence of the PARP inhibitor INO-1001. Curves showing premature deaths by heart failure and death by other causes from vehicle-treated banded, INO-1001-treated banded, and sham-operated mice. All sham operated animals survived.

There was a massive staining of collagen in the myocardium of banded mice, which was markedly reduced in the INO-1001-treated group of banded animals (Fig. 20.).

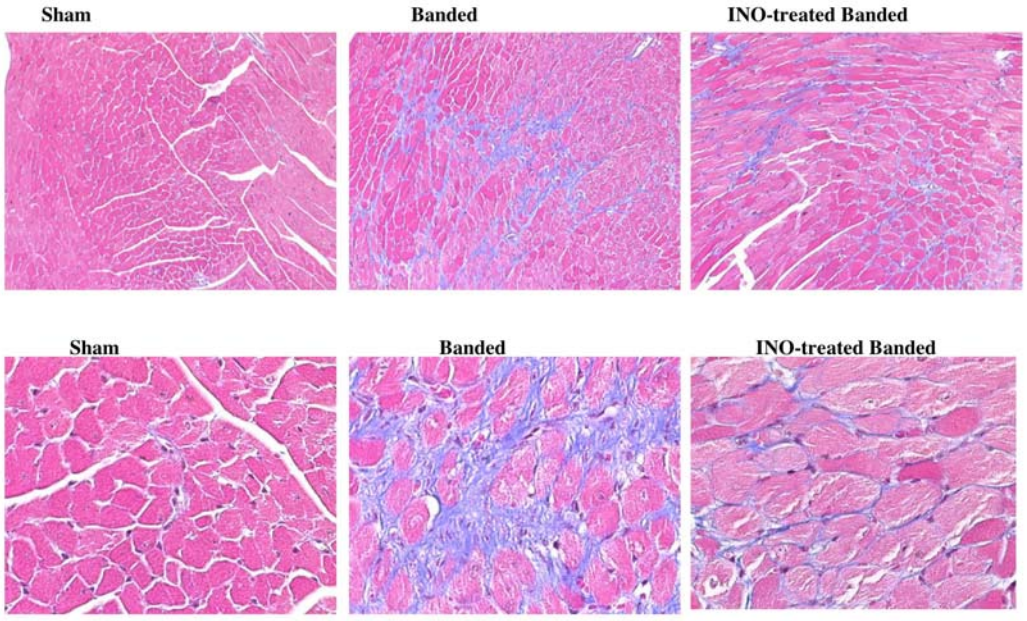

Figure 20. Effect of INO-1001 on collagen accumulation in aortic banded mouse hearts. Aortic banded and sham-operated mice were killed 9 weeks after operation. Treatment with INO-1001 after 4 weeks markedly reduced the accumulation of collagen in aortic banded mouse heart. Representative sections from four to five animals per group are shown. Bottom, higher magnification (4X) compared with the top.

The concentration of INO-1001 in plasma at 9 weeks after treatment in aortic banded mice was 1.24 ± 0.96 μM (n = 4). However, at 1 week after the start of the experiment, plasma PARP inhibitor levels amounted to only 0.27 ± 0.12 μM, indicating a gradual buildup of plasma INO-1001 concentrations in the animals subjected to its administration in the drinking water. Similarly, INO-1001 levels in the heart only amounted to 0.18 ± 0.09 μM at 1 week, whereas they increased to 0.41 ± 0.12 μM at 9 weeks. In vitro pretreatment with 1 μM INO-1001 fully prevented PARP activation in cardiac myocytes challenged with hydrogen peroxide (n = 4). At a 10 times lower concentration (0.1 μM INO-1001), PARP activation in hydrogen peroxide-challenged myocytes was reduced by 56 ± 7% (p< 0.05, n = 4).

4.2.3. Effect of INO-1001 on the load-induced PARP activation and AIF translocation

To examine whether PARP was activated in the myocardium in response to chronic pressure overload, mice were killed 1, 4, and 9 weeks after the operation. Pressure overload caused increase in PARP activity, which reached its peak at 1 week, in both vehicle-treated and INO-1001-treated banded mice hearts compared with sham-operated mice heart. PARP activation in INO-1001- treated banded mice hearts was reduced and was similar to baseline level from 4 weeks after treatment (Fig. 21).

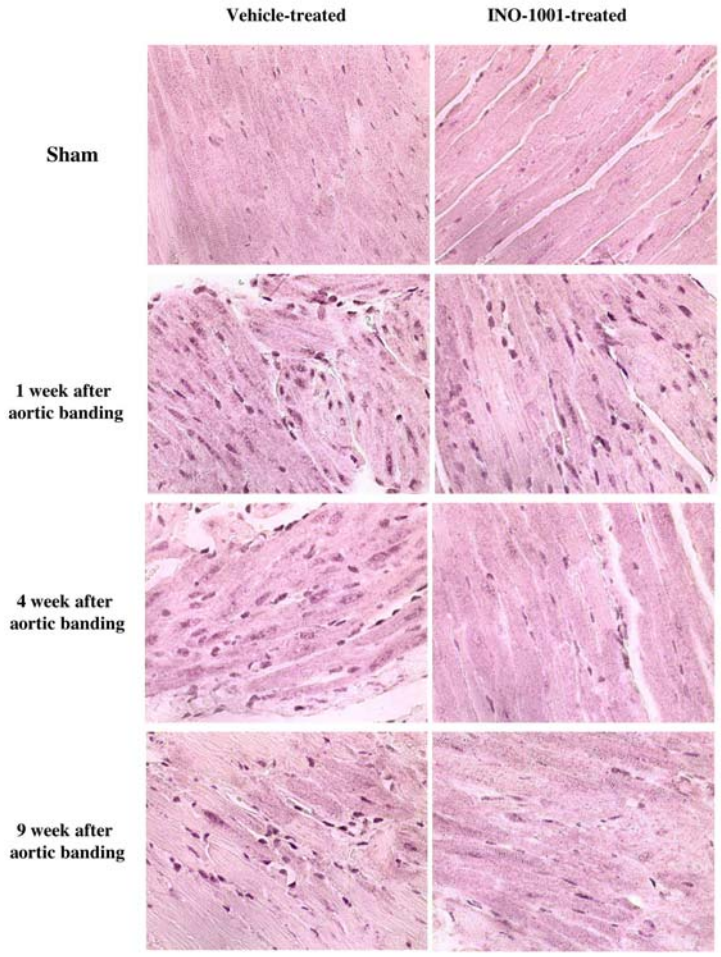

Figure 21. Effect of INO-1001 on PARP activation in aortic banded mouse hearts. Aortic banded and sham-operated mice were killed 1, 4, and 9 weeks after operation. PARP activation was detected by immunohistochemical staining as described under *Materials and Methods*. Treatment with INO-1001 after 4 weeks markedly reduced PARP activation in aortic banded mouse heart. Representative sections from four to five animals per group are shown.

Similar to the results of PARP activation, the peak of AIF translocation occurred at 1 week after aortic banding and then decreased in both groups. INO-1001 prevented AIF translocation from 4 weeks after operation (Fig. 22.). This phenomenon was also confirmed by subcellular fractionation, followed by AIF Western blotting (Fig. 23.).

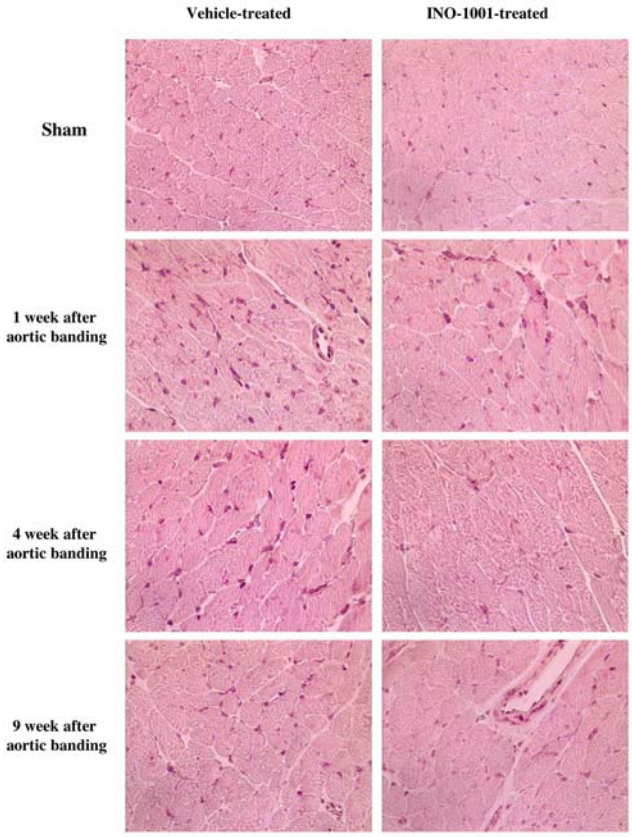

Figure 22. Effect of INO-1001 on AIF translocation in aortic banded mouse hearts. Aortic banded and sham-operated mice were killed 1, 4, and 9 weeks after operation. Treatment with INO-1001 after 4 weeks markedly reduced AIF translocation in aortic banded mouse heart.

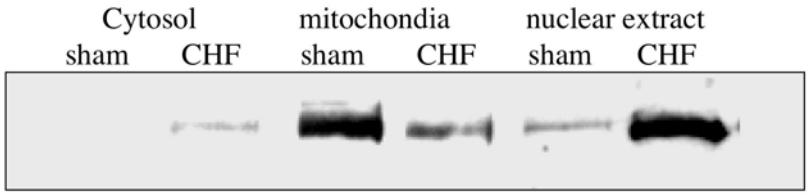

Figure 23. Evidence for myocardial AIF translocation in CHF. Aortic banded and sham-operated mice were killed at 9 weeks after operation. AIF levels in cytosolic, mitochondrial, and nuclear fractions were detected by Western blotting.

4.2.4. Studies in wild-type and PARP-1-deficient animals

To further characterize the involvement of PARP in heart failure, $PARP^{-/-}$ and wild-type littermate mice ($PARP^{+/+}$) were subjected to long-term aortic banding. Aortic banding for 29 weeks caused a significant myocardial hypertrophy in $PARP^{+/+}$ mice compared with sham-operated mice (Fig. 24.).

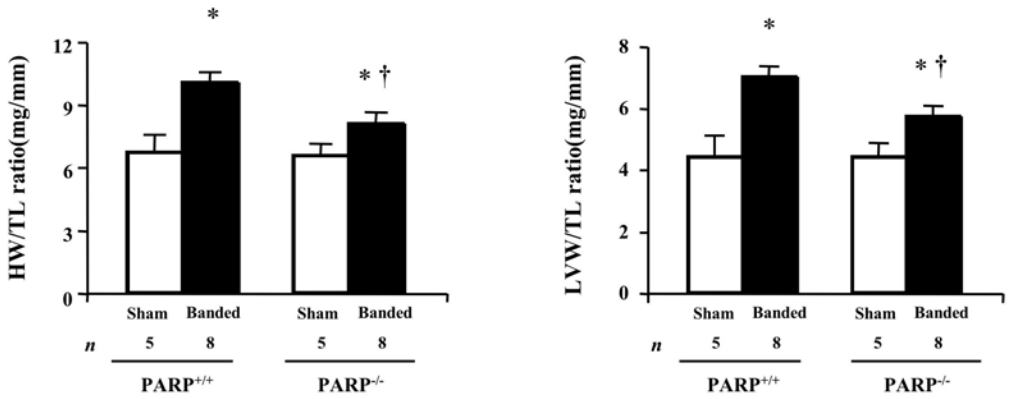

Figure 24. Effects of long-term pressure overload in $PARP^{-/-}$ mouse hearts. Heart weight to tibia length ratio in $PARP^{-/-}$ and $PARP^{+/+}$ mice were determined at 29 weeks after TAC. The error bars represent the SEM. *, $p<0.05$ versus respective sham-operative mice. †, $p<0.05$ versus $PARP^{+/+}$ mice.

The percentage of increase HW/TL and LVW/TL was 49.4% and 59.9%, respectively. The increased percentage of HW/TL and LVW/TL in $PARP^{-/-}$ mice was 23.2% and 29.5%, which was significantly ($p<0.05$) lower than in the $PARP^{+/+}$ mice. The pressure gradient was comparable in both $PARP^{-/-}$ and $PARP^{+/+}$ banded mice (96.0 ± 28.8 versus 99.4 ± 20.5 mmHg, $n = 4$ in each group). These results demonstrate that $PARP^{-/-}$ mice develop less hypertrophy compared with $PARP^{+/+}$ mice. AIF translocation from the mitochondrial to nuclear fraction was noted in the wildtype mice subjected to aortic banding, but not in the $PARP^{-/-}$ banded mice (Fig. 25.). However, the extent of these changes was less pronounced at 29 weeks than at 9 weeks, perhaps indicating that by 29 weeks of banding the peak of the AIF translocation has passed.

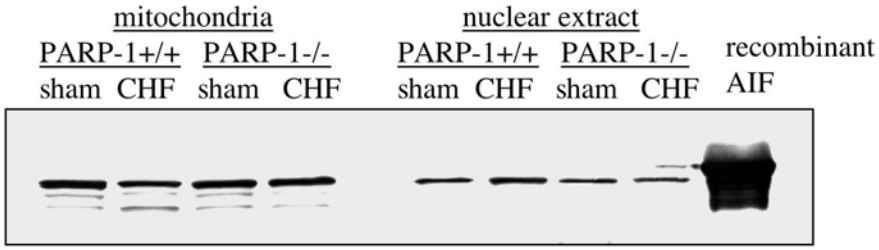

Figure 25. AIF translocation in hearts of wild-type and PARP-1-deficient mice at 29 weeks of CHF. Aortic banded wild-type and PARP-1 deficient mice were killed at 29 weeks after operation. AIF levels in mitochondrial and nuclear fractions were detected by Western blotting. In wild-type mice there was evidence for loss of AIF in mitochondrial fractions and an increase in nuclear fractions. Similar changes were not seen in the PARP-1-deficient hearts undergoing CHF.

4.3. Hydrogen sulfide attenuates myocardial ischemia-reperfusion injury by preservation of mitochondrial function

4.3.1. H_2S dose-dependently limits myocardial infarct size and preserves left ventricular structure and function

In initial studies, mice were subjected to 30 min of LV ischemia and 24 h reperfusion. H_2S donor was administered into the LV lumen at the time of reperfusion at doses ranging from (10–500 μg/kg). Evaluation of infarct size revealed a dose-response curve with 50 μg/kg displaying the most significant cytoprotection as assessed by 2,3,5-triphenyltetrazolium chloride (TTC) staining (Fig. 26 A and B). Mice receiving 50 μg/kg displayed an infarct size per area-at-risk (INF/AAR) of (13.4 ± 1.4%) as compared with vehicle treated mice (47.9 ± 2.9%), representing a 72% reduction in infarct size. Representative mid-ventricular crosssections of vehicle and H_2S (50 μg/kg) treated mice are shown in Fig. 26A. Additionally, all groups displayed similar AAR/LV (Fig. 26B). This optimal dose of 50 μg/kg was therefore used in all subsequent in vivo studies. Circulating plasma levels of the cardiac-specific isoform of troponin-I (cTnI) were evaluated as an additional marker of myocardial injury (Fig. 26C). Serum samples from mice subjected to 45 min of left coronary artery (LCA) ischemia and 4 h reperfusion receiving either vehicle or 50 μg/kg H_2S donor were found to contain 52.1 ± 1.8 vs. 33.6 ± 4.8 ng/ml per mg protein, confirming the cytoprotective effect of H_2S.

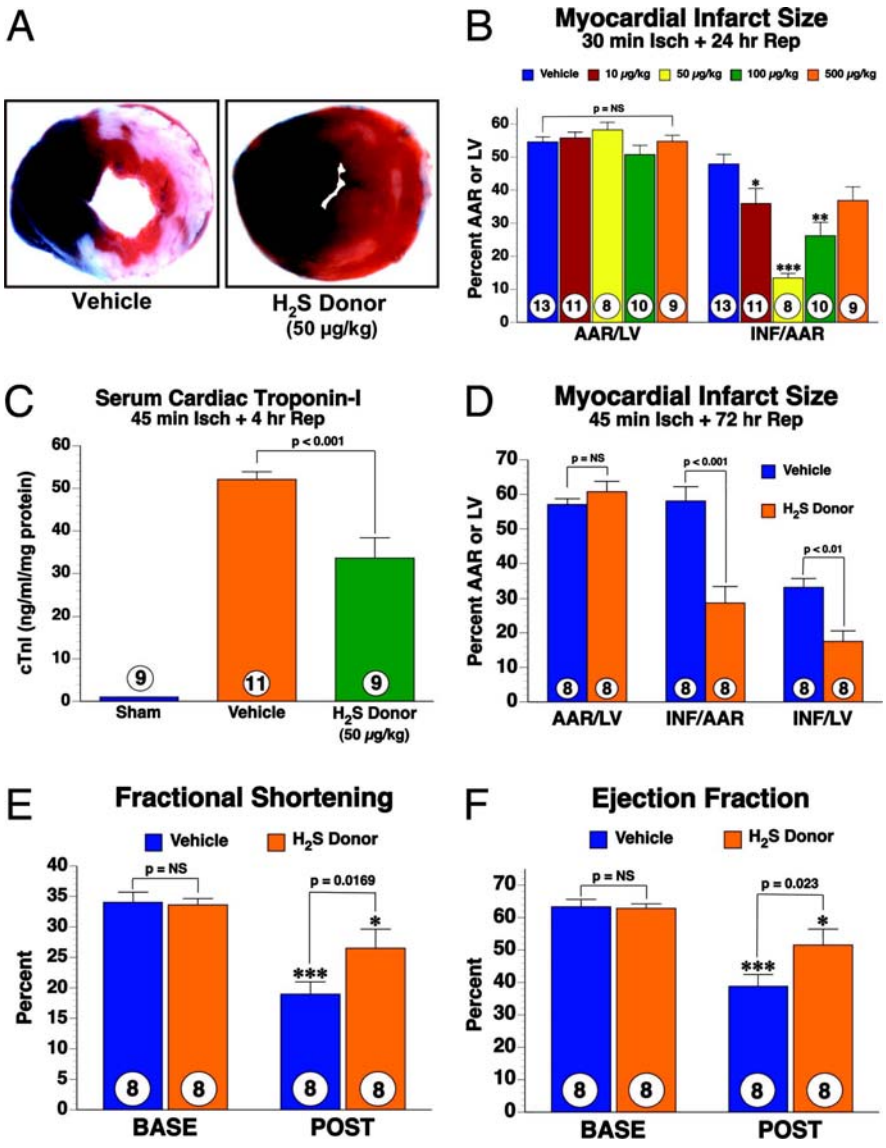

Figure 26. H_2S donor therapy in MI-R. (*A*) Representative mid-myocardial cross sections of TTC-stained hearts for vehicle and 50 µg/kg H_2S donor. Dark blue area (i.e., Evan's blue-stained), nonischemic zone; remaining area, AAR; white area, infracted tissue; red (i.e., TTC-positive), viable myocardium. (*B*) Doses of (10–500 µg/kg) or vehicle were injected i.v. at the time of reperfusion. INF/AAR revealed a U-shaped dose–response curve. (*C*) Serum cardiac troponin-I (cTnI) in sham-, vehicle-, and H_2S (50 µg/kg)-treated mice. (*D*) Myocardial infarct size after 45-min LCA ischemia and 72-h reperfusion. H_2S-treated mice displayed a significant reduction in INF/AAR as well as INF/LV. (*E*) Percent fractional shortening after myocardial infarction. Postinfarction H_2S-treated mice displayed a significant improvement as compared with vehicle-treated mice. (*F*) Percent ejection fraction after myocardial infarction. Postinfarction H_2S-treated mice displayed a significant improvement as compared with vehicle treated mice (*****, $p<0.05$, ******, $p<0.01$, *******, $p<0.001$ vs. BASE). (Circles inside bars denote *n* per group.)

Mice underwent LV echocardiographic analysis one week before 45 min of LCA ischemia and again after 72 h of reperfusion. Confirming the earlier histological findings mice receiving H_2S (50 μg/kg, i.v.) at the time of reperfusion were found to have a 51% reduction in INF/AAR as compared with vehicle treated mice (Fig. 26D). H_2S-treated mice displayed no significant increase in post-MI LV dimensions [left ventricular end-diastolic dimension (LVEDD) and left ventricular end-systolic dimension (LVESD)] as compared with vehicle treated mice which displayed significantly increased LVESD and LVEDD after MI (Table 2.). Additionally, mice receiving the H_2S donor were found to have a 21% decrease in fractional shortening 72 h after MI as compared with mice receiving vehicle, which displayed a 44% reduction in fractional shortening (Fig. 26E). In parallel, H_2S-treated mice displayed a minimal 18% reduction in ejection fraction post-MI as compared with mice receiving vehicle that displayed a 39% reduction (Fig. 26F). There were no significant differences in heart rate at baseline or post-MI between the groups (Table 2.).

Group		*n*	LVEDD, mm	LVESD, mm	HR, bpm
Base	Vehicle	8	3.69 ± 0.14	2.46 ± 0.11	423 ± 18
	H_2S	8	3.69 ± 0.11	2.45 ± 0.10	410 ± 16
Post	Vehicle	8	4.62 ± 0.15*	3.75 ± 0.20*	521 ± 11*
	H_2S	8	3.90 ± 0.17†	2.90 ± 0.24†	529 ± 12*

Table 2. MI-R echocardiographic data. Mice underwent echocardiographic analysis 1 wk before (Base) 45 min. ischemia and following 72 h reperfusion (Post). Mice received either vehicle or H_2S donor (50μg/kg i.v.) at reperfusion. (*n*, number of animals per group; LVEDD, left ventricular end-diastolic dimension; LVESD, left ventricular end-systolic dimension; HR, heart rate. *****, $p < 0.01$ vs. baseline; †, $p < 0.01$ vs. Vehicle Post.)

4.3.2. H_2S reduces myocardial inflammation after MI-R

Blinded histological analysis of heart sections stained with H&E were scored 24 h after reperfusion (Fig. 27 A and B). Mice receiving H_2S donor displayed a reduced degree of myocardial neutrophilic infiltrate, necrosis, hemorrhage, and spindle-shaped interstitial cells as compared with mice receiving vehicle. To quantify neutrophilic infiltrate myeloperoxidase (MPO) activity was analyzed 4 h after reperfusion. H_2S-treated mice

were found to have a 26% reduction in MPO activity as compared with vehicle-treated mice (Fig. 27C). Intravital microscopy of leukocyte rolling revealed that H_2S completely inhibited thrombin induced leukocyte-endothelial cell interactions (Fig. 27D). H_2S-treated mice displayed levels of leukocyte rolling similar to control levels at all time points analyzed.

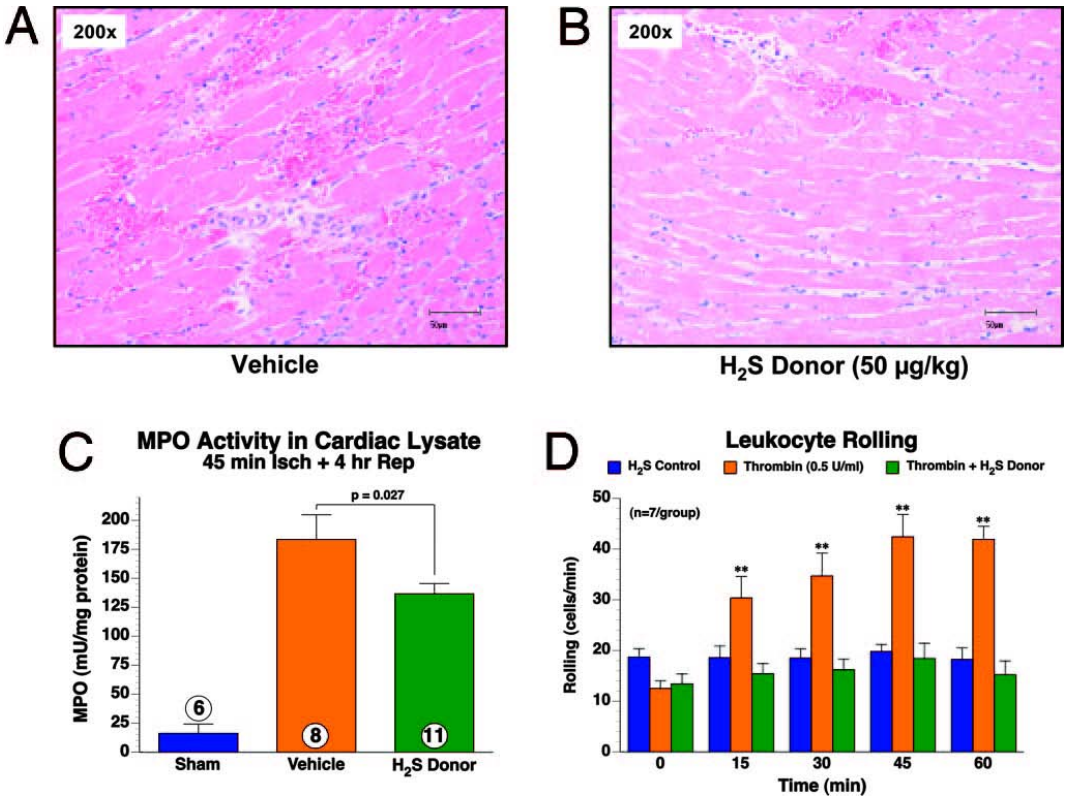

Figure 27. H_2S therapy limits the extent of myocardial inflammation. Representative H&E-stained histological images after 45 min LCA ischemia and 24 h reperfusion. (*A*) Vehicle-treated mice displayed a high degree of hemorrhage and infiltrating leukocytes within the ischemic zone. (*B*) Histopathology was attenuated in the myocardial sections of mice treated with H_2S donor (50 µg/kg). (*C*) MPO activity was significantly decreased in mice treated with H_2S donor 4 h after reperfusion. (*D*) Leukocyte rolling was reduced down to control levels in mice receiving thrombin plus H_2S donor at all time points (******, $p<0.01$ vs. all other groups, $n = 7$/group; circles inside bars denote n per group).

ELISA analysis of key myocardial cytokines after 45 min ischemia and 4 h reperfusion revealed H_2S-treated mice to have no significant increase in IL-1β as compared with sham animals (206± 21 vs. 185 ± 26 pg/mg protein). In stark contrast, vehicle-treated mice were found to have a 2.1-fold increase in IL-1β (390 ± 90 pg/mg protein). The assessment of TNF-α and IL-10 in cardiac lysate revealed no differences between any of the groups (Fig. 28).

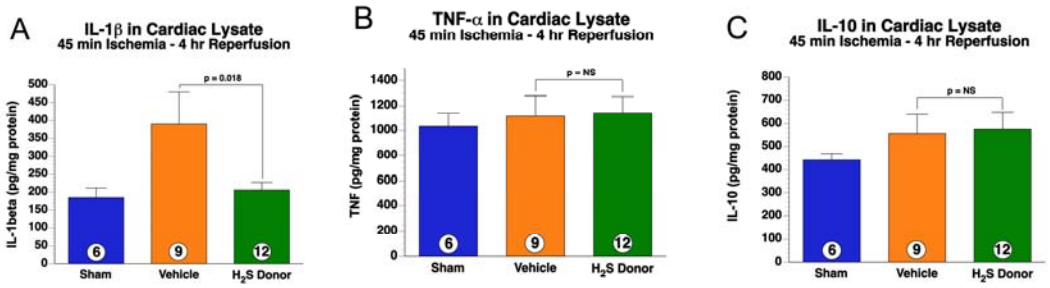

Figure 28. Myocardial cytokine levels following 45 min LCA ischemia and 4 h reperfusion. (*A*) ELISA quantified levels of myocardial IL-1β revealed a substantial (p=0.018) decrease in H_2S donor-treated mice. (*B*) There were no observed differences 4 h after reperfusion in TNF-α between any of the groups. (*C*) The Th1 cytokine IL-10 was not significantly different (p=NS) between any of the groups 4 h after reperfusion (circles inside bars denote *n* per group).

4.3.3. H_2S dose-dependently inhibits cardiac mitochondrial respiration and preserves mitochondrial function in vitro

Oxygen consumption during state 3 respiration was measured in mitochondria isolated from murine hearts. H_2S (1–50 μM) was introduced into a sealed chamber after steady-state respiration and O_2 was monitored with a Clark-type electrode. A dose dependent reduction of oxygen consumption compared with baseline was observed: (1 μM = 7%, 10 μM = 63%, 25 μM = 86%, 50 μM = 95%, Fig. 29A). Freshly isolated cardiac mitochondria were then subjected to an in vitro hypoxic assay. Mitochondria in the presence of 10 μM H_2S were found to have a significantly improved recovery of respiration rate after 30 min of hypoxia as seen by the steeper slope in Fig. 29B. The numeric results can be seen in Fig. 29C with a 36 ± 2% recovery in the vehicle-treated group as compared with a 67 ± 2% recovery in H_2S-treated mitochondria.

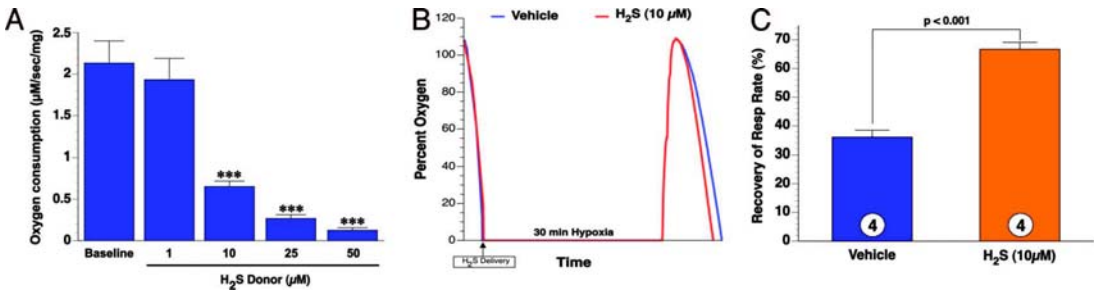

Figure 29. H_2S donor inhibits cardiac mitochondrial respiration and preserves mitochondrial function in vitro. (*A*) Cardiac mitochondrial respiratory rate. Mitochondria isolated from WT mouse hearts were analyzed for oxygen consumption in the presence of H_2S. H_2S (1–50 μM) dose-dependently reduced mitochondrial respiration. (*******, $p<0.001$, $n < 4$ per group). (*B*) Representative tracings of O_2 consumption in vehicle- and H_2S-treated (10 μM) mitochondria. Whereas both groups had similar rates of O_2 consumption before hypoxia, H_2S-treated mitochondria displayed a significantly greater rate of O_2 consumption 30 min after hypoxia as evident by a steeper slope of the red line. (*C*) Mitochondrial recovery 30 min after hypoxia. Percentage recovery of respiration rate was significantly greater in mitochondria treated with H_2S donor. Circles inside bars denote *n* per group.

4.3.4. H_2S preserves mitochondrial function and membrane integrity after in vivo MI-R injury

Cardiac mitochondria were isolated from mice subjected to 45 min ischemia and 24 h reperfusion for assessment of respiratory rate. Mitochondria isolated from vehicle-treated mice were found to have a 3.4-fold decrease in the rate of O_2 consumption (complex I substrate) as compared with sham operated animals. Mitochondria from mice receiving 50 μg/kg H_2S at reperfusion were found to have a significantly greater rate of O_2 consumption as compared with mice receiving vehicle (Fig. 30A). Mitochondria from the same groups were also analyzed for complex II efficiency. There was a 3.2-fold decrease in the rate of O_2 consumption in mitochondria isolated from vehicle-treated mice. The respiration rate in mitochondria, isolated from H_2S-treated animals, was increased 2.2-fold over mitochondria isolated from vehicle-treated animals (Fig. 30B). After 45 min of ischemia and 24 h reperfusion myocardial samples were qualitatively assessed by transmission electron microscopy for structural mitochondrial changes (Fig. 30C). Longitudinal sections of vehicle-treated hearts displayed uniform mitochondrial swelling with disorganized cristae and decreased matrix density. The presence of amorphous matrix densities or granular dense bodies, a distinctive feature of

irreversible myocardial cell injury after reperfusion, can also be seen in a number of mitochondria in vehicle-treated samples. H_2S donor-treated hearts displayed little change in mitochondrial structure. In general, mitochondria appeared highly dense with well organized cristae.

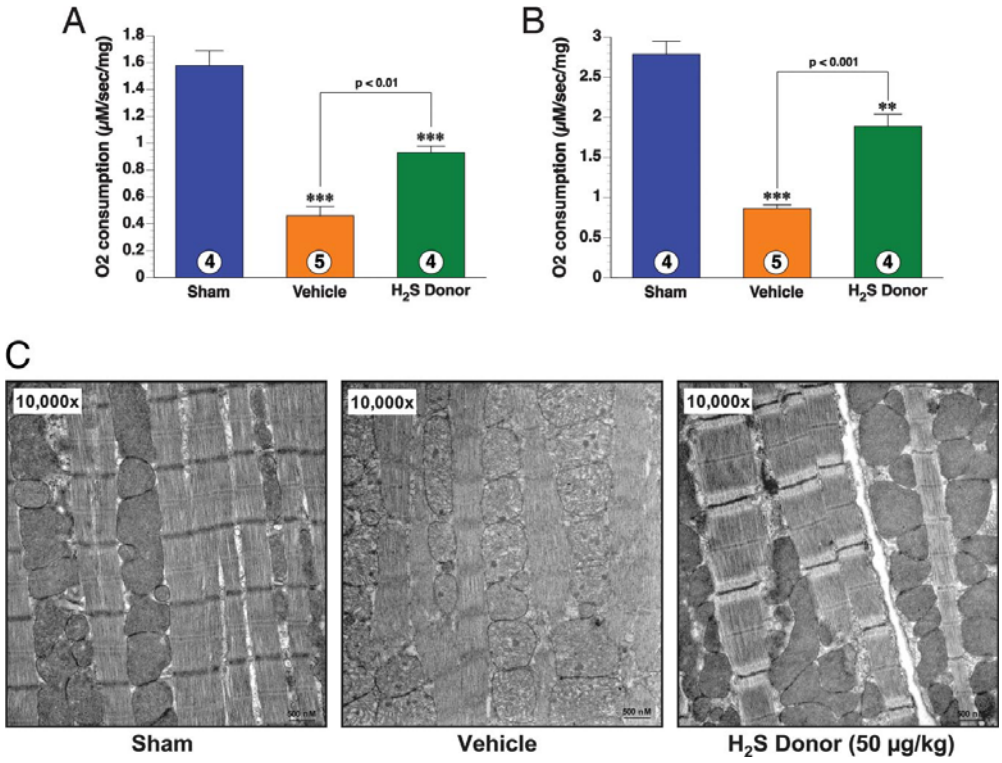

Figure 30. H_2S preserves mitochondrial function and structure after in vivo MI-R. Mitochondria were isolated from hearts after 45 min LCA ischemia and 24 h reperfusion. Mice treated with H_2S at the time of reperfusion displayed a significant improvement in mitochondrial complex I efficiency as determined by using pyruvate and malate as substrate. (*B*) The efficiency of complex II was assessed by using succinate and G3P as substrate and inhibiting complex I with rotenone. The same H_2S donor treated mice displayed significantly greater rate of O_2 consumption after MI-R (*****, $p<0.05$; ******, $p<0.01$; *******, $p<0.001$ vs. sham). Circles inside bars denote *n* per group. (*C*) After 45 min of ischemia and 24 h reperfusion, myocardial samples were qualitatively assessed by transmission electron microscopy for structural mitochondrial changes. Longitudinal sections of vehicle-treated hearts displayed uniform mitochondrial swelling with disorganized cristae and decreased matrix density. The presence of amorphous matrix densities or granular dense bodies, a distinctive feature of irreversible myocardial cell injury after reperfusion, can also be seen in a number of mitochondria in vehicle-treated samples. H_2S donor-treated hearts displayed little change in mitochondrial structure. Generally, mitochondria seemed to be highly dense with well organized cristae with little distinguishable differences from sham samples.

4.3.5. H_2S reduces cardiomyocyte apoptosis in vitro and in vivo after MI-R

Isolated adult cardiomyocytes were subjected to 6 h hypoxia and 12 h reoxygenation. Groups receiving the H_2S donor at the time of reoxygenation displayed a significant reduction in caspase-3 activity as compared with vehicle-treated myocytes (Fig. 31A). After 45 min LCA ischemia and 4 h reperfusion mouse heart samples from sham, vehicle and H_2S donor-treated mice were evaluated for TUNEL positive nuclei. H_2S donor-treated mice were found to have a 59% reduction in the number of TUNEL positive nuclei as compared with vehicle-treated animals (Fig. 31B).

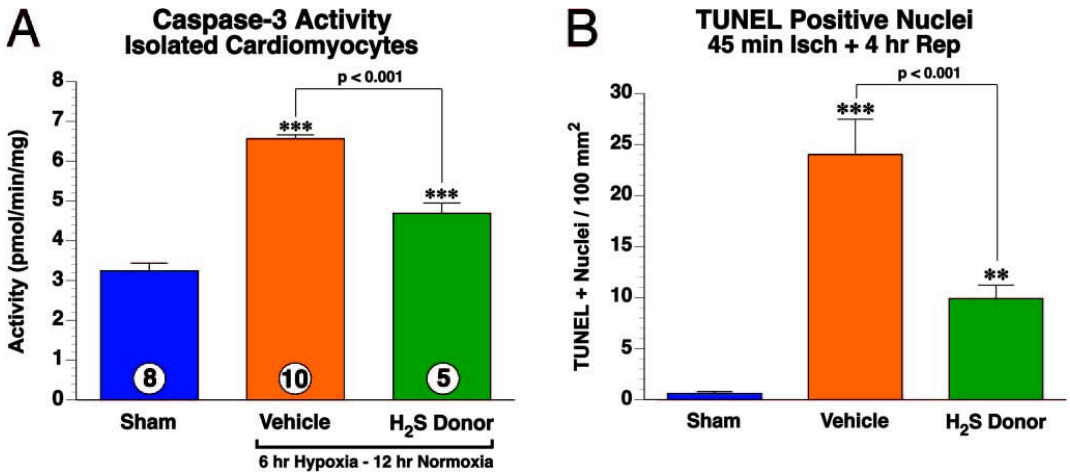

Figure 31. H_2S reduces cardiomyocyte apoptosis *in vitro* and *in vivo* after MI-R. (*A*) Isolated adult cardiomyocytes were subjected to 6 h hypoxia and 12 h reoxygenation. Groups receiving the H_2S donor (100 μM) at the time of reoxygenation displayed a significant reduction in caspase-3 activity (circles inside bars denote *n* per group). (*B*) After 45 min LCA ischemia and 4 h reperfusion, mouse heart samples from sham, vehicle, and H_2S donor-treated mice were evaluated for TUNEL-positive nuclei. H_2S donor-treated mice were found to have a 59% reduction in the number of TUNEL-positive nuclei as compared with vehicle-treated animals ($p<0.001$, n = 6 per group).

4.3.6. Hemodynamics after H_2S donor administration

Mice were implanted with radiotelemeters and subjected to femoral vein injection of H_2S. No significant effect on mean arterial blood pressure could be registered (MABP) at doses ranging from 10–500 μg/kg, as compared with vehicle-treated mice (Table 3.).

Dose-H_2S	n	Base MABP, mmHg	Post MABP, mmHg	% Decrease	Duration, s
Vehicle	6	100.1 ± 3.1	99.5 ± 3.0	0.5 ± 0.5	0.3 ± 0.3
10 μg/kg	6	100.5 ± 2.2	98.5 ± 2.8	2.1 ± 0.9	1.7 ± 0.9
50 μg/kg	6	100.1 ± 3.3	96.4 ± 2.3	3.6 ± 1.5	3.3 ± 0.8
100 μg/kg	6	104.9 ± 1.2	98.6 ± 1.5	6.0 ± 1.2	4.0 ± 0.3
500 μg/kg	6	103.5 ± 2.5	93.4 ± 2.8	9.9 ± 1.5	6.2 ± 1.6*
1 mg/kg	6	102.4 ± 2.3	64.6 ± 6.3*†	36.8 ± 6.3*†	7.4 ± 1.1*

Table 3. Alterations in blood pressure after H_2S donor administration. Mice (n = 6 per group) were implanted with radiotelemeters and doses of the H_2S donor were given via the femoral vein at various concentrations (0-1 mg/kg). Base, prior to injection, Post, minimum pressure following injection; MABP, mean arterial blood pressure.. $p<0.05$ vs. vehicle; †, $p<0.01$ vs. all other groups.

H_2S (1 mg/kg) did significantly reduce MABP from (102.4 ± 2.3 to 64.6 ± 6.3 mmHg), representing a 37% decrease that lasted for an average of 7.4 seconds followed by a period of hypertension. Assessment of heart rate revealed no significant alteration after doses ranging from 10–100 μg/kg as compared with vehicle-treated mice (Table 4.).

Dose-H_2S	n	Base HR, bpm	Post HR, bpm	% Decrease	Duration, s
Vehicle	6	460 ± 22	456 ± 21	0.9 ± 0.4	1.5 ± 0.7
10 μg/kg	6	461 ± 21	453 ± 19	1.7 ± 1.0	1.7 ± 0.8
50 μg/kg	6	467 ± 18	458 ± 17	1.8 ± 0.6	2.7 ± 0.8
100 μg/kg	6	460 ± 20	445 ± 18	3.3 ± 0.5	2.3 ± 0.2
500 μg/kg	6	462 ± 18	393 ± 29	14.2 ± 7.2*	20.7 ± 12.7
1 mg/kg	6	472 ± 17	204 ± 22*†	55.9 ± 6.0*†	148.8 ± 50.6*†

Table 4. Alterations in heart rate following H_2S donor administration Mice (n = 6 per group) were implanted with radiotelemeters and doses of the H_2S donor were given via the femoral vein at various concentrations (0-1 mg/kg). HR: heart rate; Base: prior to injection; Post: minimum HR after injection. $p<0.05$ vs. vehicle; †, $p<0.01$ vs. all other groups.

4.3.7. Mice with cardiac-restricted overexpression of cystathionine γ-lyase (αMHC-CGL-Tg) are protected against MI-R injury

The expression of CGL protein increased as can be seen in the immunoblot and calculated values of optical density in Fig. 32A. Importantly, this increase in CGL enzyme resulted in an ~2-fold increase in H_2S production by myocardial homogenates of αMHC-CGL-Tg mice as assessed by an H_2S specific electrode (Fig. 32B). αMHC-CGL-Tg mice and their WT littermates were subjected to 45 min LCA occlusion and 72 h reperfusion. TTC analysis of infarct size revealed αMHC-CGL-Tg mice to have a significant reduction in infarct size (representative mid-myocardial sections can be seen in Fig. 32C). αMHC-CGL-Tg mice exhibited a 47% reduction in INF/AAR as compared with WT littermates (Fig. 32D).

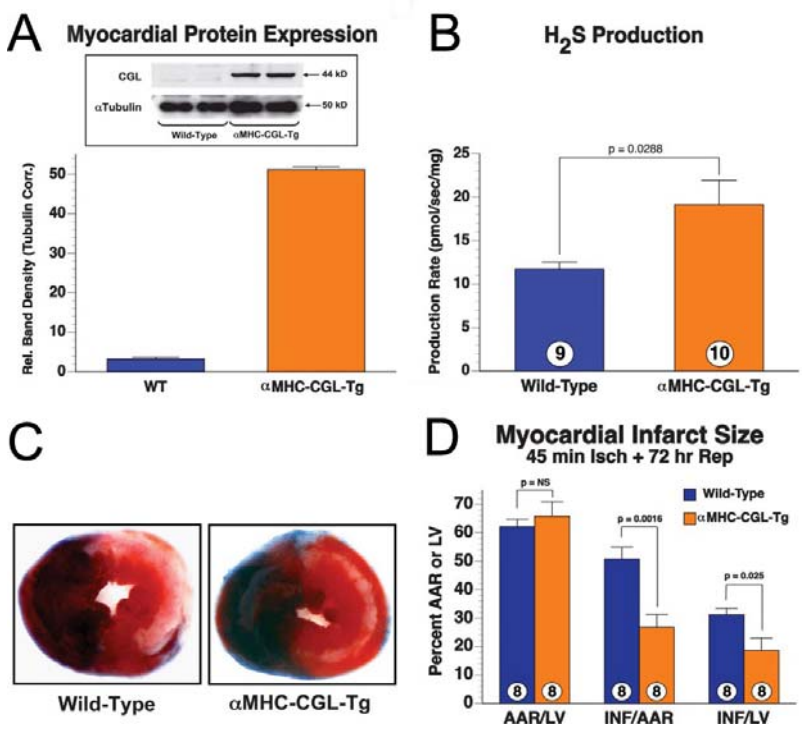

Figure 32. αMHC-CGL-Tg mice are protected against MI-R injury. (*A*) Myocardial protein expression. Increase in message translated to a significant increase in protein expression as can be seen in the immunoblot and calculated optical density. (*B*) H_2S production. The increase in CGL enzyme translated into ~2-fold increase in H_2S production by myocardial homogenates of αMHC-CGL-Tg mice as assessed by an H_2S specific electrode (circles inside bars denote *n* per group). (*C*) Representative mid-myocardial cross sections of TTC-stained hearts for WT and αMHC-CGL-Tg mice after 45 min LCA ischemia and 72 h reperfusion. (*D*) Myocardial infarct size (45 min ischemia and 72 h reperfusion). Transgenic mice displayed a reduction in infarct size per area-at-risk (INF/AAR) as compared with WT littermates. Infarct per LV (INF/LV) was also significantly reduced.

5. DISCUSSION

The present experiments demonstrated that 7-ketocholesterol was capable of activating PARP in endothelial cells and direct incubation of the rings with 7K or subcutaneous treatment with 7K did not inhibit endothelial dependent relaxation. Furthermore, endothelial cells in the vessel walls did not show PARP-activation after these treatments In the second set of experiments aortic banding in mice induced chronic heart failure, evidenced by depression of left ventricular function and hypertrophy and collagenization of the heart. The impaired cardiac function was associated with a diffuse activation of PARP in the myocardium. The ability of INO-1001 to inhibit PARP in the cardiac myocytes was confirmed via immunohistochemical detection of poly(ADP-ribose) activation. In addition, plasma and myocardial concentrations of the PARP inhibitor were found sufficient to block oxidant-induced PARP activation in cardiac myocytes in vitro. Direct functional measurements demonstrated the maintenance of cardiac output in the PARP inhibitor-treated animals undergoing aortic banding. In the last set of experiments, H_2S administered at the time of reperfusion decreased infarct size and preserved left ventricular function. The observed protection was associated with reduced myocardial inflammation, preserved mitochondrial function and reduced cardiomyocyte apoptosis after infarction. Additionally, the overexpression of the enzyme CGL resulted in subsequent increase in myocardial H_2S production, limiting the extent of MI-R injury.

5.1. Atherosclerosis and 7-ketocholesterol

Several studies examined the role of oxysterols found in oxLDL in the early pathogenesis of atherosclerosis. The excess concentration of oxysterols was shown to be cytotoxic to endothelial cells inducing apoptosis [188, 278, 279]. Other investigations showed apoptosis of vascular smooth muscle cells after treatment with cholesterol-oxides [280]. Mougenot measured arterial vasomotor responses related to oxidized LDL and indicated that the major cholesterols contributing to the atherogenic effect are the 7-ketocholesterol and 7β-hydroxicholesterol [281]. 7K was shown to inhibit arterial endothelial-dependent relaxation in the rabbit aorta [189]. Incubating BV-2 microglial

cells with 7K caused PARP-activation [190]. However the possible relation between 7K and PARP in the context of endothelial dysfunction has not yet been investigated.

Here we demonstrated the first time that 7-ketocholesterol (the main oxysterol found in oxLDL) is capable of activating PARP in endothelial cells. This activation appears to be related to NOS activity because L-NAME attenuated the effect of 7K. The phenomenon of PARP activation also appears to be dependent on intracellular oxidative stress, as pretreatment with BSO increased the degree of PARP activation. One likely scenario is that the constitutively produced NO in endothelial cell combines with superoxide, which, in turn, results in the formation of peroxynitrite, which is a known endogenous trigger of DNA single strand breakage and PARP activation. In this context, endothelial NO/peroxynitrite production may result in endothelial dysfunction, which, subsequently may damage the endothelial function, and may lead to impaired endothelial NO production later on. Such impaired NO production has previously been demonstrated after 7K treatment [189, 282, 283].

Direct incubation of the rings with 7K or subcutaneous treatment with 7K did not inhibit endothelial dependent relaxation in our experimental settings and the endothelial cells in the vessel walls did not show PARP-activation, which could be the effect of the rapid hepatic metabolism of 7K [284, 285]. The other possible explanation for these results is that 7-ketocholesterol incubation in the in vitro PARP activity studies on HUVEC cells lasted 24hrs and the incubation time for rings lasted only 2 hrs, and the technical possibilities at the time of the experiments did not allow a 24hr long incubation time.

To test the effect of 7K in a state where the vasculature may become more sensitive to oxidant stress, we utilized BSO pretreatment in mice. In previous studies it was shown that vascular rings taken from rats which had been pretreated with BSO to deplete endogenous glutathione, there was a significantly more pronounced suppression of the contractility and a significantly more pronounced (near-complete) inhibition of the endothelium-dependent relaxations after peroxynitrite exposure [267]. Here we could not find evidence that in vivo 7K would lead to apoptosis and endothelial dysfunction, even after the depletion of glutathione.

Based on the current findings, 7K is certainly capable of PARP activation in endothelial cells, but it is unlikely that 7K, on its own, may lead to endothelial dysfunction,

although it is possible that local accumulation of 7K in plaques could lead to higher, more cytotoxic concentrations. It is probable that 7K acts in synergy with other pro-atherosclerotic molecules in the early stage of atherosclerosis.

Data in the literature demonstrate that 7K can activate a variety of intracellular pathways such as PKC-activation [189], activation of ubiquitin complexes [286], calcium-dependent activation of several pro-apoptotic pathways and also the MEK-->ERK survival pathway [287], upregulation of the NAD(P)H oxidase homologue Nox-4 [288] or modulation of Ca^{++} signal and inhibition of eNOS [282]. The wide variety of possible effects indicates that 7K has numerous targets in the cells of the vascular wall - one of which could be the PARP-pathway - and the combined effects of the activation of these pathways may lead to vascular cell damage and cell death.

5.2. Chronic heart failure and poly(ADP-ribose) polymerase

The role of oxidative and nitrosative stress in chronic heart failure has been intensively investigated recently [21, 27, 28, 237-239, 246-248]. Reactive oxygen species (superoxide, hydrogen peroxide, and hydroxyl radical) are overproduced in the failing myocardium [20, 289]. There is also an overproduction of nitric oxide, due to the expression of the inducible isoform of NO synthase [290, 291]. Importantly, a recent study has suggested correlation between chronic overexpression of NO synthase and peroxynitrite generation with cardiac enlargement, conduction defects, sudden cardiac death, and, less commonly, heart failure in mice [292]. In the present, banding-induced CHF model, evidence was also found for up-regulation of the endothelial isoform of NOS [293]. The combination of NO and superoxide yields peroxynitrite, which is able to trigger DNA single strand breakage and activation of PARP [109]. Peroxynitrite generation has been demonstrated in various models of CHF, including the current model of banding [294], and this free radical has been shown to impair cardiac function via multiple mechanisms [20, 295]. The increased sensitivity of the myocytes to the toxic effects of NO has been directly demonstrated in a banding-induced cardiac hypertrophy model [296].

A recently characterized mechanism of myocardial dysfunction involves the activation of the nuclear enzyme PARP by DNA single-strand breaks generated in response to

increased oxidative and nitrosative stress. Evidence for the importance of this pathway has been demonstrated in hearts subjected to regional or global ischemia and reperfusion [297]. The mode of PARP inhibitors' cardioprotective action involves a conservation of myocardial energetics, as well as a prevention of the up-regulation of various proinflammatory pathways (cytokines, adhesion receptors, and mononuclear cell infiltration) triggered by ischemia and reperfusion [109]. It is conceivable that PARP inhibition exerts beneficial effects in the current model by affecting both above-referenced pathways of injury and also by suppressing positive feedback cycles initiated by them. It is more likely that the reduction in myocardial hypertrophy by INO-1001 (which is thought to be mediated by the up-regulation of growth factors) is mediated by the PARP-mediated modulation of signal transduction and gene expression pathways. Indeed, recent studies implicate the ability of PARP to regulate the expression of growth factors in vitro [298].

Multiple reports indicate the importance of PARP activation in the development of mitochondrial dysfunction under conditions of oxidative stress [124, 299, 300]. Even though PARP is widely considered as a nuclear enzyme, there may also be a mitochondrial isoform [299], and there is a nuclear-to mitochondrial signaling process, which initiates early mitochondrial alterations, as demonstrated in thymocytes [301], in neurons [124, 134], in cardiac myocytes in vitro [274] and in myocardial infarction in vivo [302]. The current findings, demonstrating that PARP inhibition with INO-1001 or genetic PARP deficiency reverse mitochondrial-to-nuclear translocation of AIF in CHF, are consistent with prior studies demonstrating that PARP-1 regulates the translocation of this cell death factor.

It is interesting to note that PARP inhibitor prevented PAR accumulation at 4 or 9 weeks after the banding, but this inhibitory effect is not obvious at 1 week. The same pattern was seen in Fig. 22, where the inhibition of AIF translocation by INO-1001 was less effective at 1 week than at 4 or 9 weeks. Considering the gradual increase in plasma and myocardial INO-1001 levels seen in this study, it is conceivable that myocardial INO-1001 levels at 1 week did not yet reach sufficient concentrations at the beginning of the study to provide full inhibition of PARP. Additional studies, with delayed administration of the PARP inhibitor are needed to determine the therapeutic window of

opportunity and to evaluate whether delayed treatment with PARP inhibitors is able to arrest cardiac hypertrophy or restore myocardial function in CHF.

Prior studies have demonstrated the importance of apoptosis, caspases [303, 304], and a variety of cellular pathways, including protein kinase C (PKC) activation [305, 306] in the pathogenesis of CHF. There are also many studies demonstrating TUNEL positivity in a small (approximately 0.3%) population of cells in murine CHF models [307]. In human samples, the percentage of TUNEL positivity can be higher (up to 2%) [308, 309]. What, then, is the relationship between PARP activation, AIF translocation, and the previously described pathways of apoptosis and CHF? First of all, it should be emphasized that although AIF is termed "apoptosis-inducing" factor, its role goes beyond apoptosis, and it plays a role in a variety of cell death processes (necrotic, oxidant stress induced, and mixed type) [310, 311]. Thus, AIF translocation per se should not be viewed as a hallmark or marker of apoptosis. Indeed, the very small percentage of TUNEL-positive myocytes seen in CHF myocardium is consistent with this view. AIF translocation can lead to DNA fragmentation, which, however, is caspase-independent. Therefore, its pattern is different from the typical, caspase-mediated DNA cleavage pattern and may not be detectable by conventional TUNEL assays. Furthermore, it is not yet clear whether AIF translocation in CHF is a sufficient or merely a necessary factor for its ability to induce its hallmark large-scale chromatin condensation.

It is also important to distinguish between PARP cleavage (a marker, but not necessarily an executor of apoptosis) and PARP activation (induced by DNA strand breaks). The latter process can only occur when PARP is uncleaved, because cleaved PARP is catalytically inactive [109, 312]. The fact that widespread poly(ADP-ribose) accumulation can be seen in the CHF myocardium indicates that some (possibly most of the) PARP remains in the uncleaved and functionally active state. In fact, a recent report finds no evidence for PARP cleavage in murine or human hearts with CHF [313]. The protection against CHF reported by caspase inhibitors therefore is most likely related to a pathway that is parallel and independent from the pathway governed by PARP activation.

Regarding potential connections between PKC and PARP, recent work, conducted using an in vitro model of diabetic complications (endothelial cells placed in high

glucose) demonstrates that protein kinase C activation is governed by GAPDH, and in that experimental system PARP inhibitors indirectly inhibit PKC activation, by preventing GAPDH poly(ADP-ribosyl)ation [300]. Currently, it is unknown whether PARP/PKC interactions are also present in CHF.

In a prior model of CHF induced by chronic coronary artery ligation, the phenanthridinone-based PARP inhibitor PJ34 was found to attenuate myocardial hypertrophy, and improved the endothelial function of blood vessels [132]. The current study extends these findings. The novel aspects of the current work include direct demonstration that PARP inhibition improves cardiac output, attenuates cardiac fibrosis, and tends to reduce CHF-related mortality in a model of banding induced CHF. Our results demonstrate the phenomenon of mitochondrial-to-nuclear translocation of AIF in CHF and implicates the regulatory role of PARP in this process. Recently, a study [313] demonstrated an overexpression of PARP enzyme in murine and human CHF models. Thus, the increased poly(ADP-ribose) staining seen in our studies may be a combined consequence of PARP activation and PARP upregulation.

5.3. Myocardial ischemia-reperfusion and hydrogen sulfide

In the current study, administration of H_2S at the time of reperfusion was shown to limit the extent of myocardial infarction in an in vivo murine model. A dose–response study revealed that H_2S displayed a biphasic reduction in infarct size as has previously been reported [236]. Importantly, the decrease in infarct size translated into reduced LV dilatation and improved LV function as measured by echocardiography. In an effort to further explore the role of H_2S in myocardial infarction, we generated cardiac-specific transgenic mice with overexpression of the H_2S producing enzyme CGL (αMHC-CGL-Tg), resulting in increased myocardial levels of H_2S. These mice were also found to have a reduction in infarct size after MI-R injury establishing that exogenous or endogenous increases in H_2S protect against myocardial infarction. This finding that modulation of endogenous H_2S is cardioprotective is supported by the recent work [314] which showed that pharmacologic inhibition of CGL resulted in an increase in infarct size in a rat model of MI-R.

Given that H_2S has been reported [167] to act as a vasodilator we assessed whether H_2S modulated systemic hemodynamics. A dose–response study in mice implanted with radiotelemetric pressure transducers revealed no effect on systemic blood pressure and heart rate in conscious animals until doses well outside the therapeutic range were administered. These findings ruled out the possibility that H_2S was altering afterload and thus impacting myocardial oxygen demand. We next assessed the impact of H_2S on myocardial inflammation after infarction. Histological analysis revealed a substantial decrease in hemorrhage and necrosis as well as a decrease in the number of leukocytes within the ischemic zone. MPO analysis quantitatively confirmed a significant decrease in neutrophils within the myocardial tissue after MI-R. The evaluation of inflammatory cytokines revealed myocardial levels of IL-1β to be markedly reduced to those observed in sham-operated mice. Additionally, H_2S was found to potently reduce in vivo leukocyte-endothelial cell interactions, as assessed by intravital microscopy. This finding is bolstered by a recent report [315] showing that H_2S limited aspirin-induced inflammation by inhibiting leukocyte rolling, adhesion and subsequent diapedesis. Inhibition of leukocyte transmigration is one possible mechanism by which H_2S restrains the extent of inflammation and thereby limits the extent of myocardial infarction. A number of studies [316] have cited the influence of IL-1β on the development of ischemic injury in the heart and the pathogenic role of inflammatory cytokines in the recruitment and subsequent migration of inflammatory cells into the heart [317]. Another important area of study in myocardial cytoprotection is the preservation of mitochondrial function [214, 318]. The mitochondria are unique in that not only are they the site of energy production but also a central locus in the regulation of cell death [319, 320]. The maintenance of oxidative phosphorylation to forgo myocyte death in the face of ischemic injury has long been recognized as a critical event after myocardial infarction [321]. To optimize administration of the H_2S donor for in vitro experiments we first performed a dose–response in isolated cardiac mitochondria to determine its effect on respiration. As has been previously reported in a placental cell line [322] we found a dose-dependent reduction in mitochondrial oxygen consumption followed by complete recovery to baseline. Based on these findings, we selected 10 μM, which reduced mitochondrial respiration rate by 65%, in a clear and reproducible manner. Mitochondria treated with 10 μM H_2S were found to have a significantly

greater recovery of posthypoxic respiration rate. These experiments were followed by the discovery that mitochondria isolated from mice given H_2S at the time of reperfusion (in vivo MI-R) displayed preserved mitochondrial function 24 hr following reperfusion as noted by increased complex I and II efficiency. Electron microscopy revealed a striking reduction in mitochondrial swelling and increased matrix density in mice receiving H_2S, further suggesting a prominent role for the preservation of mitochondrial function in the observed cytoprotection.

H_2S is known [160] to be a potent and reversible inhibitor of cytochrome c oxidase (complex IV of the mitochondrial electron transport chain) and the profound nature of H_2S ability to influence whole organism metabolism was recently demonstrated by its ability to induce a suspended animation-like state in mice [161]. Another possible mechanism for H_2S protective action on mitochondrial function may lie in its ability to modulate cellular respiration during reperfusion. The inhibition of mitochondrial respiration has been shown [177, 178] to protect against MI-R injury by limiting the generation of reactive oxygen species and diminishing the degree of mitochondrial uncoupling leading to decreased infarct size and preserved function. The accumulation of evidence that mitochondrial function and structure was preserved after myocardial infarction in mice treated with H_2S was further corroborated by the decreased activation of caspase-3 and a decrease in the number of TUNEL positive nuclei, suggesting that H_2S was capable of inhibiting the progression of apoptosis after MI-R injury. The capacity of H_2S to modulate apoptosis has been controversial with some groups reporting H_2S mediating apoptosis [323-326] and others citing inhibition [327-329]. However, it is important to note that none of the studies to date have used in vivo model systems and have used varying concentrations of H_2S, some well outside the physiologically relevant range.

6. CONCLUSION

Taken together, our results show that oxidative and nitrosative stress play an important role of the disease models studied. Specifically, our data suggest that although the main oxysterol component of oxLDL particles, the 7-ketocholesterol is capable of activating PARP in endothelial cells, but it cannot induce endothelial dysfunction alone. It is conceivable that 7-ketocholesterols and other oxysterols found in oxLDL may be responsible together for the development of endothelial dysfunction induced by these lipoproteins. Our experimental results also support the view that PARP activation importantly contributes to the pathogenesis of cardiovascular dysfunction in experimental models of CHF and strengthens the notion that PARP inhibition may represent a novel approach for the experimental therapy of CHF. Finally, either exogenous or endogenous increases in hydrogen sulfide at the time of reperfusion limits the extent of myocardial infarction. This protection is accompanied by a decrease in myocardial inflammation and a preservation of mitochondrial function. These results stress the importance of oxidative and nitrosative stress in the investigated cardiovascular diseases and may lead to novel approaches in the therapies of atherosclerosis, ischemic heart disease and chronic heart failure.

7. ABSTRACT

Oxidative and nitrosative stress play an important role in the pathogenesis of several cardiovascular diseases, but the involved downstream pathways are still incompletely understood. Based on recent investigations, poly(ADP-ribose) polymerase and hydrogen sulfide may play an important part in these processes. The purpose of the present thesis was to further elucidate the role of poly(ADP-ribose) polymerase and hydrogen sulfide in models of cardiovascular diseases involving free radicals. In our first experiments we investigated the effects of the main oxysterol 7-ketocholesterol on the activity of endothelial poly(ADP-ribose) polymerase and on endothelium-dependent vasorelaxant function. In further experiments we investigated the role of poly(ADP-ribose) polymerase in the process of cardiac remodeling and heart failure in a mouse model of heart failure induced by transverse aortic constriction. Finally, we investigated whether hydrogen sulfide has a potential to ameliorate myocardial ischemia-reperfusion injury in vivo and to explore what could be the possible underlying mechanism of action. Our experimental results indicate that: (1) although 7-ketocholesterol can activate poly(ADP-ribose) polymerase in endothelial cells, it is not sufficient on its own to cause impairment in the endothelium-dependent vascular reactivity; (2) poly(ADP-ribos)ylation plays an important role in the pathogenesis of banding-induced heart failure; (3) hydrogen sulfide may be of value in cytoprotection during the evolution of myocardial infarction and that either administration of hydrogen sulfide or the modulation of endogenous production may be of clinical benefit in ischemic disorders. These results stress the importance of oxidative and nitrosative stress in the investigated cardiovascular diseases and may lead to novel approaches in the therapies of atherosclerosis, ischemic heart disease and chronic heart failure.

ÖSSZEFOGLALÁS

Az oxidatív és nitrozatív stressz fontos szerepet játszik számos kardiovaszkuláris betegség kialakulásában, de az ebben szerepet játszó biokémiai útvonalak még nem teljesen tisztázottak. Az utóbbi idők vizsgálatai alapján a poli(ADP-ribóz) polimeráznak és a hidrogén szulfidnak jelentős szerepe lehet ezekben a folyamatokban. A jelen értekezés célja a poli(ADP-ribóz) polimeráz szerepének további felderítése és a hidrogén szulfid hatásainak vizsgálata volt szabad gyökökkel összefüggő kardiovaszkuláris betegségek modelljeiben. Első kísérletsorozatunkban megvizsgáltuk a legjelentősebb oxiszterol, a 7-ketokoleszterol hatását az endoteliális poli(ADP-ribóz) polimeráz aktivitására és az endotéliumfüggő vazorelaxációra. További kísérletekben a poli(ADP-ribóz) polimeráz szerepét tanulmányoztuk a szív szívelégtelenség során létrejövő átépülésében egy egér szívelégtelenség modell felhasználásával az aorta szűkítése segítségével. Végül megvizsgáltuk, hogy a hidrogén szulfid rendelkezik-e miokardiális iszkémia-reperfúziós sérülést csökkentő hatással és mi lehet ennek a mechanizmusa. Kísérleti eredményeink azt mutatják, hogy: (1) noha a 7-ketokoleszterol képes aktiválni a poli(ADP-ribóz) polimerázt endotélsejtekben, azonban önmagában nem befolyásolja az endotélfüggő vaszkuláris reaktivitást; (2) a poli(ADP-ribóz) polimeráz jelentős szerepet játszik az alkalmazott módszerrel létrehozott szívelégtelenség kialakulásában; (3) a hidrogén szulfid citoprotektív hatású lehet a miokardiális infarktus kialakulása során, és mind exogén hidrogén szulfid adása, mind az endogén termelés szabályozása klinikai előnyökkel járhat iszkémiás betegségekben. Az eredmények megerősítik az oxidatív és nitrozatív stressz szerepének jelentőségét a vizsgált kardiovaszkuláris betegségekben, valamint új megközelítésekhez vezethetnek az ateroszklerózis, az iszkémiás szívbetegség és a krónikus szívelégtelenség terápiájában.

8. REFERENCES

1. Sans S, Kesteloot H, and Kromhout D. The burden of cardiovascular diseases mortality in Europe. Task Force of the European Society of Cardiology on Cardiovascular Mortality and Morbidity Statistics in Europe. *Eur Heart J*, 1997. 18(12): p. 1231-48.
2. Dayer M and Cowie MR. Heart failure: diagnosis and healthcare burden. *Clin Med*, 2004. 4(1): p. 13-8.
3. Kesteloot H, Sans S, and Kromhout D. Dynamics of cardiovascular and all-cause mortality in Western and Eastern Europe between 1970 and 2000. *Eur Heart J*, 2006. 27(1): p. 107-13.
4. Libby P. Changing concepts of atherogenesis. *J Intern Med*, 2000. 247(3): p. 349-58.
5. Stary HC, Chandler AB, Dinsmore RE, Fuster V, Glagov S, Insull W, Jr., Rosenfeld ME, Schwartz CJ, Wagner WD, and Wissler RW. A definition of advanced types of atherosclerotic lesions and a histological classification of atherosclerosis. A report from the Committee on Vascular Lesions of the Council on Arteriosclerosis, American Heart Association. *Circulation*, 1995. 92(5): p. 1355-74.
6. Weissberg PL. Atherogenesis: current understanding of the causes of atheroma. *Heart*, 2000. 83(2): p. 247-52.
7. Fuster V. Lewis A. Conner Memorial Lecture. Mechanisms leading to myocardial infarction: insights from studies of vascular biology. *Circulation*, 1994. 90(4): p. 2126-46.
8. Selwyn AP, Kinlay S, Libby P, and Ganz P. Atherogenic lipids, vascular dysfunction, and clinical signs of ischemic heart disease. *Circulation*, 1997. 95(1): p. 5-7.
9. Davies MJ. The pathophysiology of acute coronary syndromes. *Heart*, 2000. 83(3): p. 361-6.
10. Ridker PM. Evaluating novel cardiovascular risk factors: can we better predict heart attacks? *Ann Intern Med*, 1999. 130(11): p. 933-7.
11. Tunstall-Pedoe H, Kuulasmaa K, Amouyel P, Arveiler D, Rajakangas AM, and Pajak A. Myocardial infarction and coronary deaths in the World Health

Organization MONICA Project. Registration procedures, event rates, and case-fatality rates in 38 populations from 21 countries in four continents. *Circulation*, 1994. 90(1): p. 583-612.

12. Ridker P and Libby P. Nontraditional coronary risk factors and vascular biology: the frontiers of preventive cardiology. *J Investig Med*, 1998. 46(8): p. 338-50.
13. Mann DL. Basic mechanisms of disease progression in the failing heart: the role of excessive adrenergic drive. *Prog Cardiovasc Dis*, 1998. 41(1 Suppl 1): p. 1-8.
14. de Tombe PP. Altered contractile function in heart failure. *Cardiovasc Res*, 1998. 37(2): p. 367-80.
15. McMurray JJ and Pfeffer MA. Heart failure. *Lancet*, 2005. 365(9474): p. 1877-89.
16. Armstrong PW and Moe GW. Medical advances in the treatment of congestive heart failure. *Circulation*, 1993. 88(6): p. 2941-52.
17. Droge W. Free radicals in the physiological control of cell function. *Physiol Rev*, 2002. 82(1): p. 47-95.
18. Mozsik G, Fiegler M, Juricskay I, Mezey B, and Toth K. Oxygen free radicals, lipid metabolism, and whole blood and plasma viscosity in the prevention and treatment of human cardiovascular diseases. *Bibl Nutr Dieta*, 1992(49): p. 111-24.
19. Kesmarky G, Toth K, Vajda G, Habon L, Halmosi R, and Roth E. Hemorheological and oxygen free radical associated alterations during and after percutaneous transluminal coronary angioplasty. *Clin Hemorheol Microcirc*, 2001. 24(1): p. 33-41.
20. Mihm MJ, Coyle CM, Schanbacher BL, Weinstein DM, and Bauer JA. Peroxynitrite induced nitration and inactivation of myofibrillar creatine kinase in experimental heart failure. *Cardiovasc Res*, 2001. 49(4): p. 798-807.
21. Singh N, Dhalla AK, Seneviratne C, and Singal PK. Oxidative stress and heart failure. *Mol Cell Biochem*, 1995. 147(1-2): p. 77-81.
22. Fortuno A, Olivan S, Beloqui O, San Jose G, Moreno MU, Diez J, and Zalba G. Association of increased phagocytic NADPH oxidase-dependent superoxide production with diminished nitric oxide generation in essential hypertension. *J Hypertens*, 2004. 22(11): p. 2169-75.

23. Ward NC, Hodgson JM, Puddey IB, Mori TA, Beilin LJ, and Croft KD. Oxidative stress in human hypertension: association with antihypertensive treatment, gender, nutrition, and lifestyle. *Free Radic Biol Med*, 2004. 36(2): p. 226-32.
24. Ortona E, Margutti P, Matarrese P, Franconi F, and Malorni W. Redox state, cell death and autoimmune diseases: A gender perspective. *Autoimmun Rev*, 2008. 7(7): p. 579-84.
25. Kiss L and Szabo C. The pathogenesis of diabetic complications: the role of DNA injury and poly(ADP-ribose) polymerase activation in peroxynitrite-mediated cytotoxicity. *Mem Inst Oswaldo Cruz*, 2005. 100 Suppl 1: p. 29-37.
26. Forbes JM, Coughlan MT, and Cooper ME. Oxidative stress as a major culprit in kidney disease in diabetes. *Diabetes*, 2008. 57(6): p. 1446-54.
27. Sawyer DB, Siwik DA, Xiao L, Pimentel DR, Singh K, and Colucci WS. Role of oxidative stress in myocardial hypertrophy and failure. *J Mol Cell Cardiol*, 2002. 34(4): p. 379-88.
28. Dhalla NS, Temsah RM, and Netticadan T. Role of oxidative stress in cardiovascular diseases. *J Hypertens*, 2000. 18(6): p. 655-73.
29. Brownlee M. Biochemistry and molecular cell biology of diabetic complications. *Nature*, 2001. 414(6865): p. 813-20.
30. Lee HC and Wei YH. Mitochondrial role in life and death of the cell. *J Biomed Sci*, 2000. 7(1): p. 2-15.
31. Babior BM. The NADPH oxidase of endothelial cells. *IUBMB Life*, 2000. 50(4-5): p. 267-9.
32. Babior BM, Lambeth JD, and Nauseef W. The neutrophil NADPH oxidase. *Arch Biochem Biophys*, 2002. 397(2): p. 342-4.
33. Vignais PV. The superoxide-generating NADPH oxidase: structural aspects and activation mechanism. *Cell Mol Life Sci*, 2002. 59(9): p. 1428-59.
34. Griendling KK, Sorescu D, and Ushio-Fukai M. NAD(P)H oxidase: role in cardiovascular biology and disease. *Circ Res*, 2000. 86(5): p. 494-501.
35. Griendling KK, Minieri CA, Ollerenshaw JD, and Alexander RW. Angiotensin II stimulates NADH and NADPH oxidase activity in cultured vascular smooth muscle cells. *Circ Res*, 1994. 74(6): p. 1141-8.

36. Jones SA, O'Donnell VB, Wood JD, Broughton JP, Hughes EJ, and Jones OT. Expression of phagocyte NADPH oxidase components in human endothelial cells. *Am J Physiol*, 1996. 271(4 Pt 2): p. H1626-34.
37. Jones SA, Wood JD, Coffey MJ, and Jones OT. The functional expression of p47-phox and p67-phox may contribute to the generation of superoxide by an NADPH oxidase-like system in human fibroblasts. *FEBS Lett*, 1994. 355(2): p. 178-82.
38. Suzuki YJ and Ford GD. Redox regulation of signal transduction in cardiac and smooth muscle. *J Mol Cell Cardiol*, 1999. 31(2): p. 345-53.
39. Deby C and Goutier R. New perspectives on the biochemistry of superoxide anion and the efficiency of superoxide dismutases. *Biochem Pharmacol*, 1990. 39(3): p. 399-405.
40. Ravanat JL, Di Mascio P, Martinez GR, and Medeiros MH. Singlet oxygen induces oxidation of cellular DNA. *J Biol Chem*, 2001. 276(8): p. 40601-4.
41. Kaneko T and Tahara S. Formation of 8-oxo-2'-deoxyguanosine in the DNA of human diploid fibroblasts by treatment with linoleic acid hydroperoxide and ferric ion. *Lipids*, 2000. 35(9): p. 961-5.
42. Uchida K. Role of reactive aldehyde in cardiovascular diseases. *Free Radic Biol Med*, 2000. 28(12): p. 1685-96.
43. Freeman B. Free radical chemistry of nitric oxide. Looking at the dark side. *Chest*, 1994. 105(3 Suppl): p. 79S-84S.
44. Powell SR and Tortolani AJ. Recent advances in the role of reactive oxygen intermediates in ischemic injury. I. Evidence demonstrating presence of reactive oxygen intermediates; II. Role of metals in site-specific formation of radicals. *J Surg Res*, 1992. 53(4): p. 417-29.
45. Palmer RM, Rees DD, Ashton DS, and Moncada S. L-arginine is the physiological precursor for the formation of nitric oxide in endothelium-dependent relaxation. *Biochem Biophys Res Commun*, 1988. 153(3): p. 1251-6.
46. Bredt DS, Hwang PM, and Snyder SH. Localization of nitric oxide synthase indicating a neural role for nitric oxide. *Nature*, 1990. 347(6295): p. 768-70.
47. Xie QW, Cho HJ, Calaycay J, Mumford RA, Swiderek KM, Lee TD, Ding A, Troso T, and Nathan C. Cloning and characterization of inducible nitric oxide synthase from mouse macrophages. *Science*, 1992. 256(5054): p. 225-8.

48. Lamas S, Marsden PA, Li GK, Tempst P, and Michel T. Endothelial nitric oxide synthase: molecular cloning and characterization of a distinct constitutive enzyme isoform. *Proc Natl Acad Sci U S A*, 1992. 89(14): p. 6348-52.
49. Bogdan C, Rollinghoff M, and Diefenbach A. Reactive oxygen and reactive nitrogen intermediates in innate and specific immunity. *Curr Opin Immunol*, 2000. 12(1): p. 64-76.
50. MacMicking J, Xie QW, and Nathan C. Nitric oxide and macrophage function. *Annu Rev Immunol*, 1997. 15: p. 323-50.
51. Stamler JS, Singel DJ, and Loscalzo J. Biochemistry of nitric oxide and its redox-activated forms. *Science*, 1992. 258(5090): p. 1898-902.
52. Assem M, Teyssier JR, Benderitter M, Terrand J, Laubriet A, Javouhey A, David M, and Rochette L. Pattern of superoxide dismutase enzymatic activity and RNA changes in rat heart ventricles after myocardial infarction. *Am J Pathol*, 1997. 151(2): p. 549-55.
53. Li Y, Huang TT, Carlson EJ, Melov S, Ursell PC, Olson JL, Noble LJ, Yoshimura MP, Berger C, Chan PH, Wallace DC, and Epstein CJ. Dilated cardiomyopathy and neonatal lethality in mutant mice lacking manganese superoxide dismutase. *Nat Genet*, 1995. 11(4): p. 376-81.
54. Kloner RA, Przyklenk K, and Whittaker P. Deleterious effects of oxygen radicals in ischemia/reperfusion. Resolved and unresolved issues. *Circulation*, 1989. 80(5): p. 1115-27.
55. Seiler KS and Starnes JW. Exogenous GSH protection during hypoxia-reoxygenation of the isolated rat heart: impact of hypoxia duration. *Free Radic Res*, 2000. 32(1): p. 41-55.
56. Murphy ME, Scholich H, and Sies H. Protection by glutathione and other thiol compounds against the loss of protein thiols and tocopherol homologs during microsomal lipid peroxidation. *Eur J Biochem*, 1992. 210(1): p. 139-46.
57. Scholich H, Murphy ME, and Sies H. Antioxidant activity of dihydrolipoate against microsomal lipid peroxidation and its dependence on alpha-tocopherol. *Biochim Biophys Acta*, 1989. 1001(3): p. 256-61.
58. Ernster L and Dallner G. Biochemical, physiological and medical aspects of ubiquinone function. *Biochim Biophys Acta*, 1995. 1271(1): p. 195-204.

59. Gutteridge JM and Quinlan GJ. Antioxidant protection against organic and inorganic oxygen radicals by normal human plasma: the important primary role for iron-binding and iron-oxidising proteins. *Biochim Biophys Acta*, 1993. 1156(2): p. 144-50.
60. Souza AV, Petretski JH, Demasi M, Bechara EJ, and Oliveira PL. Urate protects a blood-sucking insect against hemin-induced oxidative stress. *Free Radic Biol Med*, 1997. 22(1-2): p. 209-14.
61. Otani K, Shimizu S, Chijiiwa K, Morisaki T, Yamaguchi T, Yamaguchi K, Kuroki S, and Tanaka M. Administration of bacterial lipopolysaccharide to rats induces heme oxygenase-1 and formation of antioxidant bilirubin in the intestinal mucosa. *Dig Dis Sci*, 2000. 45(12): p. 2313-9.
62. Whiteman M, Armstrong JS, Chu SH, Jia-Ling S, Wong BS, Cheung NS, Halliwell B, and Moore PK. The novel neuromodulator hydrogen sulfide: an endogenous peroxynitrite 'scavenger'? *J Neurochem*, 2004. 90(3): p. 765-8.
63. Davies KJ, Lin SW, and Pacifici RE. Protein damage and degradation by oxygen radicals. IV. Degradation of denatured protein. *J Biol Chem*, 1987. 262(20): p. 9914-20.
64. Davies KJ, Delsignore ME, and Lin SW. Protein damage and degradation by oxygen radicals. II. Modification of amino acids. *J Biol Chem*, 1987. 262(20): p. 9902-7.
65. Stadtman ER. Oxidation of free amino acids and amino acid residues in proteins by radiolysis and by metal-catalyzed reactions. *Annu Rev Biochem*, 1993. 62: p. 797-821.
66. Hammarqvist F, Wernerman J, Ali R, von der Decken A, and Vinnars E. Addition of glutamine to total parenteral nutrition after elective abdominal surgery spares free glutamine in muscle, counteracts the fall in muscle protein synthesis, and improves nitrogen balance. *Ann Surg*, 1989. 209(4): p. 455-61.
67. Keisari Y, Braun L, and Flescher E. The oxidative burst and related phenomena in mouse macrophages elicited by different sterile inflammatory stimuli. *Immunobiology*, 1983. 165(1): p. 78-89.

68. Nathan CF and Root RK. Hydrogen peroxide release from mouse peritoneal macrophages: dependence on sequential activation and triggering. *J Exp Med*, 1977. 146(6): p. 1648-62.
69. Hampton MB, Kettle AJ, and Winterbourn CC. Inside the neutrophil phagosome: oxidants, myeloperoxidase, and bacterial killing. *Blood*, 1998. 92(9): p. 3007-17.
70. Schoonbroodt S, Legrand-Poels S, Best-Belpomme M, and Piette J. Activation of the NF-kappaB transcription factor in a T-lymphocytic cell line by hypochlorous acid. *Biochem J*, 1997. 321 (Pt 3): p. 777-85.
71. Ignarro LJ, Wood KS, and Wolin MS. Regulation of purified soluble guanylate cyclase by porphyrins and metalloporphyrins: a unifying concept. *Adv Cyclic Nucleotide Protein Phosphorylation Res*, 1984. 17: p. 267-74.
72. Gerzer R, Bohme E, Hofmann F, and Schultz G. Soluble guanylate cyclase purified from bovine lung contains heme and copper. *FEBS Lett*, 1981. 132(1): p. 71-4.
73. Rando RR and Kishi Y. Structural basis of protein kinase C activation by diacylglycerols and tumor promoters. *Biochemistry*, 1992. 31(8): p. 2211-8.
74. Ignarro LJ and Kadowitz PJ. The pharmacological and physiological role of cyclic GMP in vascular smooth muscle relaxation. *Annu Rev Pharmacol Toxicol*, 1985. 25: p. 171-91.
75. Radomski MW, Palmer RM, and Moncada S. The anti-aggregating properties of vascular endothelium: interactions between prostacyclin and nitric oxide. *Br J Pharmacol*, 1987. 92(3): p. 639-46.
76. Archer SL, Huang JM, Hampl V, Nelson DP, Shultz PJ, and Weir EK. Nitric oxide and cGMP cause vasorelaxation by activation of a charybdotoxin-sensitive K channel by cGMP-dependent protein kinase. *Proc Natl Acad Sci U S A*, 1994. 91(16): p. 7583-7.
77. Burke TM and Wolin MS. Hydrogen peroxide elicits pulmonary arterial relaxation and guanylate cyclase activation. *Am J Physiol*, 1987. 252(4 Pt 2): p. H721-32.
78. Mittal CK and Murad F. Activation of guanylate cyclase by superoxide dismutase and hydroxyl radical: a physiological regulator of guanosine 3',5'-monophosphate formation. *Proc Natl Acad Sci U S A*, 1977. 74(10): p. 4360-4.

79. White AA, Crawford KM, Patt CS, and Lad PJ. Activation of soluble guanylate cyclase from rat lung by incubation or by hydrogen peroxide. *J Biol Chem*, 1976. 251(23): p. 7304-12.
80. Wang GL, Jiang BH, Rue EA, and Semenza GL. Hypoxia-inducible factor 1 is a basic-helix-loop-helix-PAS heterodimer regulated by cellular O2 tension. *Proc Natl Acad Sci U S A*, 1995. 92(12): p. 5510-4.
81. Semenza GL. HIF-1: mediator of physiological and pathophysiological responses to hypoxia. *J Appl Physiol*, 2000. 88(4): p. 1474-80.
82. Zhu H and Bunn HF. Oxygen sensing and signaling: impact on the regulation of physiologically important genes. *Respir Physiol*, 1999. 115(2): p. 239-47.
83. Acker H. Mechanisms and meaning of cellular oxygen sensing in the organism. *Respir Physiol*, 1994. 95(1): p. 1-10.
84. Bunn HF and Poyton RO. Oxygen sensing and molecular adaptation to hypoxia. *Physiol Rev*, 1996. 76(3): p. 839-85.
85. Prabhakar NR. Oxygen sensing by the carotid body chemoreceptors. *J Appl Physiol*, 2000. 88(6): p. 2287-95.
86. Pan N and Hori H. The interaction of acteoside with mitochondrial lipid peroxidation as an ischemia/reperfusion injury model. *Adv Exp Med Biol*, 1994. 361: p. 319-25.
87. Packer L, Valenza M, Serbinova E, Starke-Reed P, Frost K, and Kagan V. Free radical scavenging is involved in the protective effect of L-propionyl-carnitine against ischemia-reperfusion injury of the heart. *Arch Biochem Biophys*, 1991. 288(2): p. 533-7.
88. Takeda N, Ota Y, Tanaka Y, Shikata C, Hayashi Y, Nemoto S, Tanamura A, Iwai T, and Nakamura I. Myocardial adaptive changes and damage in ischemic heart disease. *Ann N Y Acad Sci*, 1996. 793: p. 282-8.
89. Ambrosio G, Zweier JL, Duilio C, Kuppusamy P, Santoro G, Elia PP, Tritto I, Cirillo P, Condorelli M, Chiariello M, and et al. Evidence that mitochondrial respiration is a source of potentially toxic oxygen free radicals in intact rabbit hearts subjected to ischemia and reflow. *J Biol Chem*, 1993. 268(25): p. 18532-41.
90. Gille L and Nohl H. Analyses of the molecular mechanism of adriamycin-induced cardiotoxicity. *Free Radic Biol Med*, 1997. 23(5): p. 775-82.

91. Bogoyevitch MA, Ng DC, Court NW, Draper KA, Dhillon A, and Abas L. Intact mitochondrial electron transport function is essential for signalling by hydrogen peroxide in cardiac myocytes. *J Mol Cell Cardiol*, 2000. 32(8): p. 1469-80.
92. Sussman MS and Bulkley GB. Oxygen-derived free radicals in reperfusion injury. *Methods Enzymol*, 1990. 186: p. 711-23.
93. Savage MK and Reed DJ. Release of mitochondrial glutathione and calcium by a cyclosporin A-sensitive mechanism occurs without large amplitude swelling. *Arch Biochem Biophys*, 1994. 315(1): p. 142-52.
94. Radons J, Heller B, Burkle A, Hartmann B, Rodriguez ML, Kroncke KD, Burkart V, and Kolb H. Nitric oxide toxicity in islet cells involves poly(ADP-ribose) polymerase activation and concomitant NAD+ depletion. *Biochem Biophys Res Commun*, 1994. 199(3): p. 1270-7.
95. Lindahl T, Satoh MS, Poirier GG, and Klungland A. Post-translational modification of poly(ADP-ribose) polymerase induced by DNA strand breaks. *Trends Biochem Sci*, 1995. 20(10): p. 405-11.
96. Heller B, Wang ZQ, Wagner EF, Radons J, Burkle A, Fehsel K, Burkart V, and Kolb H. Inactivation of the poly(ADP-ribose) polymerase gene affects oxygen radical and nitric oxide toxicity in islet cells. *J Biol Chem*, 1995. 270(19): p. 11176-80.
97. Kerr JF, Wyllie AH, and Currie AR. Apoptosis: a basic biological phenomenon with wide-ranging implications in tissue kinetics. *Br J Cancer*, 1972. 26(4): p. 239-57.
98. Orrenius S, Zhivotovsky B, and Nicotera P. Regulation of cell death: the calcium-apoptosis link. *Nat Rev Mol Cell Biol*, 2003. 4(7): p. 552-65.
99. Zhang M and Chen L. Status of cytokines in ischemia reperfusion induced heart injury. *Cardiovasc Hematol Disord Drug Targets*, 2008. 8(3): p. 161-72.
100. Dinarello CA. The IL-1 family and inflammatory diseases. *Clin Exp Rheumatol*, 2002. 20(5 Suppl 27): p. S1-13.
101. Szabo C. Hydrogen sulphide and its therapeutic potential. *Nat Rev Drug Discov*, 2007. 6(11): p. 917-35.
102. Hiromatsu Y, Sato M, Yamada K, and Nonaka K. Nicotinamide and 3-aminobenzamide inhibit recombinant human interferon-gamma-induced HLA-DR

antigen expression, but not HLA-A, B, C antigen expression, on cultured human thyroid cells. *Clin Endocrinol (Oxf)*, 1992. 36(1): p. 91-5.

103. de Murcia G, Schreiber V, Molinete M, Saulier B, Poch O, Masson M, Niedergang C, and Menissier de Murcia J. Structure and function of poly(ADP-ribose) polymerase. *Mol Cell Biochem*, 1994. 138(1-2): p. 15-24.
104. de Murcia JM, Niedergang C, Trucco C, Ricoul M, Dutrillaux B, Mark M, Oliver FJ, Masson M, Dierich A, LeMeur M, Walztinger C, Chambon P, and de Murcia G. Requirement of poly(ADP-ribose) polymerase in recovery from DNA damage in mice and in cells. *Proc Natl Acad Sci U S A*, 1997. 94(14): p. 7303-7.
105. Szabo C and Dawson VL. Role of poly(ADP-ribose) synthetase in inflammation and ischaemia-reperfusion. *Trends Pharmacol Sci*, 1998. 19(7): p. 287-98.
106. Le Rhun Y, Kirkland JB, and Shah GM. Cellular responses to DNA damage in the absence of Poly(ADP-ribose) polymerase. *Biochem Biophys Res Commun*, 1998. 245(1): p. 1-10.
107. Rudat V, Kupper JH, and Weber KJ. Trans-dominant inhibition of poly(ADP-ribosyl)ation leads to decreased recovery from ionizing radiation-induced cell killing. *Int J Radiat Biol*, 1998. 73(3): p. 325-30.
108. Davidovic L, Vodenicharov M, Affar EB, and Poirier GG. Importance of poly(ADP-ribose) glycohydrolase in the control of poly(ADP-ribose) metabolism. *Exp Cell Res*, 2001. 268(1): p. 7-13.
109. Virag L and Szabo C. The therapeutic potential of poly(ADP-ribose) polymerase inhibitors. *Pharmacol Rev*, 2002. 54(3): p. 375-429.
110. Oikawa A, Tohda H, Kanai M, Miwa M, and Sugimura T. Inhibitors of poly(adenosine diphosphate ribose) polymerase induce sister chromatid exchanges. *Biochem Biophys Res Commun*, 1980. 97(4): p. 1311-6.
111. Poirier GG, de Murcia G, Jongstra-Bilen J, Niedergang C, and Mandel P. Poly(ADP-ribosyl)ation of polynucleosomes causes relaxation of chromatin structure. *Proc Natl Acad Sci U S A*, 1982. 79(11): p. 3423-7.
112. Park SD, Kim CG, and Kim MG. Inhibitors of poly(ADP-ribose) polymerase enhance DNA strand breaks, excision repair, and sister chromatid exchanges induced by alkylating agents. *Environ Mutagen*, 1983. 5(4): p. 515-25.

113. Satoh MS and Lindahl T. Role of poly(ADP-ribose) formation in DNA repair. *Nature*, 1992. 356(6367): p. 356-8.
114. Lautier D, Lagueux J, Thibodeau J, Menard L, and Poirier GG. Molecular and biochemical features of poly (ADP-ribose) metabolism. *Mol Cell Biochem*, 1993. 122(2): p. 171-93.
115. Herceg Z and Wang ZQ. Functions of poly(ADP-ribose) polymerase (PARP) in DNA repair, genomic integrity and cell death. *Mutat Res*, 2001. 477(1-2): p. 97-110.
116. Szabo C, Zingarelli B, O'Connor M, and Salzman AL. DNA strand breakage, activation of poly (ADP-ribose) synthetase, and cellular energy depletion are involved in the cytotoxicity of macrophages and smooth muscle cells exposed to peroxynitrite. *Proc Natl Acad Sci U S A*, 1996. 93(5): p. 1753-8.
117. Szabo C, Virag L, Cuzzocrea S, Scott GS, Hake P, O'Connor MP, Zingarelli B, Salzman A, and Kun E. Protection against peroxynitrite-induced fibroblast injury and arthritis development by inhibition of poly(ADP-ribose) synthase. *Proc Natl Acad Sci U S A*, 1998. 95(7): p. 3867-72.
118. Affar el B, Shah RG, Dallaire AK, Castonguay V, and Shah GM. Role of poly(ADP-ribose) polymerase in rapid intracellular acidification induced by alkylating DNA damage. *Proc Natl Acad Sci U S A*, 2002. 99(1): p. 245-50.
119. Sakamoto J, Miura T, Shimamoto K, and Horio Y. Predominant expression of Sir2alpha, an NAD-dependent histone deacetylase, in the embryonic mouse heart and brain. *FEBS Lett*, 2004. 556(1-3): p. 281-6.
120. Zhang J. Are poly(ADP-ribosyl)ation by PARP-1 and deacetylation by Sir2 linked? *Bioessays*, 2003. 25(8): p. 808-14.
121. Tissenbaum HA and Guarente L. Increased dosage of a sir-2 gene extends lifespan in Caenorhabditis elegans. *Nature*, 2001. 410(6825): p. 227-30.
122. Cheng HL, Mostoslavsky R, Saito S, Manis JP, Gu Y, Patel P, Bronson R, Appella E, Alt FW, and Chua KF. Developmental defects and p53 hyperacetylation in Sir2 homolog (SIRT1)-deficient mice. *Proc Natl Acad Sci U S A*, 2003. 100(19): p. 10794-9.

123. Vaziri H, Dessain SK, Ng Eaton E, Imai SI, Frye RA, Pandita TK, Guarente L, and Weinberg RA. hSIR2(SIRT1) functions as an NAD-dependent p53 deacetylase. *Cell*, 2001. 107(2): p. 149-59.
124. Yu SW, Wang H, Poitras MF, Coombs C, Bowers WJ, Federoff HJ, Poirier GG, Dawson TM, and Dawson VL. Mediation of poly(ADP-ribose) polymerase-1-dependent cell death by apoptosis-inducing factor. *Science*, 2002. 297(5579): p. 259-63.
125. Chiarugi A. Poly(ADP-ribose) polymerase: killer or conspirator? The 'suicide hypothesis' revisited. *Trends Pharmacol Sci*, 2002. 23(3): p. 122-9.
126. Ehrlich W, Huser H, and Kroger H. Inhibition of the induction of collagenase by interleukin-1 beta in cultured rabbit synovial fibroblasts after treatment with the poly(ADP-ribose)-polymerase inhibitor 3-aminobenzamide. *Rheumatol Int*, 1995. 15(4): p. 171-2.
127. Zingarelli B, Salzman AL, and Szabo C. Genetic disruption of poly (ADP-ribose) synthetase inhibits the expression of P-selectin and intercellular adhesion molecule-1 in myocardial ischemia/reperfusion injury. *Circ Res*, 1998. 83(1): p. 85-94.
128. Simbulan-Rosenthal CM, Ly DH, Rosenthal DS, Konopka G, Luo R, Wang ZQ, Schultz PG, and Smulson ME. Misregulation of gene expression in primary fibroblasts lacking poly(ADP-ribose) polymerase. *Proc Natl Acad Sci U S A*, 2000. 97(21): p. 11274-9.
129. Oei SL and Ziegler M. ATP for the DNA ligation step in base excision repair is generated from poly(ADP-ribose). *J Biol Chem*, 2000. 275(30): p. 23234-9.
130. Ullrich O, Ciftci O, and Hass R. Proteasome activation by poly-ADP-ribose-polymerase in human myelomonocytic cells after oxidative stress. *Free Radic Biol Med*, 2000. 29(10): p. 995-1004.
131. Pacher P, Liaudet L, Bai P, Virag L, Mabley JG, Hasko G, and Szabo C. Activation of poly(ADP-ribose) polymerase contributes to development of doxorubicin-induced heart failure. *J Pharmacol Exp Ther*, 2002. 300(3): p. 862-7.
132. Pacher P, Liaudet L, Mabley J, Komjati K, and Szabo C. Pharmacologic inhibition of poly(adenosine diphosphate-ribose) polymerase may represent a

novel therapeutic approach in chronic heart failure. *J Am Coll Cardiol*, 2002. 40(5): p. 1006-16.

133. Eliasson MJ, Sampei K, Mandir AS, Hurn PD, Traystman RJ, Bao J, Pieper A, Wang ZQ, Dawson TM, Snyder SH, and Dawson VL. Poly(ADP-ribose) polymerase gene disruption renders mice resistant to cerebral ischemia. *Nat Med*, 1997. 3(10): p. 1089-95.
134. Komjati K, Mabley JG, Virag L, Southan GJ, Salzman AL, and Szabo C. Poly(ADP-ribose) polymerase inhibition protect neurons and the white matter and regulates the translocation of apoptosis-inducing factor in stroke. *Int J Mol Med*, 2004. 13(3): p. 373-82.
135. Szabo C, Cuzzocrea S, Zingarelli B, O'Connor M, and Salzman AL. Endothelial dysfunction in a rat model of endotoxic shock. Importance of the activation of poly (ADP-ribose) synthetase by peroxynitrite. *J Clin Invest*, 1997. 100(3): p. 723-35.
136. Oliver FJ, Menissier-de Murcia J, Nacci C, Decker P, Andriantsitohaina R, Muller S, de la Rubia G, Stoclet JC, and de Murcia G. Resistance to endotoxic shock as a consequence of defective NF-kappaB activation in poly (ADP-ribose) polymerase-1 deficient mice. *Embo J*, 1999. 18(16): p. 4446-54.
137. Jagtap P, Soriano FG, Virag L, Liaudet L, Mabley J, Szabo E, Hasko G, Marton A, Lorigados CB, Gallyas F, Jr., Sumegi B, Hoyt DG, Baloglu E, VanDuzer J, Salzman AL, Southan GJ, and Szabo C. Novel phenanthridinone inhibitors of poly (adenosine 5'-diphosphate-ribose) synthetase: potent cytoprotective and antishock agents. *Crit Care Med*, 2002. 30(5): p. 1071-82.
138. Soriano FG, Liaudet L, Szabo E, Virag L, Mabley JG, Pacher P, and Szabo C. Resistance to acute septic peritonitis in poly(ADP-ribose) polymerase-1-deficient mice. *Shock*, 2002. 17(4): p. 286-92.
139. Pacher P, Cziraki A, Mabley JG, Liaudet L, Papp L, and Szabo C. Role of poly(ADP-ribose) polymerase activation in endotoxin-induced cardiac collapse in rodents. *Biochem Pharmacol*, 2002. 64(12): p. 1785-91.
140. Shimoda K, Murakami K, Enkhbaatar P, Traber LD, Cox RA, Hawkins HK, Schmalstieg FC, Komjati K, Mabley JG, Szabo C, Salzman AL, and Traber DL.

Effect of poly(ADP ribose) synthetase inhibition on burn and smoke inhalation injury in sheep. *Am J Physiol Lung Cell Mol Physiol*, 2003. 285(1): p. L240-9.

141. Burkart V, Wang ZQ, Radons J, Heller B, Herceg Z, Stingl L, Wagner EF, and Kolb H. Mice lacking the poly(ADP-ribose) polymerase gene are resistant to pancreatic beta-cell destruction and diabetes development induced by streptozocin. *Nat Med*, 1999. 5(3): p. 314-9.
142. Pieper AA, Brat DJ, Krug DK, Watkins CC, Gupta A, Blackshaw S, Verma A, Wang ZQ, and Snyder SH. Poly(ADP-ribose) polymerase-deficient mice are protected from streptozotocin-induced diabetes. *Proc Natl Acad Sci U S A*, 1999. 96(6): p. 3059-64.
143. Hung TH, Skepper JN, Charnock-Jones DS, and Burton GJ. Hypoxia-reoxygenation: a potent inducer of apoptotic changes in the human placenta and possible etiological factor in preeclampsia. *Circ Res*, 2002. 90(12): p. 1274-81.
144. Martinet W, Knaapen MW, De Meyer GR, Herman AG, and Kockx MM. Elevated levels of oxidative DNA damage and DNA repair enzymes in human atherosclerotic plaques. *Circulation*, 2002. 106(8): p. 927-32.
145. Pacher P, Mabley JG, Soriano FG, Liaudet L, Komjati K, and Szabo C. Endothelial dysfunction in aging animals: the role of poly(ADP-ribose) polymerase activation. *Br J Pharmacol*, 2002. 135(6): p. 1347-50.
146. Pacher P, Mabley JG, Soriano FG, Liaudet L, and Szabo C. Activation of poly(ADP-ribose) polymerase contributes to the endothelial dysfunction associated with hypertension and aging. *Int J Mol Med*, 2002. 9(6): p. 659-64.
147. Smith RP and Gosselin RE. Hydrogen sulfide poisoning. *J Occup Med*, 1979. 21(2): p. 93-7.
148. Abe K and Kimura H. The possible role of hydrogen sulfide as an endogenous neuromodulator. *J Neurosci*, 1996. 16(3): p. 1066-71.
149. Wang R. Two's company, three's a crowd: can H2S be the third endogenous gaseous transmitter? *Faseb J*, 2002. 16(13): p. 1792-8.
150. Zhao W, Zhang J, Lu Y, and Wang R. The vasorelaxant effect of H(2)S as a novel endogenous gaseous K(ATP) channel opener. *Embo J*, 2001. 20(21): p. 6008-16.
151. Kimura H. Hydrogen sulfide induces cyclic AMP and modulates the NMDA receptor. *Biochem Biophys Res Commun*, 2000. 267(1): p. 129-33.

152. Hosoki R, Matsuki N, and Kimura H. The possible role of hydrogen sulfide as an endogenous smooth muscle relaxant in synergy with nitric oxide. *Biochem Biophys Res Commun*, 1997. 237(3): p. 527-31.
153. Li L, Bhatia M, Zhu YZ, Zhu YC, Ramnath RD, Wang ZJ, Anuar FB, Whiteman M, Salto-Tellez M, and Moore PK. Hydrogen sulfide is a novel mediator of lipopolysaccharide-induced inflammation in the mouse. *Faseb J*, 2005. 19(9): p. 1196-8.
154. Bhatia M, Wong FL, Fu D, Lau HY, Moochhala SM, and Moore PK. Role of hydrogen sulfide in acute pancreatitis and associated lung injury. *Faseb J*, 2005. 19(6): p. 623-5.
155. Wang R. The gasotransmitter role of hydrogen sulfide. *Antioxid Redox Signal*, 2003. 5(4): p. 493-501.
156. Beauchamp RO, Jr., Bus JS, Popp JA, Boreiko CJ, and Andjelkovich DA. A critical review of the literature on hydrogen sulfide toxicity. *Crit Rev Toxicol*, 1984. 13(1): p. 25-97.
157. Coleman JE. Mechanism of action of carbonic anhydrase. Subtrate, sulfonamide, and anion binding. *J Biol Chem*, 1967. 242(22): p. 5212-9.
158. Hill BC, Woon TC, Nicholls P, Peterson J, Greenwood C, and Thomson AJ. Interactions of sulphide and other ligands with cytochrome c oxidase. An electron-paramagnetic-resonance study. *Biochem J*, 1984. 224(2): p. 591-600.
159. Klentz RD and Fedde MR. Hydrogen sulfide: effects on avian respiratory control and intrapulmonary CO2 receptors. *Respir Physiol*, 1978. 32(3): p. 355-67.
160. Nicholls P. Inhibition of cytochrome c oxidase by sulphide. *Biochem Soc Trans*, 1975. 3(2): p. 316-9.
161. Blackstone E, Morrison M, and Roth MB. H2S induces a suspended animation-like state in mice. *Science*, 2005. 308(5721): p. 518.
162. Jeong SO, Pae HO, Oh GS, Jeong GS, Lee BS, Lee S, Kim du Y, Rhew HY, Lee KM, and Chung HT. Hydrogen sulfide potentiates interleukin-1beta-induced nitric oxide production via enhancement of extracellular signal-regulated kinase activation in rat vascular smooth muscle cells. *Biochem Biophys Res Commun*, 2006. 345(3): p. 938-44.

163. Qingyou Z, Junbao D, Weijin Z, Hui Y, Chaoshu T, and Chunyu Z. Impact of hydrogen sulfide on carbon monoxide/heme oxygenase pathway in the pathogenesis of hypoxic pulmonary hypertension. *Biochem Biophys Res Commun*, 2004. 317(1): p. 30-7.
164. Ryter SW, Alam J, and Choi AM. Heme oxygenase-1/carbon monoxide: from basic science to therapeutic applications. *Physiol Rev*, 2006. 86(2): p. 583-650.
165. Oh GS, Pae HO, Lee BS, Kim BN, Kim JM, Kim HR, Jeon SB, Jeon WK, Chae HJ, and Chung HT. Hydrogen sulfide inhibits nitric oxide production and nuclear factor-kappaB via heme oxygenase-1 expression in RAW264.7 macrophages stimulated with lipopolysaccharide. *Free Radic Biol Med*, 2006. 41(1): p. 106-19.
166. Boehning D and Snyder SH. Novel neural modulators. *Annu Rev Neurosci*, 2003. 26: p. 105-31.
167. Zhao W and Wang R. H(2)S-induced vasorelaxation and underlying cellular and molecular mechanisms. *Am J Physiol Heart Circ Physiol*, 2002. 283(2): p. H474-80.
168. Lee SW, Cheng Y, Moore PK, and Bian JS. Hydrogen sulphide regulates intracellular pH in vascular smooth muscle cells. *Biochem Biophys Res Commun*, 2007. 358(4): p. 1142-7.
169. Kiss L, Deitch EA, and Szabo C. Hydrogen sulfide decreases adenosine triphosphate levels in aortic rings and leads to vasorelaxation via metabolic inhibition. *Life Sci*, 2008. 83(17-18): p. 589-94.
170. Yan H, Du J, and Tang C. The possible role of hydrogen sulfide on the pathogenesis of spontaneous hypertension in rats. *Biochem Biophys Res Commun*, 2004. 313(1): p. 22-7.
171. Bhatia M, Sidhapuriwala J, Moochhala SM, and Moore PK. Hydrogen sulphide is a mediator of carrageenan-induced hindpaw oedema in the rat. *Br J Pharmacol*, 2005. 145(2): p. 141-4.
172. Mok YY, Atan MS, Yoke Ping C, Zhong Jing W, Bhatia M, Moochhala S, and Moore PK. Role of hydrogen sulphide in haemorrhagic shock in the rat: protective effect of inhibitors of hydrogen sulphide biosynthesis. *Br J Pharmacol*, 2004. 143(7): p. 881-9.

173. Szabo C and Salzman AL. Inhibition of ATP-activated potassium channels exerts pressor effects and improves survival in a rat model of severe hemorrhagic shock. *Shock*, 1996. 5(6): p. 391-4.
174. Pan TT, Feng ZN, Lee SW, Moore PK, and Bian JS. Endogenous hydrogen sulfide contributes to the cardioprotection by metabolic inhibition preconditioning in the rat ventricular myocytes. *J Mol Cell Cardiol*, 2006. 40(1): p. 119-30.
175. Fiorucci S, Antonelli E, Distrutti E, Rizzo G, Mencarelli A, Orlandi S, Zanardo R, Renga B, Di Sante M, Morelli A, Cirino G, and Wallace JL. Inhibition of hydrogen sulfide generation contributes to gastric injury caused by anti-inflammatory nonsteroidal drugs. *Gastroenterology*, 2005. 129(4): p. 1210-24.
176. Meng QH, Yang G, Yang W, Jiang B, Wu L, and Wang R. Protective effect of hydrogen sulfide on balloon injury-induced neointima hyperplasia in rat carotid arteries. *Am J Pathol*, 2007. 170(4): p. 1406-14.
177. Chen Q, Moghaddas S, Hoppel CL, and Lesnefsky EJ. Reversible blockade of electron transport during ischemia protects mitochondria and decreases myocardial injury following reperfusion. *J Pharmacol Exp Ther*, 2006. 319(3): p. 1405-12.
178. Chen Q, Camara AK, Stowe DF, Hoppel CL, and Lesnefsky EJ. Modulation of electron transport protects cardiac mitochondria and decreases myocardial injury during ischemia and reperfusion. *Am J Physiol Cell Physiol*, 2007. 292(1): p. C137-47.
179. Daugherty A. Mouse models of atherosclerosis. *Am J Med Sci*, 2002. 323(1): p. 3-10.
180. Laursen JB, Somers M, Kurz S, McCann L, Warnholtz A, Freeman BA, Tarpey M, Fukai T, and Harrison DG. Endothelial regulation of vasomotion in apoE-deficient mice: implications for interactions between peroxynitrite and tetrahydrobiopterin. *Circulation*, 2001. 103(9): p. 1282-8.
181. Zhang C, Yang J, and Jennings LK. Attenuation of neointima formation through the inhibition of DNA repair enzyme PARP-1 in balloon-injured rat carotid artery. *Am J Physiol Heart Circ Physiol*, 2004. 287(2): p. H659-66.
182. Benko R, Pacher P, Vaslin A, Kollai M, and Szabo C. Restoration of the endothelial function in the aortic rings of apolipoprotein E deficient mice by

pharmacological inhibition of the nuclear enzyme poly(ADP-ribose) polymerase. *Life Sci*, 2004. 75(10): p. 1255-61.

183. Steinberg D, Parthasarathy S, Carew TE, Khoo JC, and Witztum JL. Beyond cholesterol. Modifications of low-density lipoprotein that increase its atherogenicity. *N Engl J Med*, 1989. 320(14): p. 915-24.
184. Ishigaki Y, Katagiri H, Gao J, Yamada T, Imai J, Uno K, Hasegawa Y, Kaneko K, Ogihara T, Ishihara H, Sato Y, Takikawa K, Nishimichi N, Matsuda H, Sawamura T, and Oka Y. Impact of plasma oxidized low-density lipoprotein removal on atherosclerosis. *Circulation*, 2008. 118(1): p. 75-83.
185. Schmid W, Lee A, Son J, Koller E, and Volf I. Hypochlorite-oxidized low density lipoproteins reduce production and bioavailability of nitric oxide in RAW 264.7 macrophages by distinct mechanisms. *Life Sci*, 2008. 83(1-2): p. 50-8.
186. Poredos P. Endothelial dysfunction in the pathogenesis of atherosclerosis. *Int Angiol*, 2002. 21(2): p. 109-16.
187. Foncea R, Carvajal C, Almarza C, and Leighton F. Endothelial cell oxidative stress and signal transduction. *Biol Res*, 2000. 33(2): p. 89-96.
188. Zhou Q, Wasowicz E, Handler B, Fleischer L, and Kummerow FA. An excess concentration of oxysterols in the plasma is cytotoxic to cultured endothelial cells. *Atherosclerosis*, 2000. 149(1): p. 191-7.
189. Deckert V, Duverneuil L, Poupon S, Monier S, Le Guern N, Lizard G, Masson D, and Lagrost L. The impairment of endothelium-dependent arterial relaxation by 7-ketocholesterol is associated with an early activation of protein kinase C. *Br J Pharmacol*, 2002. 137(5): p. 655-62.
190. Diestel A, Aktas O, Hackel D, Hake I, Meier S, Raine CS, Nitsch R, Zipp F, and Ullrich O. Activation of microglial poly(ADP-ribose)-polymerase-1 by cholesterol breakdown products during neuroinflammation: a link between demyelination and neuronal damage. *J Exp Med*, 2003. 198(11): p. 1729-40.
191. Acute myocardial infarction: pre-hospital and in-hospital management. The Task Force on the Management of Acute Myocardial Infarction of the European Society of Cardiology. *Eur Heart J*, 1996. 17(1): p. 43-63.
192. Powell SR, Hall D, and Shih A. Copper loading of hearts increases postischemic reperfusion injury. *Circ Res*, 1991. 69(3): p. 881-5.

193. Bolli R and McCay PB. Use of spin traps in intact animals undergoing myocardial ischemia/reperfusion: a new approach to assessing the role of oxygen radicals in myocardial "stunning". *Free Radic Res Commun*, 1990. 9(3-6): p. 169-80.
194. Kevin LG, Camara AK, Riess ML, Novalija E, and Stowe DF. Ischemic preconditioning alters real-time measure of O2 radicals in intact hearts with ischemia and reperfusion. *Am J Physiol Heart Circ Physiol*, 2003. 284(2): p. H566-74.
195. Maupoil V, Rochette L, Tabard A, Clauser P, and Harpey C. Evolution of free radical formation during low-flow ischemia and reperfusion in isolated rat heart. *Cardiovasc Drugs Ther*, 1990. 4 Suppl 4: p. 791-5.
196. Merrill GF. Acetaminophen and low-flow myocardial ischemia: efficacy and antioxidant mechanisms. *Am J Physiol Heart Circ Physiol*, 2002. 282(4): p. H1341-9.
197. Pietri S, Culcasi M, and Cozzone PJ. Real-time continuous-flow spin trapping of hydroxyl free radical in the ischemic and post-ischemic myocardium. *Eur J Biochem*, 1989. 186(1-2): p. 163-73.
198. Ilangovan G, Liebgott T, Kutala VK, Petryakov S, Zweier JL, and Kuppusamy P. EPR oximetry in the beating heart: myocardial oxygen consumption rate as an index of postischemic recovery. *Magn Reson Med*, 2004. 51(4): p. 835-42.
199. Becker LB, vanden Hoek TL, Shao ZH, Li CQ, and Schumacker PT. Generation of superoxide in cardiomyocytes during ischemia before reperfusion. *Am J Physiol*, 1999. 277(6 Pt 2): p. H2240-6.
200. Vanden Hoek TL, Li C, Shao Z, Schumacker PT, and Becker LB. Significant levels of oxidants are generated by isolated cardiomyocytes during ischemia prior to reperfusion. *J Mol Cell Cardiol*, 1997. 29(9): p. 2571-83.
201. Lee JW, Bobst EV, Wang YG, Ashraf MM, and Bobst AM. Increased endogenous ascorbyl free radical formation with singlet oxygen scavengers in reperfusion injury: an EPR and functional recovery study in rat hearts. *Cell Mol Biol (Noisy-le-grand)*, 2000. 46(8): p. 1383-95.
202. Riess ML, Camara AK, Kevin LG, An J, and Stowe DF. Reduced reactive O2 species formation and preserved mitochondrial NADH and [Ca2+] levels during

short-term 17 degrees C ischemia in intact hearts. *Cardiovasc Res*, 2004. 61(3): p. 580-90.

203. Stowe DF, Aldakkak M, Camara AK, Riess ML, Heinen A, Varadarajan SG, and Jiang MT. Cardiac mitochondrial preconditioning by Big Ca2+-sensitive K+ channel opening requires superoxide radical generation. *Am J Physiol Heart Circ Physiol*, 2006. 290(1): p. H434-40.
204. Duan J and Karmazyn M. Relationship between oxidative phosphorylation and adenine nucleotide translocase activity of two populations of cardiac mitochondria and mechanical recovery of ischemic hearts following reperfusion. *Can J Physiol Pharmacol*, 1989. 67(7): p. 704-9.
205. Flameng W, Andres J, Ferdinande P, Mattheussen M, and Van Belle H. Mitochondrial function in myocardial stunning. *J Mol Cell Cardiol*, 1991. 23(1): p. 1-11.
206. Kajiyama K, Pauly DF, Hughes H, Yoon SB, Entman ML, and McMillin-Wood JB. Protection by verapamil of mitochondrial glutathione equilibrium and phospholipid changes during reperfusion of ischemic canine myocardium. *Circ Res*, 1987. 61(2): p. 301-10.
207. Lemasters JJ and Nieminen AL. Mitochondrial oxygen radical formation during reductive and oxidative stress to intact hepatocytes. *Biosci Rep*, 1997. 17(3): p. 281-91.
208. Lesnefsky EJ, Tandler B, Ye J, Slabe TJ, Turkaly J, and Hoppel CL. Myocardial ischemia decreases oxidative phosphorylation through cytochrome oxidase in subsarcolemmal mitochondria. *Am J Physiol*, 1997. 273(3 Pt 2): p. H1544-54.
209. Piper HM, Sezer O, Schleyer M, Schwartz P, Hutter JF, and Spieckermann PG. Development of ischemia-induced damage in defined mitochondrial subpopulations. *J Mol Cell Cardiol*, 1985. 17(9): p. 885-96.
210. Rouslin W. Mitochondrial complexes I, II, III, IV, and V in myocardial ischemia and autolysis. *Am J Physiol*, 1983. 244(6): p. H743-8.
211. Ueta H, Ogura R, Sugiyama M, Kagiyama A, and Shin G. O2-. spin trapping on cardiac submitochondrial particles isolated from ischemic and non-ischemic myocardium. *J Mol Cell Cardiol*, 1990. 22(8): p. 893-9.

212. Asimakis GK and Conti VR. Myocardial ischemia: correlation of mitochondrial adenine nucleotide and respiratory function. *J Mol Cell Cardiol*, 1984. 16(5): p. 439-47.
213. Lesnefsky EJ, Gudz TI, Migita CT, Ikeda-Saito M, Hassan MO, Turkaly PJ, and Hoppel CL. Ischemic injury to mitochondrial electron transport in the aging heart: damage to the iron-sulfur protein subunit of electron transport complex III. *Arch Biochem Biophys*, 2001. 385(1): p. 117-28.
214. Lesnefsky EJ, Moghaddas S, Tandler B, Kerner J, and Hoppel CL. Mitochondrial dysfunction in cardiac disease: ischemia--reperfusion, aging, and heart failure. *J Mol Cell Cardiol*, 2001. 33(6): p. 1065-89.
215. Lesnefsky EJ, Gudz TI, Moghaddas S, Migita CT, Ikeda-Saito M, Turkaly PJ, and Hoppel CL. Aging decreases electron transport complex III activity in heart interfibrillar mitochondria by alteration of the cytochrome c binding site. *J Mol Cell Cardiol*, 2001. 33(1): p. 37-47.
216. Lesnefsky EJ, Slabe TJ, Stoll MS, Minkler PE, and Hoppel CL. Myocardial ischemia selectively depletes cardiolipin in rabbit heart subsarcolemmal mitochondria. *Am J Physiol Heart Circ Physiol*, 2001. 280(6): p. H2770-8.
217. Chen Q, Vazquez EJ, Moghaddas S, Hoppel CL, and Lesnefsky EJ. Production of reactive oxygen species by mitochondria: central role of complex III. *J Biol Chem*, 2003. 278(38): p. 36027-31.
218. Han D, Antunes F, Canali R, Rettori D, and Cadenas E. Voltage-dependent anion channels control the release of the superoxide anion from mitochondria to cytosol. *J Biol Chem*, 2003. 278(8): p. 5557-63.
219. Rytomaa M and Kinnunen PK. Evidence for two distinct acidic phospholipid-binding sites in cytochrome c. *J Biol Chem*, 1994. 269(3): p. 1770-4.
220. Salamon Z and Tollin G. Interaction of horse heart cytochrome c with lipid bilayer membranes: effects on redox potentials. *J Bioenerg Biomembr*, 1997. 29(3): p. 211-21.
221. Spooner PJ and Watts A. Cytochrome c interactions with cardiolipin in bilayers: a multinuclear magic-angle spinning NMR study. *Biochemistry*, 1992. 31(41): p. 10129-38.

222. Ott M, Robertson JD, Gogvadze V, Zhivotovsky B, and Orrenius S. Cytochrome c release from mitochondria proceeds by a two-step process. *Proc Natl Acad Sci U S A*, 2002. 99(3): p. 1259-63.
223. Shidoji Y, Hayashi K, Komura S, Ohishi N, and Yagi K. Loss of molecular interaction between cytochrome c and cardiolipin due to lipid peroxidation. *Biochem Biophys Res Commun*, 1999. 264(2): p. 343-7.
224. Gadd ME, Broekemeier KM, Crouser ED, Kumar J, Graff G, and Pfeiffer DR. Mitochondrial iPLA2 activity modulates the release of cytochrome c from mitochondria and influences the permeability transition. *J Biol Chem*, 2006. 281(11): p. 6931-9.
225. Korsmeyer SJ, Wei MC, Saito M, Weiler S, Oh KJ, and Schlesinger PH. Pro-apoptotic cascade activates BID, which oligomerizes BAK or BAX into pores that result in the release of cytochrome c. *Cell Death Differ*, 2000. 7(12): p. 1166-73.
226. Borutaite V and Brown GC. Mitochondria in apoptosis of ischemic heart. *FEBS Lett*, 2003. 541(1-3): p. 1-5.
227. Borutaite V, Budriunaite A, Morkuniene R, and Brown GC. Release of mitochondrial cytochrome c and activation of cytosolic caspases induced by myocardial ischaemia. *Biochim Biophys Acta*, 2001. 1537(2): p. 101-9.
228. Borutaite V, Jekabsone A, Morkuniene R, and Brown GC. Inhibition of mitochondrial permeability transition prevents mitochondrial dysfunction, cytochrome c release and apoptosis induced by heart ischemia. *J Mol Cell Cardiol*, 2003. 35(4): p. 357-66.
229. Chen M, He H, Zhan S, Krajewski S, Reed JC, and Gottlieb RA. Bid is cleaved by calpain to an active fragment in vitro and during myocardial ischemia/reperfusion. *J Biol Chem*, 2001. 276(33): p. 30724-8.
230. Gottlieb RA, Burleson KO, Kloner RA, Babior BM, and Engler RL. Reperfusion injury induces apoptosis in rabbit cardiomyocytes. *J Clin Invest*, 1994. 94(4): p. 1621-8.
231. Hausenloy DJ and Yellon DM. The mitochondrial permeability transition pore: its fundamental role in mediating cell death during ischaemia and reperfusion. *J Mol Cell Cardiol*, 2003. 35(4): p. 339-41.

232. Lesnefsky EJ, Chen Q, Slabe TJ, Stoll MS, Minkler PE, Hassan MO, Tandler B, and Hoppel CL. Ischemia, rather than reperfusion, inhibits respiration through cytochrome oxidase in the isolated, perfused rabbit heart: role of cardiolipin. *Am J Physiol Heart Circ Physiol*, 2004. 287(1): p. H258-67.
233. Korge P, Ping P, and Weiss JN. Reactive oxygen species production in energized cardiac mitochondria during hypoxia/reoxygenation: modulation by nitric oxide. *Circ Res*, 2008. 103(8): p. 873-80.
234. Di Lisa F, Canton M, Menabo R, Kaludercic N, and Bernardi P. Mitochondria and cardioprotection. *Heart Fail Rev*, 2007. 12(3-4): p. 249-60.
235. Bian JS, Yong QC, Pan TT, Feng ZN, Ali MY, Zhou S, and Moore PK. Role of hydrogen sulfide in the cardioprotection caused by ischemic preconditioning in the rat heart and cardiac myocytes. *J Pharmacol Exp Ther*, 2006. 316(2): p. 670-8.
236. Johansen D, Ytrehus K, and Baxter GF. Exogenous hydrogen sulfide (H2S) protects against regional myocardial ischemia-reperfusion injury--Evidence for a role of K ATP channels. *Basic Res Cardiol*, 2006. 101(1): p. 53-60.
237. Cohn JN. Structural changes in cardiovascular disease. *Am J Cardiol*, 1995. 76(15): p. 34E-37E.
238. Gerdes AM, Liu Z, and Zimmer HG. Changes in nuclear size of cardiac myocytes during the development and progression of hypertrophy in rats. *Cardioscience*, 1994. 5(3): p. 203-8.
239. MacLellan WR and Schneider MD. Death by design. Programmed cell death in cardiovascular biology and disease. *Circ Res*, 1997. 81(2): p. 137-44.
240. Olivetti G, Capasso JM, Sonnenblick EH, and Anversa P. Side-to-side slippage of myocytes participates in ventricular wall remodeling acutely after myocardial infarction in rats. *Circ Res*, 1990. 67(1): p. 23-34.
241. Weber KT, Anversa P, Armstrong PW, Brilla CG, Burnett JC, Jr., Cruickshank JM, Devereux RB, Giles TD, Korsgaard N, Leier CV, and et al. Remodeling and reparation of the cardiovascular system. *J Am Coll Cardiol*, 1992. 20(1): p. 3-16.
242. Mann DL and Spinale FG. Activation of matrix metalloproteinases in the failing human heart: breaking the tie that binds. *Circulation*, 1998. 98(17): p. 1699-702.

243. Litwin SE and Bridge JH. Enhanced Na(+)-Ca2+ exchange in the infarcted heart. Implications for excitation-contraction coupling. *Circ Res*, 1997. 81(6): p. 1083-93.
244. Morgan JP, Erny RE, Allen PD, Grossman W, and Gwathmey JK. Abnormal intracellular calcium handling, a major cause of systolic and diastolic dysfunction in ventricular myocardium from patients with heart failure. *Circulation*, 1990. 81(2 Suppl): p. III21-32.
245. Radi R, Beckman JS, Bush KM, and Freeman BA. Peroxynitrite-induced membrane lipid peroxidation: the cytotoxic potential of superoxide and nitric oxide. *Arch Biochem Biophys*, 1991. 288(2): p. 481-7.
246. Beckman JS and Koppenol WH. Nitric oxide, superoxide, and peroxynitrite: the good, the bad, and ugly. *Am J Physiol*, 1996. 271(5 Pt 1): p. C1424-37.
247. Weinstein DM, Mihm MJ, and Bauer JA. Cardiac peroxynitrite formation and left ventricular dysfunction following doxorubicin treatment in mice. *J Pharmacol Exp Ther*, 2000. 294(1): p. 396-401.
248. Kooy NW, Lewis SJ, Royall JA, Ye YZ, Kelly DR, and Beckman JS. Extensive tyrosine nitration in human myocardial inflammation: evidence for the presence of peroxynitrite. *Crit Care Med*, 1997. 25(5): p. 812-9.
249. Ischiropoulos H. Biological tyrosine nitration: a pathophysiological function of nitric oxide and reactive oxygen species. *Arch Biochem Biophys*, 1998. 356(1): p. 1-11.
250. Barrans JD, Allen PD, Stamatiou D, Dzau VJ, and Liew CC. Global gene expression profiling of end-stage dilated cardiomyopathy using a human cardiovascular-based cDNA microarray. *Am J Pathol*, 2002. 160(6): p. 2035-43.
251. Elsasser A, Suzuki K, and Schaper J. Unresolved issues regarding the role of apoptosis in the pathogenesis of ischemic injury and heart failure. *J Mol Cell Cardiol*, 2000. 32(5): p. 711-24.
252. Guerra S, Leri A, Wang X, Finato N, Di Loreto C, Beltrami CA, Kajstura J, and Anversa P. Myocyte death in the failing human heart is gender dependent. *Circ Res*, 1999. 85(9): p. 856-66.
253. Hein S, Arnon E, Kostin S, Schonburg M, Elsasser A, Polyakova V, Bauer EP, Klovekorn WP, and Schaper J. Progression from compensated hypertrophy to

failure in the pressure-overloaded human heart: structural deterioration and compensatory mechanisms. *Circulation*, 2003. 107(7): p. 984-91.

254. Knaapen MW, Davies MJ, De Bie M, Haven AJ, Martinet W, and Kockx MM. Apoptotic versus autophagic cell death in heart failure. *Cardiovasc Res*, 2001. 51(2): p. 304-12.
255. Kang PM and Izumo S. Apoptosis and heart failure: A critical review of the literature. *Circ Res*, 2000. 86(11): p. 1107-13.
256. Clerk A, Cole SM, Cullingford TE, Harrison JG, Jormakka M, and Valks DM. Regulation of cardiac myocyte cell death. *Pharmacol Ther*, 2003. 97(3): p. 223-61.
257. Condorelli G, Morisco C, Stassi G, Notte A, Farina F, Sgaramella G, de Rienzo A, Roncarati R, Trimarco B, and Lembo G. Increased cardiomyocyte apoptosis and changes in proapoptotic and antiapoptotic genes bax and bcl-2 during left ventricular adaptations to chronic pressure overload in the rat. *Circulation*, 1999. 99(23): p. 3071-8.
258. Teiger E, Than VD, Richard L, Wisnewsky C, Tea BS, Gaboury L, Tremblay J, Schwartz K, and Hamet P. Apoptosis in pressure overload-induced heart hypertrophy in the rat. *J Clin Invest*, 1996. 97(12): p. 2891-7.
259. Kang PM, Yue P, Liu Z, Tarnavski O, Bodyak N, and Izumo S. Alterations in apoptosis regulatory factors during hypertrophy and heart failure. *Am J Physiol Heart Circ Physiol*, 2004. 287(1): p. H72-80.
260. Bartunek J, Vanderheyden M, Knaapen MW, Tack W, Kockx MM, and Goethals M. Deoxyribonucleic acid damage/repair proteins are elevated in the failing human myocardium due to idiopathic dilated cardiomyopathy. *J Am Coll Cardiol*, 2002. 40(6): p. 1097-103; discussion 1104-5.
261. de Boer RA, van Veldhuisen DJ, van der Wijk J, Brouwer RM, de Jonge N, Cole GM, and Suurmeijer AJ. Additional use of immunostaining for active caspase 3 and cleaved actin and PARP fragments to detect apoptosis in patients with chronic heart failure. *J Card Fail*, 2000. 6(4): p. 330-7.
262. Koda M, Takemura G, Kanoh M, Hayakawa K, Kawase Y, Maruyama R, Li Y, Minatoguchi S, Fujiwara T, and Fujiwara H. Myocytes positive for in situ markers for DNA breaks in human hearts which are hypertrophic, but neither failed nor

dilated: a manifestation of cardiac hypertrophy rather than failure. *J Pathol*, 2003. 199(2): p. 229-36.

263. Ziegler M and Oei SL. A cellular survival switch: poly(ADP-ribosyl)ation stimulates DNA repair and silences transcription. *Bioessays*, 2001. 23(6): p. 543-8.
264. Purcell NH and Molkentin JD. Is nuclear factor kappaB an attractive therapeutic target for treating cardiac hypertrophy? *Circulation*, 2003. 108(6): p. 638-40.
265. Hassa PO, Buerki C, Lombardi C, Imhof R, and Hottiger MO. Transcriptional coactivation of nuclear factor-kappaB-dependent gene expression by p300 is regulated by poly(ADP)-ribose polymerase-1. *J Biol Chem*, 2003. 278(46): p. 45145-53.
266. Wang ZQ, Auer B, Stingl L, Berghammer H, Haidacher D, Schweiger M, and Wagner EF. Mice lacking ADPRT and poly(ADP-ribosyl)ation develop normally but are susceptible to skin disease. *Genes Dev*, 1995. 9(5): p. 509-20.
267. Cuzzocrea S, Zingarelli B, O'Connor M, Salzman AL, and Szabo C. Effect of L-buthionine-(S,R)-sulphoximine, an inhibitor of gamma-glutamylcysteine synthetase on peroxynitrite- and endotoxic shock-induced vascular failure. *Br J Pharmacol*, 1998. 123(3): p. 525-37.
268. Rockman HA, Ross RS, Harris AN, Knowlton KU, Steinhelper ME, Field LJ, Ross J, Jr., and Chien KR. Segregation of atrial-specific and inducible expression of an atrial natriuretic factor transgene in an in vivo murine model of cardiac hypertrophy. *Proc Natl Acad Sci U S A*, 1991. 88(18): p. 8277-81.
269. Khan TA, Ruel M, Bianchi C, Voisine P, Komjati K, Szabo C, and Sellke FW. Poly(ADP-ribose) polymerase inhibition improves postischemic myocardial function after cardioplegia-cardiopulmonary bypass. *J Am Coll Surg*, 2003. 197(2): p. 270-7.
270. Murthy KG, Xiao CY, Mabley JG, Chen M, and Szabo C. Activation of poly(ADP-ribose) polymerase in circulating leukocytes during myocardial infarction. *Shock*, 2004. 21(3): p. 230-4.
271. Pacher P, Liaudet L, Soriano FG, Mabley JG, Szabo E, and Szabo C. The role of poly(ADP-ribose) polymerase activation in the development of myocardial and endothelial dysfunction in diabetes. *Diabetes*, 2002. 51(2): p. 514-21.

272. Shiva S, Brookes PS, and Darley-Usmar VM. Methods for measuring the regulation of respiration by nitric oxide. *Methods Cell Biol*, 2007. 80: p. 395-416.
273. Soriano FG, Virag L, and Szabo C. Diabetic endothelial dysfunction: role of reactive oxygen and nitrogen species production and poly(ADP-ribose) polymerase activation. *J Mol Med*, 2001. 79(8): p. 437-48.
274. Chen M, Zsengeller Z, Xiao CY, and Szabo C. Mitochondrial-to-nuclear translocation of apoptosis-inducing factor in cardiac myocytes during oxidant stress: potential role of poly(ADP-ribose) polymerase-1. *Cardiovasc Res*, 2004. 63(4): p. 682-8.
275. Gottlieb RA, Giesing HA, Engler RL, and Babior BM. The acid deoxyribonuclease of neutrophils: a possible participant in apoptosis-associated genome destruction. *Blood*, 1995. 86(6): p. 2414-8.
276. Ouedraogo R, Gong Y, Berzins B, Wu X, Mahadev K, Hough K, Chan L, Goldstein BJ, and Scalia R. Adiponectin deficiency increases leukocyte-endothelium interactions via upregulation of endothelial cell adhesion molecules in vivo. *J Clin Invest*, 2007. 117(6): p. 1718-26.
277. Koenitzer JR, Isbell TS, Patel HD, Benavides GA, Dickinson DA, Patel RP, Darley-Usmar VM, Lancaster JR, Jr., Doeller JE, and Kraus DW. Hydrogen sulfide mediates vasoactivity in an O2-dependent manner. *Am J Physiol Heart Circ Physiol*, 2007. 292(4): p. H1953-60.
278. Lizard G, Deckert V, Dubrez L, Moisant M, Gambert P, and Lagrost L. Induction of apoptosis in endothelial cells treated with cholesterol oxides. *Am J Pathol*, 1996. 148(5): p. 1625-38.
279. Lizard G, Monier S, Cordelet C, Gesquiere L, Deckert V, Gueldry S, Lagrost L, and Gambert P. Characterization and comparison of the mode of cell death, apoptosis versus necrosis, induced by 7beta-hydroxycholesterol and 7-ketocholesterol in the cells of the vascular wall. *Arterioscler Thromb Vasc Biol*, 1999. 19(5): p. 1190-200.
280. Yin J, Chaufour X, McLachlan C, McGuire M, White G, King N, and Hambly B. Apoptosis of vascular smooth muscle cells induced by cholesterol and its oxides in vitro and in vivo. *Atherosclerosis*, 2000. 148(2): p. 365-74.

281. Mougenot N, Lesnik P, Ramirez-Gil JF, Nataf P, Diczfalusy U, Chapman MJ, and Lechat P. Effect of the oxidation state of LDL on the modulation of arterial vasomotor response in vitro. *Atherosclerosis*, 1997. 133(2): p. 183-92.
282. Millanvoye-Van Brussel E, Topal G, Brunet A, Do Pham T, Deckert V, Rendu F, and David-Dufilho M. Lysophosphatidylcholine and 7-oxocholesterol modulate Ca2+ signals and inhibit the phosphorylation of endothelial NO synthase and cytosolic phospholipase A2. *Biochem J*, 2004. 380(Pt 2): p. 533-9.
283. Lee CS, Joe EH, and Jou I. Oxysterols suppress inducible nitric oxide synthase expression in lipopolysaccharide-stimulated astrocytes through liver X receptor. *Neuroreport*, 2006. 17(2): p. 183-7.
284. Lyons MA, Samman S, Gatto L, and Brown AJ. Rapid hepatic metabolism of 7-ketocholesterol in vivo: implications for dietary oxysterols. *J Lipid Res*, 1999. 40(10): p. 1846-57.
285. Lyons MA and Brown AJ. 7-Ketocholesterol delivered to mice in chylomicron remnant-like particles is rapidly metabolised, excreted and does not accumulate in aorta. *Biochim Biophys Acta*, 2001. 1530(2-3): p. 209-18.
286. Martinet W, De Bie M, Schrijvers DM, De Meyer GR, Herman AG, and Kockx MM. 7-ketocholesterol induces protein ubiquitination, myelin figure formation, and light chain 3 processing in vascular smooth muscle cells. *Arterioscler Thromb Vasc Biol*, 2004. 24(12): p. 2296-301.
287. Berthier A, Lemaire-Ewing S, Prunet C, Montange T, Vejux A, Pais de Barros JP, Monier S, Gambert P, Lizard G, and Neel D. 7-Ketocholesterol-induced apoptosis. Involvement of several pro-apoptotic but also anti-apoptotic calcium-dependent transduction pathways. *Febs J*, 2005. 272(12): p. 3093-104.
288. Pedruzzi E, Guichard C, Ollivier V, Driss F, Fay M, Prunet C, Marie JC, Pouzet C, Samadi M, Elbim C, O'Dowd Y, Bens M, Vandewalle A, Gougerot-Pocidalo MA, Lizard G, and Ogier-Denis E. NAD(P)H oxidase Nox-4 mediates 7-ketocholesterol-induced endoplasmic reticulum stress and apoptosis in human aortic smooth muscle cells. *Mol Cell Biol*, 2004. 24(24): p. 10703-17.
289. Ekelund UE, Harrison RW, Shokek O, Thakkar RN, Tunin RS, Senzaki H, Kass DA, Marban E, and Hare JM. Intravenous allopurinol decreases myocardial

oxygen consumption and increases mechanical efficiency in dogs with pacing-induced heart failure. *Circ Res*, 1999. 85(5): p. 437-45.

290. Fukuchi M, Hussain SN, and Giaid A. Heterogeneous expression and activity of endothelial and inducible nitric oxide synthases in end-stage human heart failure: their relation to lesion site and beta-adrenergic receptor therapy. *Circulation*, 1998. 98(2): p. 132-9.
291. Vejlstrup NG, Bouloumie A, Boesgaard S, Andersen CB, Nielsen-Kudsk JE, Mortensen SA, Kent JD, Harrison DG, Busse R, and Aldershvile J. Inducible nitric oxide synthase (iNOS) in the human heart: expression and localization in congestive heart failure. *J Mol Cell Cardiol*, 1998. 30(6): p. 1215-23.
292. Mungrue IN, Gros R, You X, Pirani A, Azad A, Csont T, Schulz R, Butany J, Stewart DJ, and Husain M. Cardiomyocyte overexpression of iNOS in mice results in peroxynitrite generation, heart block, and sudden death. *J Clin Invest*, 2002. 109(6): p. 735-43.
293. Dai ZK, Tan MS, Chai CY, Yeh JL, Chou SH, Chiu CC, Jeng AY, Chen IJ, and Wu JR. Upregulation of endothelial nitric oxide synthase and endothelin-1 in pulmonary hypertension secondary to heart failure in aorta-banded rats. *Pediatr Pulmonol*, 2004. 37(3): p. 249-56.
294. Bouloumie A, Bauersachs J, Linz W, Scholkens BA, Wiemer G, Fleming I, and Busse R. Endothelial dysfunction coincides with an enhanced nitric oxide synthase expression and superoxide anion production. *Hypertension*, 1997. 30(4): p. 934-41.
295. Pacher P, Liaudet L, Bai P, Mabley JG, Kaminski PM, Virag L, Deb A, Szabo E, Ungvari Z, Wolin MS, Groves JT, and Szabo C. Potent metalloporphyrin peroxynitrite decomposition catalyst protects against the development of doxorubicin-induced cardiac dysfunction. *Circulation*, 2003. 107(6): p. 896-904.
296. Brookes PS, Zhang J, Dai L, Zhou F, Parks DA, Darley-Usmar VM, and Anderson PG. Increased sensitivity of mitochondrial respiration to inhibition by nitric oxide in cardiac hypertrophy. *J Mol Cell Cardiol*, 2001. 33(1): p. 69-82.
297. Szabo G, Liaudet L, Hagl S, and Szabo C. Poly(ADP-ribose) polymerase activation in the reperfused myocardium. *Cardiovasc Res*, 2004. 61(3): p. 471-80.

298. Obrosova IG, Minchenko AG, Frank RN, Seigel GM, Zsengeller Z, Pacher P, Stevens MJ, and Szabo C. Poly(ADP-ribose) polymerase inhibitors counteract diabetes- and hypoxia-induced retinal vascular endothelial growth factor overexpression. *Int J Mol Med*, 2004. 14(1): p. 55-64.

299. Du L, Zhang X, Han YY, Burke NA, Kochanek PM, Watkins SC, Graham SH, Carcillo JA, Szabo C, and Clark RS. Intra-mitochondrial poly(ADP-ribosylation) contributes to NAD+ depletion and cell death induced by oxidative stress. *J Biol Chem*, 2003. 278(20): p. 18426-33.

300. Du X, Matsumura T, Edelstein D, Rossetti L, Zsengeller Z, Szabo C, and Brownlee M. Inhibition of GAPDH activity by poly(ADP-ribose) polymerase activates three major pathways of hyperglycemic damage in endothelial cells. *J Clin Invest*, 2003. 112(7): p. 1049-57.

301. Virag L, Salzman AL, and Szabo C. Poly(ADP-ribose) synthetase activation mediates mitochondrial injury during oxidant-induced cell death. *J Immunol*, 1998. 161(7): p. 3753-9.

302. Xiao CY, Chen M, Zsengeller Z, and Szabo C. Poly(ADP-ribose) polymerase contributes to the development of myocardial infarction in diabetic rats and regulates the nuclear translocation of apoptosis-inducing factor. *J Pharmacol Exp Ther*, 2004. 310(2): p. 498-504.

303. Hayakawa Y, Chandra M, Miao W, Shirani J, Brown JH, Dorn GW, 2nd, Armstrong RC, and Kitsis RN. Inhibition of cardiac myocyte apoptosis improves cardiac function and abolishes mortality in the peripartum cardiomyopathy of Galpha(q) transgenic mice. *Circulation*, 2003. 108(24): p. 3036-41.

304. Chandrashekhar Y, Sen S, Anway R, Shuros A, and Anand I. Long-term caspase inhibition ameliorates apoptosis, reduces myocardial troponin-I cleavage, protects left ventricular function, and attenuates remodeling in rats with myocardial infarction. *J Am Coll Cardiol*, 2004. 43(2): p. 295-301.

305. Takeishi Y, Chu G, Kirkpatrick DM, Li Z, Wakasaki H, Kranias EG, King GL, and Walsh RA. In vivo phosphorylation of cardiac troponin I by protein kinase Cbeta2 decreases cardiomyocyte calcium responsiveness and contractility in transgenic mouse hearts. *J Clin Invest*, 1998. 102(1): p. 72-8.

306. Koide Y, Tamura K, Suzuki A, Kitamura K, Yokoyama K, Hashimoto T, Hirawa N, Kihara M, Ohno S, and Umemura S. Differential induction of protein kinase C isoforms at the cardiac hypertrophy stage and congestive heart failure stage in Dahl salt-sensitive rats. *Hypertens Res*, 2003. 26(5): p. 421-6.
307. Jiang L, Huang Y, Hunyor S, and dos Remedios CG. Cardiomyocyte apoptosis is associated with increased wall stress in chronic failing left ventricle. *Eur Heart J*, 2003. 24(8): p. 742-51.
308. Di Napoli P, Taccardi AA, Grilli A, Felaco M, Balbone A, Angelucci D, Gallina S, Calafiore AM, De Caterina R, and Barsotti A. Left ventricular wall stress as a direct correlate of cardiomyocyte apoptosis in patients with severe dilated cardiomyopathy. *Am Heart J*, 2003. 146(6): p. 1105-11.
309. Hughes SE. Detection of apoptosis using in situ markers for DNA strand breaks in the failing human heart. Fact or epiphenomenon? *J Pathol*, 2003. 201(2): p. 181-6.
310. Cregan SP, Dawson VL, and Slack RS. Role of AIF in caspase-dependent and caspase-independent cell death. *Oncogene*, 2004. 23(16): p. 2785-96.
311. Hong SJ, Dawson TM, and Dawson VL. Nuclear and mitochondrial conversations in cell death: PARP-1 and AIF signaling. *Trends Pharmacol Sci*, 2004. 25(5): p. 259-64.
312. Duriez PJ and Shah GM. Cleavage of poly(ADP-ribose) polymerase: a sensitive parameter to study cell death. *Biochem Cell Biol*, 1997. 75(4): p. 337-49.
313. Pillai JB, Russell HM, Raman J, Jeevanandam V, and Gupta MP. Increased expression of poly(ADP-ribose) polymerase-1 contributes to caspase-independent myocyte cell death during heart failure. *Am J Physiol Heart Circ Physiol*, 2005. 288(2): p. H486-96.
314. Sivarajah A, McDonald MC, and Thiemermann C. The production of hydrogen sulfide limits myocardial ischemia and reperfusion injury and contributes to the cardioprotective effects of preconditioning with endotoxin, but not ischemia in the rat. *Shock*, 2006. 26(2): p. 154-61.
315. Zanardo RC, Brancaleone V, Distrutti E, Fiorucci S, Cirino G, and Wallace JL. Hydrogen sulfide is an endogenous modulator of leukocyte-mediated inflammation. *Faseb J*, 2006. 20(12): p. 2118-20.

316. Pomerantz BJ, Reznikov LL, Harken AH, and Dinarello CA. Inhibition of caspase 1 reduces human myocardial ischemic dysfunction via inhibition of IL-18 and IL-1beta. *Proc Natl Acad Sci U S A*, 2001. 98(5): p. 2871-6.
317. Jones SP, Trocha SD, Strange MB, Granger DN, Kevil CG, Bullard DC, and Lefer DJ. Leukocyte and endothelial cell adhesion molecules in a chronic murine model of myocardial reperfusion injury. *Am J Physiol Heart Circ Physiol*, 2000. 279(5): p. H2196-201.
318. Murphy E and Steenbergen C. Preconditioning: the mitochondrial connection. *Annu Rev Physiol*, 2007. 69: p. 51-67.
319. Foo RS, Mani K, and Kitsis RN. Death begets failure in the heart. *J Clin Invest*, 2005. 115(3): p. 565-71.
320. Kroemer G, Galluzzi L, and Brenner C. Mitochondrial membrane permeabilization in cell death. *Physiol Rev*, 2007. 87(1): p. 99-163.
321. Jennings RB and Ganote CE. Structural changes in myocardium during acute ischemia. *Circ Res*, 1974. 35 Suppl 3: p. 156-72.
322. Leschelle X, Goubern M, Andriamihaja M, Blottiere HM, Couplan E, Gonzalez-Barroso MD, Petit C, Pagniez A, Chaumontet C, Mignotte B, Bouillaud F, and Blachier F. Adaptative metabolic response of human colonic epithelial cells to the adverse effects of the luminal compound sulfide. *Biochim Biophys Acta*, 2005. 1725(2): p. 201-12.
323. Yang G, Sun X, and Wang R. Hydrogen sulfide-induced apoptosis of human aorta smooth muscle cells via the activation of mitogen-activated protein kinases and caspase-3. *Faseb J*, 2004. 18(14): p. 1782-4.
324. Yang G, Wu L, and Wang R. Pro-apoptotic effect of endogenous H_2S on human aorta smooth muscle cells. *Faseb J*, 2006. 20(3): p. 553-5.
325. Baskar R, Li L, and Moore PK. Hydrogen sulfide-induces DNA damage and changes in apoptotic gene expression in human lung fibroblast cells. *Faseb J*, 2007. 21(1): p. 247-55.
326. Cao Y, Adhikari S, Ang AD, Moore PK, and Bhatia M. Mechanism of induction of pancreatic acinar cell apoptosis by hydrogen sulfide. *Am J Physiol Cell Physiol*, 2006. 291(3): p. C503-10.

327. Rose P, Moore PK, Ming SH, Nam OC, Armstrong JS, and Whiteman M. Hydrogen sulfide protects colon cancer cells from chemopreventative agent beta-phenylethyl isothiocyanate induced apoptosis. *World J Gastroenterol*, 2005. 11(26): p. 3990-7.
328. Hu LF, Lu M, Wu ZY, Wong PT, and Bian JS. Hydrogen sulfide inhibits rotenone-induced apoptosis via preservation of mitochondrial function. *Mol Pharmacol*, 2009. 75(1): p. 27-34.
329. Rinaldi L, Gobbi G, Pambianco M, Micheloni C, Mirandola P, and Vitale M. Hydrogen sulfide prevents apoptosis of human PMN via inhibition of p38 and caspase 3. *Lab Invest*, 2006. 86(4): p. 391-7.

9. PUBLICATION LIST

9.1. Publications related to the present thesis

Xiao CY, Chen M, Zsengellér Zs, Li H, **Kiss L**, Kollai M, Szabó C. Poly (ADP-ribose) polymerase promotes cardiac remodeling, contractile failure and translocation of apoptosis-inducing factor in a murine experimental model of aortic banding and heart failure. *J Pharmacol Exp Ther*, 2005. 312(3): p. 891-8. **IF: 4.098**

Elrod JW, Calvert JW, Morrison J, Doeller JE, Kraus DW, Tao L, Jiao X, Scalia R, **Kiss L**, Szabó C, Kimura H, Chow CW, Lefer DJ. Hydrogen sulfide attenuates myocardial ischemia-reperfusion injury by preservation of mitochondrial function. *Proc Natl Acad Sci U S A,* 2007. 104(39): p. 15560-5. **IF: 9.598**

Kiss L, Chen M, Gerő D, Módis K, Lacza Zs, Szabó C. Effects of 7-ketocholesterol on the activity of endothelial poly (ADP-ribose) polymerase (PARP) and on endothelium-dependent relaxant function. *Int J Mol Med,* 2006. 18(6): p. 1113-7. **IF: 1.854**

9.2. Publications not related to the present thesis

Módis K, **Kiss L**, Szabó C. The clinical relevance and pathogenesis of the endothelial dyfunction syndrome in atherosclerosis and cardiovascular diseases. *Praxis*, 2005. February

Kiss L, Szabó C. The pathogenesis of diabetic complications: the role of DNA injury and poly(ADP-ribose) polymerase activation in peroxynitrit-mediated cytotoxicity. *Mem Inst Oswaldo Cruz,* 2005. 100(1): p. 29-37. **IF: 0.847**

Módis K, **Kiss L**, Csaba Szabó C. cGMP phosphodiesterase-inhibitors and their clinical applications. *Praxis,* 2005 April

Kiss L, Módis K, Szabó C. The role of uric acid and xanthine-oxidase inhibitors in cardiovascular diseases. *Praxis*, 2005 June

Lacza Zs, Pankotai E, Csordás A, Gerő D, **Kiss L**, Horváth EM, Kollai M, Busija DW, Szabó C. Mitochondrial NO and reactive nitrogen species production: does mtNOS exist? *Nitric Oxide*, 2006. 14(2): p. 162-8. **IF: 2.509**

Csordás A, Pankotai E, Snipes JA, Cselenyák A, Sárszegi Zs, Cziráki A, Gaszner B, Papp L, Benkő R, **Kiss L**, Kovács E, Kollai M, Csaba Szabó C, Busija DW, Lacza Zs. Human heart mitochondria do not produce physiologically relevant quantities of nitric oxide. *Life Sci,* 2007. 80(7): p. 633-7. **IF: 2.257**

Seabra AB, Pankotai E, Fehér M, Somlai Á, **Kiss L**, Bíró L, Szabó C, Kollai M, de Oliveira MG, Lacza Zs. S-nitrosoglutathione-containing hydrogel increases dermal blood flow in streptozotocin-induced diabetic rats. *Br J Dermatol*, 2007. 156(5): p. 814-8. **IF: 3.503**

Horváth EM, Benkő R, Gerő D, **Kiss L**, Szabó C. Treatment with insulin inhibits poly(ADP-ribose)polymerase activation in a rat model of endotoxemia. *Life Sci*, 2008. 82(3-4): p. 205-9. **IF: 2.257**

Esechie A, **Kiss L**, Oláh G, Horváth EM, Hawkins H, Szabó C, Traber DL. Protective effect of hydrogen sulfide in a murine model of combined burn and smoke inhalation-induced acute lung injury. *Clin Sci*, 2008. 115(3): p. 91-7. **IF: 3.900**

Kiss L, Deitsch EA, Szabó C. Hydrogen sulfide decreases adenosine triphosphate levels in aortic rings and leads to vasorelaxation via metabolic inhibition. *Life Sci*, 2008. 83(17-18): p. 589-94. **IF: 2.257**

10. ACKNOWLEDGEMENTS

I would like to express my gratitude to Professor Csaba Szabó, my supervisor, for his guidance on straightforward thinking and scientific know-how and for giving me the opportunity to work at the Inotek Pharmaceuticals Corporation and at the University of Medicine and Dentistry of New Jersey. These experiences helped me a lot to achieve my scientific goals and improved my skills in designing and performing experimental protocols. I also thank Professor Márk Kollai for his help in initiating my scientific career in his lab and my biology teacher András Gömöry for his lectures sparkling my interest in biology and medicine. I would like to thank also all contributors and all co-authors for their work and help through all my work. Finally, I thank my family and my friends for their support during my studies.

11. APPENDIX (Paper I-III)